DICHOPTIC MULTIFOCAL VISUAL EVOKED POTENTIALS IN GLAUCOMA DETECTION, AND THEIR STRUCTURAL AND FUNCTIONAL CORRELATES.

Dr John Charles Montague Leaney MBBS, BE (Chem)

Department of Ophthalmology and Visual Sciences

Australian School of Advanced Medicine

Date of Submission

20th April 2015

This thesis is submitted for the degree of Doctor of Philosophy

Contents

Summary

Glaucoma is the leading cause of preventable blindness in the western world. Effective treatment of glaucoma relies on early detection of a disease that is without symptoms in the initial stages. Identification of damage often relies on visual field testing which can be unreliable. The Multifocal VEP (mfVEP) was developed to provide an objective measure of visual field function in glaucoma. The use of inter-eye asymmetry analysis provides a sensitive way to detect subtle, early changes in glaucoma. The newly designed dichoptic (binocular) mfVEP creates a testing environ which is most conducive to calculating inter-eye asymmetry, as both eyes are tested at the same time, under the same conditions. However the sensitivity of this testing technology, the role of inter-ocular suppression in asymmetry analysis and the ideal stimulus for detecting glaucoma using dichoptic mfVEP are largely unknown. Experiments focusing on dichoptic mfVEP and interocular suppression demonstrated sensitivity to eccentricity, contrast and speed of presentation. Building on these relationships, dichoptic mfVEP with targeted stimuli was shown to be more effective than monocular in detecting unilateral early glaucoma.

Furthermore this project sought to provide further insight into the structure/function relationship that underlies the pathogenesis of glaucoma by studying correlations of glaucomatous field defects as detected by Humphrey visual field testing and mfVEP with structural changes characterised by high resolution retinal imaging techniques. The results showing that newer imaging technologies exhibited closer correlation to glaucomatous change but that the relationship is still variable highlighted the one of the many challenges in monitoring glaucoma. Correlation analysis comparing HVF and mfVEP showed similarities in structure-function patterns.

Declaration of originality

I certify that the work in this thesis entitled "Dichoptic multifocal visual evoked potentials in glaucoma detection, and their structural and functional correlates" has not previously been submitted for a degree nor has it been submitted as part of requirements for a degree to any other university or institution other than Macquarie University.

I also certify that the thesis is an original piece of research and it has been written by me. Any help and assistance that I have received in my research work and the preparation of the thesis itself have been appropriately acknowledged.

In addition, I certify that all information sources and literature used are indicated in the thesis.

The research presented in this thesis was approved by Macquarie University Ethics Review Committee, reference number: HE25SEP2009-D00139 on May 2009

Dr John Charles Montague Leaney

29th of June 2014

Acknowledgements

I would like to extend my sincerest thanks to my supervisors Professor Stuart Graham and Associate Professor Alexander Klistorner. Their unwavering support has proved invaluable in the entirety of this thesis. Their depth of knowledge and expertise in this area is unparalleled and I have greatly benefited from their time and effort. Professor Graham's extensive knowledge on glaucoma and application of mfVEP has been fundamental to the direction of my research. Professor Klistorner has nurtured, with Professor Graham, mfVEP through many years of research and I was lucky enough to be involved in part of this process.

I would like to show my appreciation to the researchers with whom I have worked – namely Dr Prema Sriram and Martin Lee. I would also like to thank all of the willing volunteers who have given up their time to participate in the clinical experiments, especially Drs Mojtaba Golzan, Johnson Thie and Deepa Viswanathan. Thank you to my father, Professor Leaney, for reading and editing my thesis from start to finish.

Thank you to Macquarie University for providing the scholarship and ongoing support throughout this endeavour. The staff and students at the Australian School of Advanced Medicine have been influential and have created an environment that fosters collaboration and academic excellence.

Lastly, I wish to express my gratitude to my family, friends and above all my wife.

Publications arising from this thesis

1. Leaney J, Klistorner A, Arvind H, Graham SL

   Dichoptic Suppression of mfVEP Amplitude: Effect of Retinal Eccentricity and Simulated Unilateral Visual Impairment. Investigative Ophthalmology & Visual Science, 2010. **51**(12): p. 6549-6555.

2. Leaney J, Healey PR, Lee M, Graham S L.

   Correlation of structural retinal nerve fibre layer parameters and functional measures using Heidelberg Retinal Tomography and Spectralis spectral domain optical coherence tomography at different levels of glaucoma severity. Clinical & Experimental Ophthalmology, 2012. **40**(8): p. 802-812.

Prepared for Publication

1. Leaney J, Klistorner A, Graham SL.

   Stimulation speed, but not contrast determines degree of dichoptic suppression of mfVEP.

   Prepeared for submission to Documenta Ophthalmologica

Published abstracts and presentations

1. Leaney J, Klistorner A, Arvind H, Graham SL

   Dichoptic Suppression of mfVEP Amplitude: Effect of Retinal Eccentricity and Simulated Unilateral Visual Impairment.

   Poster presentation - Poster number: 10A-2373-ARVO at the American society for Research in Vision and Ophthalmology (ARVO) conference. 2009, Fort Lauderdale, USA.

2. Leaney J, Klistorner A, Arvind H, Graham SL

   Dichoptic Suppression of mfVEP Amplitude: Effect of Retinal Eccentricity and Simulated Unilateral Visual Impairment.

   Oral presentation - *International Society for Clinical Electrophysiology of Vision* (ISCEV) Annual conference. 2010, Freemantle, Australia.

3. Leaney J, Healey PR, Lee M, Graham S L.

   Correlation of RNFL Loss with Visual Field Using HRT 3 and Spectralis OCT at Different Levels of Glaucoma Severity

   Oral presentation – Royal Australia and New Zealand College of Ophthalmologists (RANZCO), annual conference. 2010, Adelaide, Australia

4. Leaney J, Healey PR, Lee M, Graham S L.

   Correlation of structural retinal nerve fibre layer parameters and functional measures using Heidelberg Retinal Tomography and Spectralis spectral domain optical coherence tomography at different levels of glaucoma severity.

   Oral Presentation at the American society for Research in Vision and Ophthalmology (ARVO) conference. 2011 Fort Lauderdale, Florida, USA.

Publications I contributed to during my thesis not included as chapters

1. Cordina RL, Nakhla S, O'Meagher S, Leaney J, Graham S, Celermajer DS.

   Widespread endotheliopathy in adults with cyanotic congenital heart disease.

   Cardiol Young. 2014 Mar 25:1-9. [Epub ahead of print]

2. Golzan SM, Graham SL, J. Leaney, A. Avolio, "

   Dynamic Association between retinal venous pulsatility and intraocular pressure changes

   J Current Eye Research, 2011, 36(1), pp 53-59

3. Golzan SM, Avolio A, Leaney J, Cordina R, Celermajer DS, Graham SL,

   Spontaneous Retinal Venous Pulsatility in Patients with Cyanotic Congenital Heart Disease

   J of Heart and Vessels, *In Press* 2011

Thesis hypotheses and research questions

Hypotheses

1. The dichoptic mfVEP shows variable levels of inter-ocular suppression depending on stimulus presentation
2. The dichoptic mfVEP can be adapted to provide optimal detection of early glaucoma
3. Changes identified by the dichoptic mfVEP reflect local functional and structural defects as detected by visual field testing and retinal imaging techniques

Specific questions

Broadly divided into visual function and retinal nerve structure areas, the questions are:

- Visual function
  - Can a redesigned dichoptic mfVEP accurately measure normal mfVEP traces and provide useful measurements of disease states?
  - Is there a benefit in using fast stimulation dichoptic mfVEP for detection of early glaucoma?
    - If there is a benefit, what are the underlying mechanisms?
    - Is there increased asymmetry using dichoptic over monocular stimulation and what is the relationship to eccentricity?
  - Can the dichoptic mfVEP be used as a clinical tool for detection of early unilateral glaucomatous optic neuropathy
- Retinal structure
  - Do the new structural nerve head imaging devices, SD-OCT or HRT, provide reliable markers of structural damage, and which is the most accurate for use in glaucoma?
  - Is there a relationship between SD-OCT nerve head parameters and mfVEP responses and how does this compare with the current gold standard of functional testing (HVF)?

- Is there an advantage of using these new technologies either individually or in combination?

Thesis outline

Chapter 1 – Literature review

This chapter explores the current research on the pathogenesis glaucoma and importance of early detection. It highlights the importance of the relationship between structural and functional changes in glaucoma and how accurately predicting function from early structural change can lead to the early diagnosis of glaucomatous optic neuropathy. Structural and functional measures in current glaucoma diagnosis are outlined. Work on the use of electrophysiology in the detection and monitoring of glaucoma and the evolution of dichoptic stimulation is also covered. The mechanisms underlying dichoptic suppression are explained and their relevance to dichoptic mfVEP, namely in increasing glaucoma detection. Finally the comparison of mfVEP monocular and dichoptic stimulation is addressed and the current use of both is detailed.

Chapter 2 – Materials and Methods

This chapter describes the technologies used in this thesis which assess structural and functional changes in glaucoma. Methods of statistical analysis are detailed and the reasons for utilizing them. Recruitment of subjects for the trials and the studies in which they are involved are explained.

Chapter 3 - Dichoptic Suppression of mfVEP Amplitude: Effect of Retinal Eccentricity and Simulated Unilateral Visual Impairment

Dichoptic mfVEP has been previously shown to possess advantages over monocular mfVEP in the detection of glaucoma through enhancing asymmetry between eyes through dichoptic suppression. To further understand the mechanisms underlying this phenomena a study on normal subjects with simulated visual impairment was undertaken to assess the factors influencing dichoptic suppression, namely degree of suppression and eccentricity.

Chapter 4 - Stimulation speed, but not contrast determines degree of dichoptic suppression of mfVEP.

This section follows from chapter 3 in exploring dichoptic suppression in dichoptic mfVEP and the influence of speed of presentation and contrast level on dichoptic suppression. The study explores these issues to gain deeper understanding about factors that can be adjusted to alter levels of dichoptic suppression. The finding that dichoptic suppression is influenced by speed of presentation but not contrast aids understanding of the types of retinal ganglion cells involved and potential targets in the non-redundant pathways involved in glaucomatous optic nerve damage.

Chapter 5 - Comparison of low luminance contrast (LLA) and blue on yellow (BonY) stimulation with fast and slow presentation in the detection of glaucoma

This study incorporates the two preceding chapters into a clinical pilot study comparing degree of inter-eye asymmetry in four stimulus conditions to identify a sensitive stimulus for use in a larger clinical study. The study develops the thesis that faster stimulation increases dichoptic suppression and targeting of the koniocellular RGC pathway could increase rates of detection in early unilateral glaucoma.

Chapter 6 - The role of interocular suppression in the detection of glaucomatous defects using dichoptic mfVEP fast blue on yellow stimulation

Applying the findings of chapters 3 -5, this study used the stimulus characteristics of fast, blue on yellow dichoptic and monocular mfVEP to explore the differences between monocular and dichoptic stimulation, comparing these technologies with the gold standard of Humphrey visual field testing. Finding that there was greater asymmetry in dichoptic stimulation versus monocular and that this asymmetry was accurate to the side of disease, demonstrated the sensitivity and accuracy of dichoptic mfVEP.

Chapter 7 - Correlation of disc parameters with visual field indices using scanning laser and SD-OCT at different levels of glaucoma severity

In order to provide a deeper understanding upon which to explore the structural and functional changes in mfVEP, this study looked at the correlation between structural and functional parameters in optic nerve head imaging and Humphrey visual field testing technologies. The study thus provided a foundation upon which to explore structural and functional changes seen with mfVEP.

Chapter 8 - Structure/function correlations of novel and conventional perimetry technologies

Correlation between structural and functional changes in a glaucoma disease detection technology is an indirect indicator of the accuracy of the technology for diagnosing glaucomatous disease. By measuring the correlation coefficients of dichoptic and monocular mfVEP against those of HVF, as established in the previous chapter, we provided insight into the strengths and weaknesses, in the detection of glaucoma, of monocular and dichoptic mfVEP both globally and segmentally.

Contributions to each chapter

Chapter 1 – Research, writing

Chapter 2 – Experimentation, analysis and writing

Chapter 3 – Experimental work, analysis and writing

Chapter 4 – Experimental work, analysis and writing

Chapter 5 –Experimental work, analysis and writing

Chapter 6 – Most experimental work (20% of experimental work was performed by PhD candidate Prema Sriram), all analysis and writing

Chapter 7 – Writing and analysis - testing by orthoptists at Eye Associates Clinic

Chapter 8 – Experimental work, analysis and writing

Chapter 9 - Writing

List of Abbreviations

Amp	Amplitude
Candel	Candella
D	Dichoptic
DS	Dichoptic Suppression
HRT	Heidelberg Retinal Tomograph
HVF	Humphrey Visual Field
M	Monocular
mfVEP	Multifocal Visually Evoked Potentials
OCT	Optical Coherence Tomography
RAC	Relative Asymmetry Coefficient
RGC	Retinal Ganglion Cell
V	Volts

Chapter 1 INTRODUCTION AND LITERATURE REVIEW

Summary

This chapter provides background information on glaucomatous optic neuropathy, current understanding on structure and function in glaucoma, use of electrophysiology in clinical and research settings and an exploration of the challenges facing contemporary glaucoma detection.

1 INTRODUCTION

Primary open angle glaucoma is the leading cause of preventable blindness in the western world[1]. Effective treatment of glaucoma relies on early detection of a disease that is without symptoms until it is in a very advanced stage. There is a complex structure-function relationship between glaucomatous visual field changes and structural optic nerve damage. Predicting and understanding the structure-function relationship is important in making the primary diagnosis and in assessing disease severity. This is important as glaucoma is a disease in which early treatment can prevent blindness with reduction of intraocular pressure. Study of the structure-function relationship provides important insight into the strengths and weaknesses of structural imaging and visual field testing technologies. Indeed, patients can lose 30% of their retinal nerve fibre layer and have no demonstrable field defect[2]. Conversely, one third of the retinal nerve fibre layer can be lost before it is classified as abnormal using current imaging technologies.[3]

Glaucoma is a challenging diagnosis as identification of disease often relies on visual field testing that is unreliable initially and takes time and skill to utilise effectively. Multifocal visually evoked potential (mfVEP) provides an objective measure of visual field function in glaucoma which attempts to redress some of the difficulties with current subjective testing technologies. The use of inter-eye asymmetry provides a sensitive method to detect subtle, early changes in glaucoma by comparing intrinsically symmetrical cortical responses that are almost identical in normal eyes. Dichoptic (binocular) mfVEP creates a testing environ which is the most conducive to calculating inter-eye asymmetry as both eyes are tested at the same time, under the same conditions. However the sensitivity of this testing technology for disease detection, the role of inter-ocular suppression in asymmetry analysis, the relationship of mfVEP functional changes to manifest structural changes and the ideal stimulus for detecting glaucoma using dichoptic mfVEP all require further study.

2 GLAUCOMATOUS OPTIC NEUROPATHY (GON)

2.1 BACKGROUND

Glaucoma is the leading cause of preventable irreversible blindness in the world [1]. Effective treatment centres around early detection and lowering of intraocular pressures [4]. Primary open angle glaucoma is the most common type of glaucoma seen in the western world affecting 1-2% of the population over 40 years of age, with rising incidence with increasing age[5]. The economic burden of the disease will rise steeply in accordance with the ageing population, with projections for the total cost to more than double in the next 20 years from $1.9 billion to $4.3 billion in total costs.[6]

There are multiple subclassifications of GON dependent upon the mechanism of altered intraocular pressure at the optic nerve head, broadly divided into – congenital, primary open angle, primary closed angle, secondary open angle and secondary closed angle[7].

Primary open angle glaucoma (POAG) refers to the development of pathological optic nerve changes, arcuate visual field defects or a combination of these features in the presence of an open angle in the trabecular meshwork. While there is not complete agreement between specialists about the definitive characteristics of POAG there a number of signs can exist in isolation or together that point towards a diagnosis of glaucoma. (Table 1-1)

SIGN	DESCRIPTION
Cup-to-disc ratio	Increased, usually >0.6
	Asymmetry between eyes, usually >0.2
	Vertical elongation, usually denoting loss of rim inferiorly or superiorly
Neuroretinal rim	Notching or focal loss
	Pallor
	Sloped rim is common temporally and is not a specific sign
Nerve fibre layer	Localized wedge defects
	Can be diffuse in advanced disease

SIGN	DESCRIPTION
	Often in relation with splinter haemorrhage
Vascular	Disc splinter haemorrhages
	Overpass with loss of rim underneath
	Bayonetting
	Narrowing, can be diffuse or focal
	Nasalization mostly with advanced cupping
Peripapillary atrophy	Common but not specific to glaucoma

Table 1-1 - Common signs associated with glaucomatous optic neuropathy (from Glaucoma: Volume 1 Medical Diagnosis and Therapy[8])

In order for glaucoma to be diagnosed there should be evidence of progression of the visual field loss or developing neural retinal rim loss. It is a diagnosis over space and time, with progressive structural changes correlating with functional changes. Thus it is a difficult diagnosis for some patients who may manifest very subtle optic nerve head changes that have no corresponding visual field defect.

Although POAG can proceed via a number of routes the end result is either abnormal force on a normal nerve or normal force on an abnormal nerve, resulting in visual field loss, most often progressing peripherally to centrally. POAG is thought to have three main underlying pathologic influences –intraocular pressure that is beyond the limits of the optic nerve to withstand[9,10], abnormal blood flow dynamics [11-13] and structural characteristics[14] all of which can combine to cause pathological visual loss as a result of optic nerve damage seen as neural rim thinning. In POAG, the damage to the nerve is the result of accumulated excessive force on optic nerve axons resulting in altered axoplasmic flow, retrograde neural degeneration[7] and progressive decline in the optic nerve

axon population[7]. This leads to the end result of decline in the retinal ganglion cell population at the optic nerve head.

2.2 RISK FACTORS FOR GON

The most reproducible and widely accepted risk factor for POAG is intraocular pressure (IOP) greater than 21mmHg[15]. This has been well established in many large, multi-centered studies.[10,16] There are other significant factors which include family history [17], refractive error[18] (higher myopes are more at risk of developing glaucoma), optic head cup-disc ratio[9] (larger cup disc ratio is associated with increased risk of developing POAG), African-American race[17], altered optic nerve head blood supply (patients with normal tension glaucoma often have vasospastic tendencies)[19,20] and increasing age[11] (prevalence of GON increases sharply above age 80). Other factors that are still to be definitively studied are diabetes and hypertension.

2.3 INTRAOCULAR PRESSURE MEASUREMENT

Detection of POAG is the most crucial step in glaucoma management as the disease is insidious in onset and progression, with patient observed manifestations of the disease only in late stages. Lowering of IOP remains the most effective and well-studied mechanism for reducing the rates of progression to glaucomatous optic neuropathy (GON) – this has been demonstrated by the Early Manifest Glaucoma Trial (EMGT)[16] where at 6 years, treatment significantly lowered risk of progression. The study demonstrated that there was a good correlation between IOP reduction and delaying glaucoma progression such that 1mmHg reduction resulted in a 10% reduction in progression of visual field loss. In the Ocular Hypertension Treatment Study (OHTS)[10] there was also shown to be benefit in reducing rates of progression by reduction of IOP, resulting in a 50% reduction in disease progression versus the non-treatment arm.

The fundamental method of detection of glaucoma is the testing of intraocular pressure (IOP). Large studies[9] have consistently found that raised IOP is a strong predictor of the risk of developing glaucoma. Of all the risk factors identified in the pathogenesis of POAG, only IOP is modifiable.

3 FUNCTIONAL MEASURES OF THE VISUAL FIELD IN GLAUCOMA

Assessment of the function of the optic nerve involves stimulation and measurement of the visual field response in a repeatable, structured and timely efficient manner. The most commonly used functional tests in glaucoma assessment are Humphrey visual field testing, electrophysiological methods (VEP and ERG types) and frequency doubling technology. An overview of the technologies is presented in Table 1-2.

3.1 SUBJECTIVE VISUAL FIELD TESTING

Subjective visual field testing relies on the subject's response for measurement of visual field function. Humphrey Visual Field testing (HVF) is the most commonly used test for visual field assessment of glaucomatous visual field loss[8]. The principle behind HVF, similar to a number of other examples of static automated perimetry (SAP) technologies, is establishing the threshold at which the subject can perceive light at pre-determined points in the visual field. For HVF, this process is completed for 56 points in the visual field but relies heavily on the user response to the stimulus, meaning HVF is a subjective field test. The most widely used program is the Swedish Interactive Testing Algorithm (SITA) which was developed to decrease testing time whilst still testing full threshold sensitivity.

There are a number of problems with subjective testing in general and HVF in particular – the lack of interchangeability between SITA and full threshold testing in longitudinal follow-up and the short-term fluctuation with patients owing to a number of physical and psychophysical factors. Further factors include fatigue of the patient, media opacities (although the pattern standard deviation (PSD) does attempt to counteract this), refractive errors, false-positive errors, false negative errors and a learning effect that typically takes up to 3 fields to be assured the results are a true representation of the visual function [8]. The aforementioned difficulties underscore the variability of subjective testing and the problems that can be somewhat addressed with objective field testing[21].

3.2 FREQUENCY DOUBLING TECHNOLOGY

Frequency doubling technology (FDT), as used in detection of glaucoma, utilizes the properties of magnocellular retinal ganglion cells to attempt to stimulate non-redundant pathways thought to be damaged in early glaucoma [22]. FDT uses the spatial frequency doubling illusion and a subject's

perception of the point at which the illusion is reached. In normals this will be at a certain level of contrast, in glaucomatous eyes the contrast level will be higher indicating magnocellular injury.

FDT is a subjective test however it does appear to have comparatively better detection of early glaucoma than SITA and better prediction of progression[23]. Owing to a number of limitations of traditional FDT, such a low spatial resolution, FDT Matrix (Carl-Zeiss Meditc, Dublin, CA) was developed using a Bayesian probability algorithm and greater spatial resolution.

3.3 Short Wave Automated Perimetry (SWAP)

SWAP was also developed to test the non-redundant pathways thought to be affected in early glaucoma [24]. In the case of SWAP, the test design, based upon SITA protocols, uses a blue stimulus on a saturating yellow background to stimulate short wave cones. The koniocellular RGCs corresponding to the short wave cones make up less than 10% of the total RGC population[25], thus changes in this non-redundant population can be an early sign of POAG.

Test	Field (degrees)	Stimulus type	Stimulus size (degrees)	Testing time (mins/eye)	Targeted RGC?
HVF	24	White on white	0.47	5-10	All
mfVEP	24	Commonly low contrast achromatic	Scaled to cortical representation	7-12	Depends on stimulus
FDT	30	Frequency doubling achromatic	10x10	4-5	Magnocellular
SWAP	24	Blue on yellow	1.8	10-15	Koniocellular
PERG	Full field	Pattern change	10-20	5	All
PhNR	Full field	Flash	large	5	All

Table 1-2 - Visual field assessment technologies used in the assessment of glaucoma [8] pp 115-147

3.4 ELECTROPHYSIOLOGY IN GLAUCOMA

Electrophysiology in the detection of glaucoma can be broadly divided into electroretinogram (ERG) and visually evoked potential (VEP) techniques. For glaucoma detection using ERG the pattern ERG (PERG), photopic negative response (PhNR) and multifocal ERG (mfERG) provide the most useful information regarding glaucoma diagnosis and progression. Useful VEP measures are essentially restricted to the use of mfVEP as other measures, such as pattern or flash VEP, are not sensitive enough to detect early or subtle glaucomatous change.

3.4.1 THE ELECTRORETINOGRAM IN GLAUCOMA

The ERG is a sensitive measure of the function of the retina, using either corneal or conjunctival electrodes, to light stimuli. The full field ERG is composed of five signals which are characterised by the type of photic stimulation and dark/light adaptation state of the retina. As per the ISCEV 2009 standard[26](Figure 1-1), there are three dark-adapted stimuli with flash intensities of 0.01 cdm^{-2} for rod response, 3.0 $cdsm^{-2}$ for rod/cone mixed response and oscillatory 3.0 $cdsm^{-2}$ for muller, glial and astroglial responses. There are additionally two light adapted 3.0 $cdsm^{-2}$ stimuli – flash and oscillatory which are both representative of the pure cone responses with the oscillatory response more sensitive to early abnormalities in the cone system[27].

The scotopic 0.01 ERG response is a smooth curve with a single peak (b-wave) representing a rod bipolar response. The second of the scotopic (3.0 ERG) stimuli is a high intensity stimulus producing a signal representing a mixed rod-cone response seen as a large a-wave and b-wave. The oscillatory potentials are seen as high frequency wavelets on the b-waves. The photopic 3.0 ERG demonstrates a smaller amplitude a and b wave compared with the scotopic response but faster a and b wave response representative of the light adapted state. Lastly the 30 Hz flicker photopic response demonstrates a high frequency, uniform wave which is sensitive to early cone dysfunction.

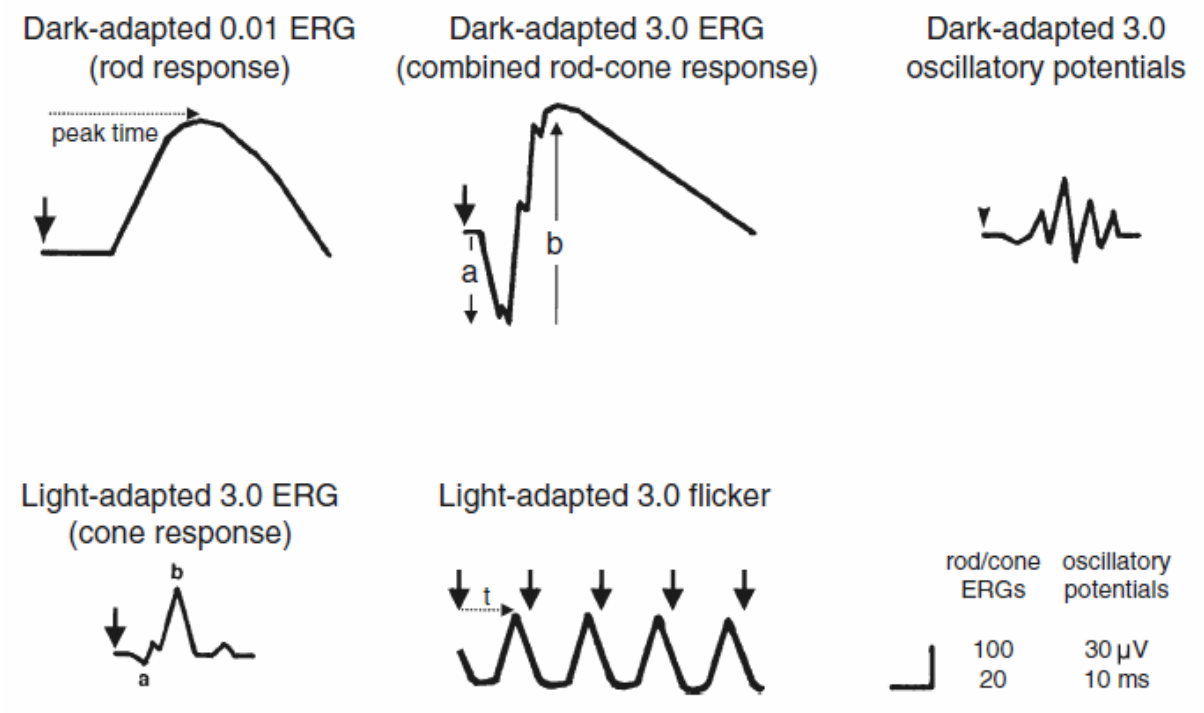

Figure 1-1 - ISCEV standard response curves for full field ERG (diagram from ISCEV 2009 standard)[26]

3.4.1.1 PERG

A PERG signal is generated by using a high-contrast patterned stimulus on a television monitor and is sensitive to changes in the health of the RGCs[28]. The patient is light adapted and the stimulus covers the central 20° of the visual field. The PERG response has shown to be sensitive to early glaucoma showing abnormalities in amplitude, phase or interocular asymmetry in 69% of patients tested[29]. More recently studies have shown that PERG can be an early glaucoma indicator in ocular hypertension with a sensitivity of 80% and a specificity of 71% 1 year before conversion to demonstrable glaucomatous disease[30]. Fundamentally the PERG signal relies on the normal functioning of the RGCs although the levels of RGC dysfunction do not always closely correlate to the structural changes seen on OCT[31].

3.4.1.2 MFERG

Multifocal ERGs, despite the promise shown with PERG, have limited use in the detection and monitoring of glaucoma. The principle of the mfERG is similar to full field ERG but using multiple stimuli in often hexagonal shape on a computer monitor, typically around 100 points and up to 50° of eccentricity. The stimuli are presented in a pseudo random fashion using an m-sequence paradigm to

cross correlate the displayed stimulation with the recorded ERG responses[27]. Early work in experimental[32] and clinical glaucoma[33] demonstrated abnormalities of mfERG recordings associated with glaucomatous change. However application of these findings in reproducible clinical studies have been challenging[34]. This is most likely due to the way mfERG is recorded(ie outer retinal greater than inner retinal function), in glaucoma the optic nerve head component is predominantly affected but this doesn't result in focal loss appearing on mfERG testing, hence there is limited sensitivity even in moderate glaucoma. More recent work has focused on central amplitude changes demonstrating ganglion cell complex damage and corresponding mfERG photopic negative response (PhNR) changes in glaucoma[35].

3.4.1.3 PHOTOPIC NEGATIVE RESPONSE (PHNR)

The PhNR, as part of the flash ERG, originates from the RGCs and is therefore of interest in glaucoma. It is seen as a slow negative wave after the positive b-wave[36] and was observed in monkeys with glaucoma and was isolated to the RGCs by injection of tetrodotoxin[37] . In human POAG, there was a demonstrated reduction of the PhNR sensitive to early glaucoma (MD<-6dB) [38] but with declining sensitivity with increasing glaucoma severity. Further published work has demonstrated a linear relationship between RNFL parameters and PhNR in the superotemporal and inferotemporal regions using scanning laser ophthalmoscopy and laser scanning polarimetry[39]. More recently ganglion cell complex thickness has been shown to be correlated to PhNR amplitude and PhNR/b-wave amplitude ratio in central retinal areas.[40]

3.4.2 THE VEP IN GLAUCOMA

The traditional VEP in glaucoma (flash or pattern), whilst being a sensitive measure of optic nerve function is primarily driven by the macula and therefore not suited to detection of peripheral field changes. However, before the advent of multifocal techniques, there were useful applications of VEP recordings in glaucoma detection. VEP latencies were shown to be correlated to severity and location of visual field defects.[41,42] Additionally stimulation of the blue-yellow opponent pathways also yielded reasonable sensitivity and specificity for glaucoma detection[43].

3.4.2.1 GENERATION OF THE VEP SIGNAL

The visual evoked potential is thought to arise from the action potential generated from activation of the RGCs in the inner retina [44]. Photons enter the eye stimulating the photoreceptors to undergo phototransduction in the form of graded hyperpolarisation (and off-centre depolarisation) in a centre surround fashion. Through graded action potentials and a series of excitatory and inhibitory neurotransmitters the signal is further transmitted to on-bipolar cells (with lateral inhibition via amacrine and horizontal cells) and then to on-centre ganglion cells[44]. The action potential generated at the level of the ganglion cell represents the 1st in a 2 synapse link that stretches from retinal ganglion cell to striate cortex. The 1st synapse occurs at the level of the lateral geniculate nucleus (LGN) where ganglion cells are arranged in a retinotopic manner, the 2nd synapse is located in the striate cortex where the neurons from the LGN synapse at various sub-layers of layer 4 of the striate cortex, depending on ganglion cell type. The striate cortex represents the first area where there is a complete map of the visual field, with central field magnification. It is at this level that the visually evoked potentials are recorded and are derived from the action potentials generated at layer 4 of the visual cortex. The structure of the visual cortex as related to the visual field allows correlation between action cortical action potentials and retinal ganglion cell responses to visual stimuli.

The conventional VEP signal is characterised in signal analysis by amplitude and latency. The typical pattern reversal stimulus VEP signal has 3 identifying peaks upon which the amplitude and latency are calculated (Figure 1-2); N75 is the first large negative peak and occurs 75msec in the normal population, P100 is the first large positive peak at 100msec and N135 the second large negative peak at 135msec. Amplitude is calculated as the difference between the N75 and P100 peaks[26] with latency as the time from onset to the largest peak.

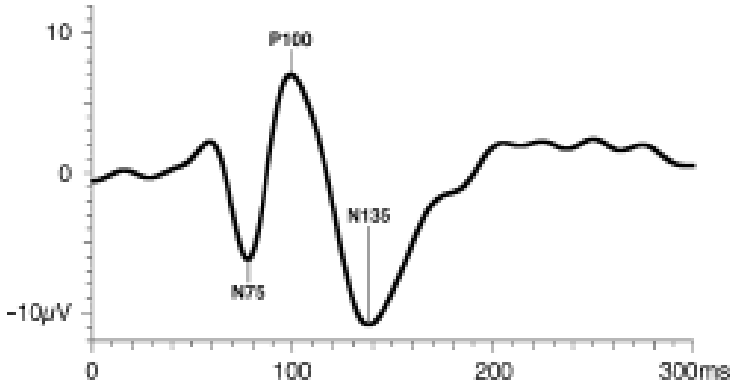

Figure 1-2 - ISCEV standard VEP waveform[26]

3.4.3 MULTIFOCAL VISUALLY EVOKED POTENTIALS

Multifocal visually evoked potentials are a more recent development in the functional visual field assessment tools. Using computer-driven visual stimuli and occipital electroencephalogram recordings, a measurement of the sensitivity of 56 points over 24 degrees of eccentricity is obtained. Unlike subjective visual field testing where the sensitivity of the retina relies on patient response, the mfVEP measures retinal sensitivity by amplitude of the cortically measured VEP wave. Repeated measurements of the visual field decrease signal to noise ratio to an acceptable level.

Multifocal visually evoked potentials have a number of applications in assessment of ocular pathology, most prominently in multiple sclerosis[45,46] and glaucoma[47-50]. MfVEP benefits from a number of advantages for testing patients – it is an objective test so minimizing the errors associated with subjective testing[51] as seen with Humphrey visual field testing, it has good repeat testing in the hands of a skilled operator[52,53] , it doesn't require repeat testing to confirm presence of a defect as subjective testing does [54], it can assess the pathway from retinal ganglion cell to occipital lobe with a high degree of accuracy [55] and there is a wide body of knowledge substantiating its use.

MfVEP does suffer from a number of disadvantages compared to the most commonly used field testing modality, Humphrey visual field testing. There is a need for a skilled operator to align the electrodes appropriately to ensure correct readings[56], to repeat the test the operator must align the electrodes to the same surface anatomical landmarks, the testing time is usually 15-25 minutes in

length, the results need to be interpreted by a skilled clinician and there are a number of diseases which can obscure the relationship between ganglion cell amplitude and mfVEP readings (such as cataract, uncorrected vision/high astigmatism, lesions anywhere from the optic nerve to the occipital lobe, retinal dystrophies)[51,57]. The visual field representation as derived from the cortical signals is affected by eccentricity which is somewhat addressed by the cortical magnification factor.

3.4.3.1 THE MONOCULAR MULTIFOCAL VEP IN GLAUCOMA

The first mfVEP recorded was described in 1994 by Baseler et al. using pattern and luminance reversal, in the first series of experiments the test regions were 64 equal sized patches and thus were not scaled for eccentricity [58]. Within the same publication, with the addition of cortical scaling, signal generation and robustness was enhanced but not to the point of clinical utility. The group concluded that clinical testing with the VEP was not feasible due to the ubiquitous cortical convolutions of the inferior segment of V1.

Despite the conclusions of Baseler et al. mfVEP continued to improve in recording paradigms, eccentricity of visual field tested, signal analysis, minimization of noise and sensitivity and specificity in disease detection. Work by Klistorner and Graham, Hood and others, refined the testing procedures in monocular mfVEP improving on electrode placement[56], electroencephalogram (EEG) scaling[52], fixation targets[59], check size[60] and stimulation type[61,62].

Graham et al, in 2005, reported 97.5% sensitivity for detecting glaucoma in patients with established field loss and 95% for patients with early glaucoma[47]. MfVEP also compared favourably in their study with HVF as demonstrated by a correlation coefficient of r=0.78[47].

The sensitivity of mfVEP, using achromatic high luminance contrast, was significantly improved with the development of a new blue on yellow stimulus, designed to target the non-redundant koniocellular pathways.[48,49] Comparison of the blue on yellow with black and white demonstrated a sensitivity of 100% for eyes with SAP defects whereas black and white had 92.2% sensitivity[48]. Again a strong correlation was calculated between SAP and mfVEP amplitudes (r=0.73). Further research in preperimetric glaucoma patients demonstrated the utility of blue on yellow stimulation when using

amplitude asymmetry analysis when comparing to RNFL asymmetry as measured with OCT[49]. This body of research served to highlight the sensitive nature of asymmetry analysis, correlating functional mfVEP changes to structural RNFL damage which preceded the development of a demonstrable visual field defect.

Signal analysis for mfVEP, as defined by the ISCEV standard, identifies 3 distinct peaks: C1 - positive at 75ms, C2 - negative at 125ms and C3 – positive at 150ms. MfVEP, as used by the Graham and Klistorner research group, stimulus is a pattern onset/offset type which has greater variability in peaks and troughs. The definition of mfVEP the amplitude, for the Graham and Klistorner group, is taken as the difference between the largest positive and negative deflections.

Similarly to mfERG, mfVEP stimulation is driven by pseudo-random binary sequences (PRBS) (m-sequence) so that the presentation at each location is random and independent of other locations. Each binary sequence has a 50% probability of being 1 or 0 at any point of time. In a frame sequence lasting 18 frames, element 1 is represented by two consecutive states: pattern on, lasting two frames of the screen, when the stimulus pattern was displayed, and pattern off, lasting 16 frames, when the whole segment was diffusely illuminated with an intensity of the mean luminance. Element 0 consisted of the pattern-off state for 18 frames. M-sequence is necessary to allow for pseudo-randomness in presentation and for correlation of signals necessary for processing.

3.4.3.2 RECORDING THE MFVEP

Recording of the VEP is through EEG skin contact electrodes, traditionally 1cm above the inion with a reference electrode placed mid forehead. Various mfVEP recording positions have been tried[63] with some success. The research group of Graham and Klistorner uses four gold cup electrodes (Grass, West Warwick, RI) mounted in an occipital cross-electrode holder for bipolar recording. Two electrodes are positioned 4 cm on either side of the inion: one in the midline 2.5 cm above the inion and one 4.5 cm below the inion. Electrical signals are recorded along four channels as the difference between superior and inferior and between left and right, and obliquely between the left and inferior and right and inferior electrodes. A ground electrode is placed on one ear lobe. Cortical responses are amplified 100,000 times and band-pass filtered (1–20 Hz). Uniquely designed software

correlates the responses with the stimulating PRBS and attributes the calculated signals to the respective segments of the visual field. This software scales the responses to the background EEG to reduce the interindividual variability.[52] For every segment, the largest peak-to-trough amplitude of each wave within the interval of 60 to 200 ms is determined for each channel. The wave of maximum amplitude from each segment in the field from the four channels is automatically selected, and the software creates a combined topographic map.[64]

The mfVEP display consists of a cortically scaled dartboard (Figure 1-3) with 56 segments arranged in five concentric rings (1°–2.5°, 2.5°–5°, 5°–10°, 10°–16°, and 16°–24°) and a central fixation target extending up to 0.5°. The stimulus in any segment consists of a 4x4 check pattern, the chromaticity and contrast chosen to suit the testing requirements. Segment size is scaled according to the cortical magnification factor (CMF)[65]. Corresponding to the size of the segments, the size of the individual checks also increases with eccentricity (Figure 1-3). A central fixation target is presented that consists of rotating and slowly changing letters.

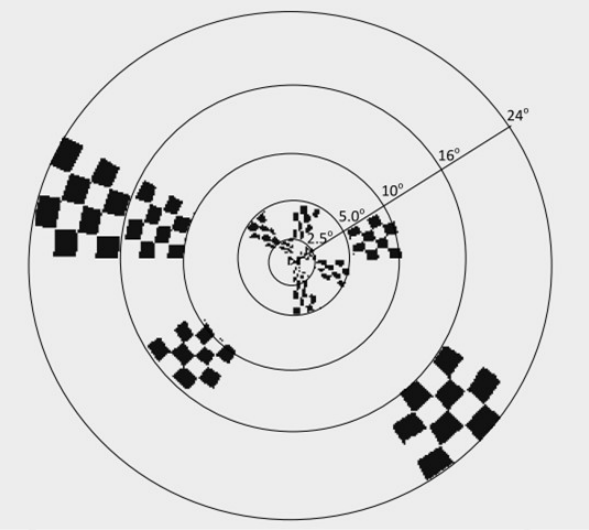

Figure 1-3 - mfVEP stimulus displaying checker-board pattern, cortically scaled with stimulation to 24 degrees of eccentricity

3.4.3.3 Use of Asymmetry Analysis

As mfVEP is subject to wide variations in signal size[66] and in order to obtain improved accuracy when judging whether a signal is normal or abnormally reduced, the use of inter-eye asymmetry is a useful

tool in detecting early glaucoma.[67]. Inter-eye asymmetry is based upon the principle that the cortical signals from each retina should be identical [68] as the site of generation of signal at the striate cortex is almost identical. If there is a significant difference between the two eyes, as based upon asymmetry analysis using an age-matched normals database, there is a high suspicion that the site of the reduced signal is abnormal. Initially it was thought that mfVEP recordings would have to rely entirely on asymmetry analysis due to the wide variation of amplitudes[58]. Research into detection of glaucoma [64] showed that signal changes alone could be enough to distinguish abnormal areas. Asymmetry analysis still remains a mainstay of mfVEP testing in addition to monocular amplitude and latency analysis.

Generalised use of asymmetry analysis[69] has been verified as sensitive to early glaucomatous defects. In studies performed by Graham et al. there were significantly higher relative asymmetry coefficient (RAC) values between eyes of subjects with glaucoma and glaucoma suspects when compared to a group of normals. The symmetry of normal RACs was such that it was found to be a very sensitive technique for picking up subtle differences in visual fields. These findings were also shown by Hood et al[68]. Some deficiencies of the technique, which are true for dichoptic recordings, were identified in both papers. These include that it would be difficult to compare asymmetry if the corresponding retinal locations in each eye were equally affected; if there is post chiasmal damage on either side; and, any other functional or structural disease the interfering with the normal ganglion cell functioning.

Utilizing asymmetry in preperimetric glaucoma detection, Arvind et al[49] showed the effectiveness of using interocular asymmetry to more accurately identify changes with blue on yellow monocular mfVEP. Such a finding indicates the sensitivity of interocular asymmetry to diagnose glaucoma despite there being no demonstrable visual field defects (i.e. pre-perimetric disease).

3.4.3.4 DEVELOPMENT OF DICHOPTIC MFVEP

Dichoptic visually evoked potentials were first recorded by Lennerstrand[70] in 1978 using a polaroid checker board pattern viewed through rotating polaroid discs. Lennerstrand et al reported a 50% or greater reduction in amplitude signal size owing to the dioptric stimulation conditions. In these experiments patients with binocular vision abnormalities, such as abnormal stereo vision, were shown to have less of a reduction in the VEP amplitude for the dominant eye. This continued on a spectrum to those patients who were stereoblind, their dominant eye having a similar amplitude to their monocular recordings. This observation was important as it provided the basis for a series of experiments and observations detailing the cortical nature of interocular suppression.

At the same time as the above experiments, Lennerstrand investigated dioptic stimulation using red and blue grating and checker board patterns[71]. He demonstrated one of the fundamental features of interocular suppression, namely that it was minimized with patterns that were disparate enough to produce binocular rivalry and maximized when patterns were identical in shape. Lennerstrand noted that these findings supported "spatial frequency and orientation selective channels in the human visual system"[71]. This is of fundamental importance as the dichoptic mfVEP stimulation conditions resemble a situation where the patterns are identical in shape for a given retinotopic location and thus are primed to cause maximum interocular suppression.

In 2005 James et al demonstrated the feasibility of recording dichoptic mfVEP using liquid crystal polarizing shutters[62]. However this did not represent true dichoptic recording technique as it alternatively stimulated the eyes rather than having true dichoptic recording conditions which dictate that the eyes are both presented stimuli simultaneously. Further to this luminance was reduced substantially although the authors report that the amplitudes recorded were similar to other labs[62]. James et al did highlight some of the benefits of dichoptic recording which included decreased intereye variability and reduced overall recording time as well as the benefit of temporal sparseness on recording amplitudes. These results were supported by the work of Maddess et al. in examining the effect of contrast on amplitude response using temporally sparse stimuli.[72]

Arvind et al built on the work of James et al. by demonstrating the viability of dichoptic mfVEP using virtual reality (VR) goggles[73]. Using pseudo random binary sequences (PRBS), virtual reality goggle screens presented dichoptically, but temporally separated, checkerboard stimuli. PRBS have been demonstrated by Sato et al[74] to enable stimulus presentation and accurate cross-correlation in testing conventional dichoptic VEPs. Furthermore the same group had shown that the amplitude size in dichoptic presentation was luminance dependent and decreasing luminance in one eye caused a decrease amplitude in that eye and an increased amplitude in the contralateral eye[74]. In experiments by Arvind et al. the temporal separation was shown to be important in the stimulus design as it directly affected the degree of interocular suppression and thus the size of recorded cortical amplitudes[73]. A slower rate of stimulus presentation, thus greater temporal separation, was chosen by this group so as to guarantee a suitable stimulus amplitude size and therefore adequate signal to noise ratio. Design limitations with the VR goggles used by Arvind et al. meant that the clinical applications were restricted. These limitations included lack of pupil monitoring which limited the ability to ensure fixation throughout testing. The field of visual stimulation was limited to 16 degrees of eccentricity, owing to the optics of the goggles[75].

Despite the above problems, Arvind et al did demonstrate that the dichoptic mfVEP measured with VR goggles was a more sensitive method, than monocular alone, for detection of glaucoma[75]. They hypothesized that the simultaneous recording conditions afforded tighter asymmetry in the normals database and thus a more sensitive statistical test of abnormal asymmetry. In addition they postulated that having a unilateral defect, with the addition of interocular suppression, could further suppress the defect and thus further decrease amplitude in the affected segment and subsequently increase asymmetry[76].

Graham et al. and Arvind further postulated that the phenomenon of interocular suppression could aid in the earlier detection of glaucoma using asymmetry analysis[76]. As interocular suppression involves the interaction of retinotopically corresponding binocular neurons at layer 4 of V1 and is related to the temporal closeness of mfVEP stimuli – the amplitude of the resulting signal as recorded for each eye is a function of the size of each binocular signal and the closeness in timing. If

the signals are of equal magnitude it follows that they will be equally reduced. However if one segment is affected by glaucoma the corresponding segment could be comparatively increased in amplitude owing to the gain/suppression characteristics of the binocular neuron. Upon this basis was the theory that there could be an increase in asymmetry as the glaucomatous signal was further reduced by IS and the non-affected segment was “released”.

Asymmetry analysis can be enhanced through the use of dichoptic recording conditions, through having the eyes recorded under the same psychophysical conditions and through potentially enhancing the asymmetry between a diseased segments and its correspondingly normal segment in each eye possibly through interocular suppression[76]. The first aspect of the nature of increased asymmetry in dichoptic recording addresses one the fundamental difficulties with visual field testing, namely the differing conditions that each eye is tested under. By testing both eyes simultaneously this is somewhat addressed. The second aspect of the postulated benefits of dichoptic mfVEP recording, the interplay between corresponding segments of the two eyes, through interocular suppression, provides an important stepping stone for investigating the mechanisms for maximizing asymmetry in dichoptic testing and for selecting a stimulus which enhances the strengths of dichoptic mfVEP.

Whilst the above research has sought to elucidate a better understanding of the mechanisms underlying interocular suppression it is still a poorly understood area especially as monocular inhibitory mechanisms play an unquantified role in interocular suppression.

3.4.4 USES OF MFVEP

MfVEP is not routinely used in the clinical assessment of glaucoma, despite having good evidence that it is as effective as standard automated perimetry (SAP)[77] in detecting glaucomatous visual field defects. The inter-test variability is comparatively better than SAP[78] and it is fundamentally an objective rather than a subjective test. However the length of testing, need for expert interpretation and the skill required of the operator to perform quality testing limit its widespread use. In its current form, mfVEP, despite its limitations can still provide an adjunct to assessing patients seen to

have structural changes but having normal SAP testing. This is especially true for dichoptic mfVEP as the increase in detection reported by Arvind et al[75] is useful in highlighting early, unilateral defects.

4 STRUCTURAL MEASURES OF THE OPTIC NERVE IN GLAUCOMA

The assessment of the optic nerve is of key importance in the diagnosis and monitoring of glaucoma. Physician assessment of the optic nerve and RNFL is the cornerstone of good glaucoma management, more recently it has been aided by the advent of sophisticated imaging devices which can enhance the ability of the physician to slow down progression due to glaucomatous optic neuropathy. These devices assess the structure of the posterior segment using confocal optics and laser inferometry technologies.

It should be noted that the gold standard of glaucoma diagnosis is double blinded physician assessment using stereoscopic photos of the optic nerve. This assessment is fundamental in detecting glaucomatous optic neuropathy in conjunction with current structural and functional tests.

4.1 SCANNING LASER OPHTHALMOSCOPY (SLO)

Scanning laser ophthalmoscopy (SLO) is based upon confocal optics principles utilising a 670nm diode laser to scan the optic nerve head at set intervals to obtain slices for three dimensional reconstruction[8]. Slices are taken from lamina cribrosa to the anterior surface of the retina centred around the optic nerve head. The operator receives information regarding multiple indices of the nerve head, the most important for glaucoma being the retinal nerve fibre layer thickness.

The most commonly used SLO in clinical practice is the Heidelberg Retinal Tomograph (HRT) III, which produces static and longitudinal analysis of the height of the retinal nerve fibre for glaucoma diagnosis and progression. The slices are taken in a 15^{o} (difference between confocal laser beams) scan diameter with 3 scans averaged for mean topography.

4.2 SPECTRAL DOMAIN OPTICAL COHERENCE TOMOGRAPHY (SD-OCT)

Optical coherence tomography (OCT) utilises a Michelson inferometer which measures the time taken for a beam of light to be reflected versus a reference beam [79] , this indicates the degree of

reflectivity of a layer in the eye thus its optical characteristics. Using similar principles to ultrasound, OCT incorporates an A-scan to provide depth reference and B-scan to provide morphology. The combination of the 2 scans allows a three dimensional reconstruction of the area in question from retina to optic nerve.

Spectral domain optical coherence tomography (SD-OCT) is the latest major development in OCT technology advancement. Spectral domain refers the spectral separation of the light detectors which are analysed with Fourier transformation to provide greater clarity and resolution of OCT images.

5 STRUCTURE AND FUNCTION IN GLAUCOMA

The relationship between the structure of the retinal nerve fibre layer and the visual function of the retina it subserves is fundamental to glaucoma diagnosis and management. While extensive research has been performed into structure-function correlations, there is still debate over the nature of the relationship and the reasons for the many inconsistencies[80].

5.1 BACKGROUND

Glaucomatous optic neuropathy is characterised by a pathognomonic pattern of optic disc changes matched with visual field loss (Figure 1-4).

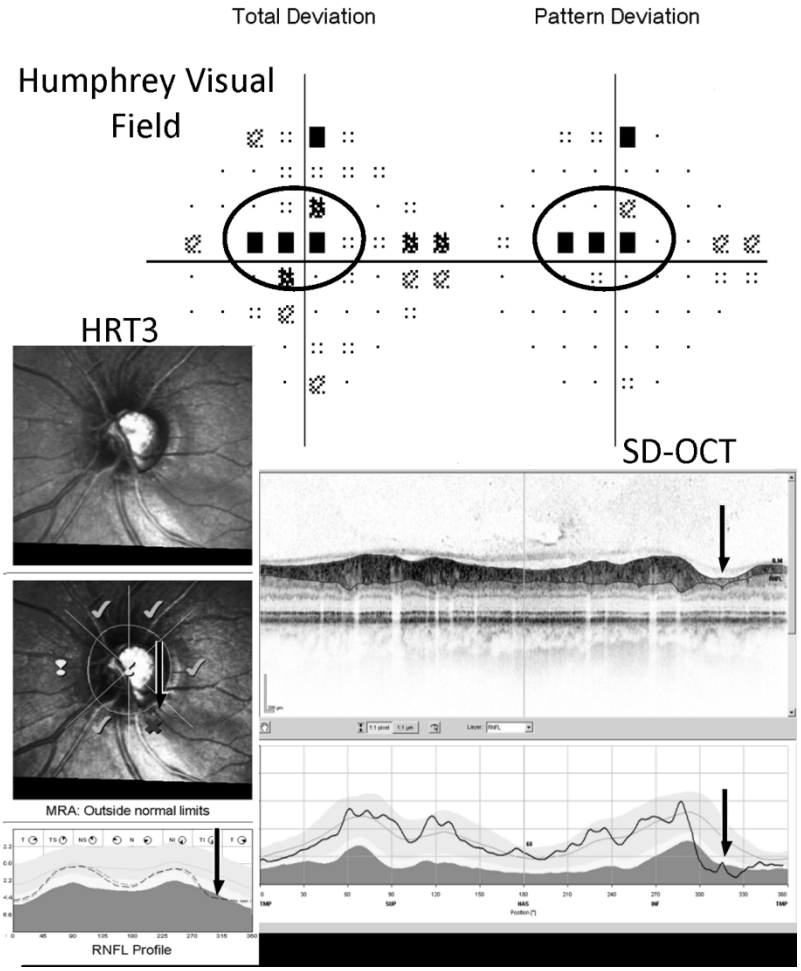

Figure 1-4 - Typical glaucomatous field defect on HVF with corresponding RNFL loss on HRT and SD-OCT (arrow)

The typical field loss in a high tension POAG patient is an arcuate visual field loss coupled with a corresponding notched or thinned retinal nerve fibre layer. These changes are often temporally separate, indeed Drance [81] and colleagues found that structural change (optic disc changes) preceded functional change. Other studies have shed more light on the relationship between structure and function [15,82] but finding that the relationships do not demonstrate the high correlations (between structure and function) as expected, indeed there is inconsistency between different structural measurement devices and, inter-alia, functional measurement devices as well.[83-85]

A number of factors may contribute to this – the substantial variation in normal RNFL thicknesses, the disease processes involved in the pathogenesis of glaucoma which include many factors that affect the structure-function relationship[86,87], and the limitations of the instruments used to measure structural and functional status[88-90].

Whilst the above factors can cloud the relationship between structural and functional changes, the importance of characterising this relationship cannot be understated, especially with respect to current and emerging technologies. As structure often precedes function, characterising the earliest structural changes can lead to early glaucoma diagnosis and treatment[16,91]. Similarly, characterising subtle functional changes, those that are recognised as being part of a glaucomatous disease spectrum, can also provide an avenue into earlier detection. As early detection provides the best possible chance to prevent irreversible visual loss, the understanding of the structure-function relationship underpins optimum glaucoma management.

5.2 STRUCTURE/FUNCTION MODELS IN GLAUCOMA

As research into glaucoma has progressed, so has the appreciation of the complicated nature between structural change and functional correlations. In order to explain these changes a number of groups have developed models, largely based upon HVF testing, to relate structure to function. These include those by Garway-Heath[92], Negi[93] and others[94].

5.2.1 HUMPHREY VISUAL FIELD TO RNFL MODELS

Garway-Heath et al[92] produced a structure function map that related sectors of RNFL to visual field areas based upon observational data of glaucomatous nerves and HVF testing using 98,821 visual fields from a Moorfields database(Figure 1-5). Using Pearson's correlation coefficients, the team calculated the most likely RNFL sectoral change that was associated with the HVF functional change.

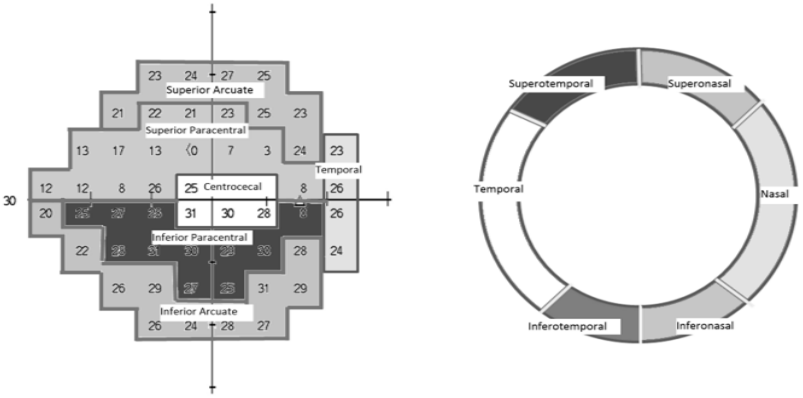

Figure 1-5 - Structure function map relating HVF locations (left) to circumpapillary RNFL locations (right)

Whilst the model does have flaws, it does provide a plausible map with which to relate structure to function. Other models by Gardiner et al[95], using ONH tomography and standard automated perimetry(SAP), and Hood[96,97] using OCT RNFL and SAP producing a linear relationship between RNFL and sensitivity, have added further information to the modelling of structure and function. Efforts have been made predict visual function from structure, a recent example being the Bayesian framework based model constructed by Zhu et al[98]. It must be recognised that there are a number of sources of error which obscure the structure-function relationship which were identified by Hood et al[99] largely arising from structural measurement errors including epiretinal membranes, blood vessels included in the optic nerve head scan, oedema and individual variations in field to disc mapping. Owing to the wide variation in optic nerve morphology, the severity of disease was found to be an important moderator in the structure function relationship[100], adding to the above factors it highlights that the measurement of visual fields is a subjective process with intrinsic variability. Work has been performed examining the mathematical relationship between visual field sensitivity measured in the logarithmic scale of decibels and the RNFL parameters which are inherently linear. Hood[99] and others[96,101] have suggested that the relationship is linear when the decibel measurements are anti-logged and that this should be the paradigm in order to model glaucomatous changes with greater accuracy.

The above confounders emphasise the challenges faced in obtained detailed understanding of glaucoma pathogenesis.

5.2.2 MFVEP VISUAL FIELD TO HVF MODELS

Significantly less research has been undertaken in the field of mfVEP structure function relationships. A recently devised model is shown in Figure 1-6, relating HVF to mfVEP with OCT is represented in four quadrants. The model was devised by Hood[102] to relate HVF, OCT and mfVEP. The model was subsequently utilised by Laron[103] to study the effectiveness of mfVEP over HVF for detecting visual field damage caused by multiple sclerosis. Balachandran[104] applied the model below in his work on glaucoma investigating the relationship between objective structural testing in the form of HRT and functional testing with mfVEP.

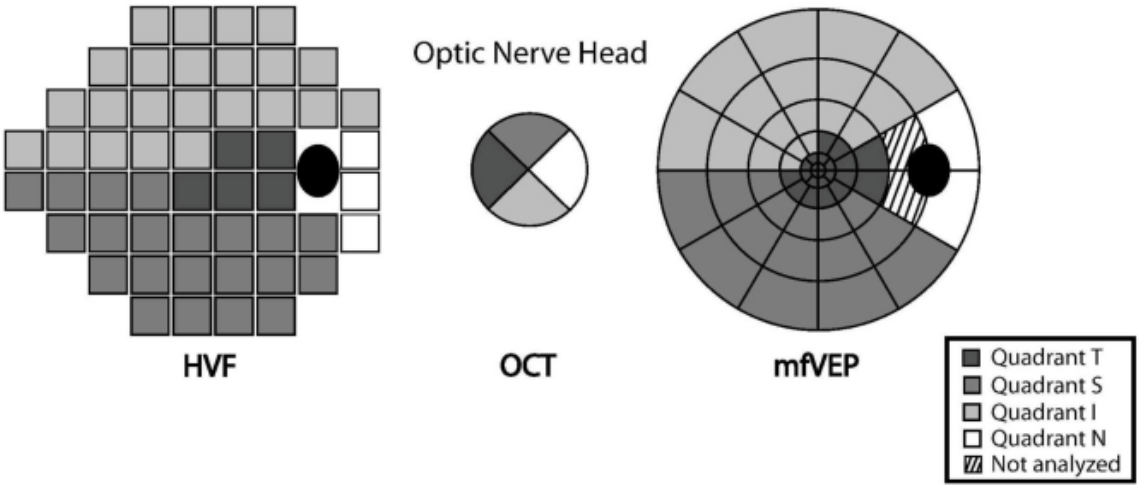

Figure 1-6 - Structure-function model devised by Laron et al relating HVF, OCT and mfVEP

5.3 Unanswered questions in structure/function research

Whilst there has been significant research into structure and function relationships, there are still a number of unexplored areas relating to the accuracy of newer structural testing modalities (namely spectral domain OCT) and the relationships that exist for mfVEP and HVF with these structural testing modalities. Certainly there has been no work into the structure function correlations of dichoptic mfVEP as it relates to HVF and OCT.

6 Neural pathways and visual processing

Understanding the neural pathways of the human visual system underpins the appreciation of the structure-function relationship in glaucoma. Identification of selective visual pathways has led to greater understanding of how and why glaucoma progresses. The modulation of binocular input at the level of the occipital cortex and its use in glaucoma detection is important for advancing the understanding of glaucoma as a whole.

Converting light into electrical nervous impulses to convey information to the brain is the primary function of the human visual system. From the photoreceptor layer in the outer retina, light is converted from photons to neurochemical impulses by phototransduction. The cascade of reactions from photoreceptor to retinal ganglion cell, to lateral geniculate nucleus and finally occipital lobe is

the fundamental pathway subserving the acquisition of visual information. The ganglion cells are the crucial link between retina and cortex but only provide basic information in need of further processing by the extrastriate areas mostly in the temporal and parietal lobes.

6.1 RETINAL GANGLION CELLS OF THE VISUAL PROCESSING SYSTEM

Visual information from optic nerve to occipital cortex is processed along three major retino-geniculo-cortical pathways: parvocellular, magnocellular and koniocellular[25]. The parvocellular pathway, which constitutes about 80% of retinal ganglion cells is responsible for processing of high contrast, low temporal and high spatial frequency information while the magnocellular pathway conveys information about low contrast and low spatial frequency achromatic images and has higher temporal resolution[105,106] . The distribution of parvocellular and magnocellular neurons across retina is also different. Whilst the central visual field is dominated by P-cell, the relative number of magnocellular neurons increases with retinal eccentricity by the factor of ten[107]. The third, koniocellular pathway, conveys blue-on/yellow-off colour signals to the brain.

6.1.1 MAGNOCELLULAR RETINAL GANGLION CELLS

Magnocellular RGCs (parasol cells) are characterized by the large neurons for which they are named. Magnocellular cells have properties which enhance the peripheral retina's ability to pick up motion and low contrast information[44]. They respond to luminance contrast, high temporal and low spatial frequency stimuli. Magnocellular cells have a centre surround receptive field organisation, a transient response to stimuli and a high axon speed (2m/s)[44]. Magnocellular cells project to layer 4Ca of the striate cortex. These properties are suited to high speed, low contrast stimuli mfVEP stimuli. Owing to the paucity of magnocellular RGCs compared to parvocellular cells, they are potential targets as they are considered part of the non-redundant population of RGCs in the retina.

6.1.2 PARVOCELLULAR RETINAL GANGLION CELLS

Parvocellular RGCs (midget cells) are characterised by small, centrally concentrated cells with centre/surround receptive field organisation.[44] They have a small dendritic field size, are wavelength selective (i.e. have colour opponent receptive fields) and preferentially respond to high spatial frequency, low contrast sensitivity and low temporal frequency stimuli. Their response is sustained

and they have a medium axon speed of 4m/c[44] The parvocellular RGCs project to layer 4Cb of the striate cortex with limited projections to layer 6 and 4A[25].

6.1.3 KONIOCELLULAR CELLS

The smallest and least studied RGCs are the koniocellular population, having a variable receptive field organisation, large dendritic field size and receiving stimulation from blue wavelengths[44]. The koniocellular cells have a low preferred spatial frequency, intermediate contrast sensitivity and intermediate temporal frequency. They also exhibit a mixture of sustained and transient responses to stimuli with a low axon conduction speed at > 5msec. In short, the koniocellular cells fall in between the magno and parvo cellular RGCs in terms of most characteristics. They project to layer IIIb cytochrome oxidase blobs in the striate cortex. Similar to magnocellular cells, owing to the smaller population, koniocellular cells are also considered to be part of a non-redundant group of RGCs.

6.1.4 INTRINSICALLY PHOTOSENSITIVE RETINAL GANGLION CELLS (IP- RGCS)

Recently there has been the discovery [44] pointing to a fourth population of RGCs, the intrinsically photosensitive RGCs, making up about 3% of the total RGCs these cells are responsible for the moderation of circadian rhythm, pupil size and sleep-wake cycle conveying information to the pineal gland[44]. The cells branch from the optic nerve to the mid brain before the LGN, the cells are stimulated by light independent of photoreceptors and are the only RGCs to contain melanopsin.

6.2 VISUAL PROCESSING IN THE OCCIPITAL CORTEX

The occipital cortex is divided into 6 layers, layers I to IVB outputting to the extrastriate areas, layer IVCα receiving magnocellular input, layer IVCβ parvocellular and layer IVA koniocellular input[44]. Layer V and layer VI output to subcortical areas such as the midbrain and thalamus with some feedback to LGN.

Information conveyed by the retinal ganglion cells arrives at the occipital cortex (V1, Brodmann area 17) and feeds into layer IVC where the RGC input remains segregated into right and left eyes, the segregation representing the ocular dominance columns of V1[44] . These columns are important for balancing input from left and right eyes and for facilitating single binocular vision. The importance of

single binocular vision is fundamental to stereopsis and the balancing of signals from competing visual inputs. There are a multitude of other processes that take place in the V1 which enable useful signals to be sent to and from V1.

Processing above the level of the occipital cortex is divided into two streams – ventral and dorsal. The ventral stream is primarily concerned with processing of the "what" information i.e. object recognition through orientation, colour sensitivity and binocular disparity[44] through a pathway extending from V2to V4 and then the temporal lobe. The dorsal stream is oriented to the "where" information i.e. motion, direction and disparity sensitivity [44] through a pathway extending from V2 to middle temporal area (MT) and V3 to the parietal lobe. These pathways are fundamental to understanding the reasons for higher-order processing abnormalities and their effect on interocular suppression.

6.3 INTEROCULAR(DICHOPTIC) SUPPRESSION

Interocular suppression is a vital phenomenon that allows for cortical adaptation to changing visual stimuli.[108] Efficient neural processing of images is facilitated if images are single and coherent. The processing of dichoptic images and the role of interocular suppression has been utilised previously to substantially improve glaucoma detection[75].

Lennestrand[70] , in experiments using visual evoked recordings (VER) and dioptic stimulation, showed suppression was largest when patterns were the same shape – this served to separate interocular suppression from the process of binocular rivalry, as rivalry was predominantly present with oppositely oriented orthogonal gratings.

While the origins of interocular suppression are not universally agreed, Sengpiel [109] stipulated that the adjacent ocular dominance columns in layer 4C of V1 likely account for the reduction of signal size observed with the phenomenon of interocular suppression. Sengpiel had previously written[108] that interocular suppression took place at the level of the binocular neurons at the primary visual cortex and further supplemented this research with studies on feline visual systems demonstrating that interocular suppression was strongest at the central field. As he showed that the spatial pattern

of interocular suppression closely matched the cortical representation of the stimulus he stipulated that interocular suppression was related to the functional architecture of V1. This suppression took place between "neighbouring cortical columns of opposite ocular dominance"[109].

Callaway reports from Macaque monkeys[25] that blobs located above the ocular dominance columns in V1 possessed neurons with greater contrast sensitivity and selectivity for lower spatial frequencies and that the blobs' functions in layer 2 and 3 of V1 were indicative of the properties of their functional location i.e. ocular dominance columns. This could indicate that ocular dominance columns were most affected by contrast and would be selective for lower spatial frequencies. This is turn could indicate that, as ocular dominance columns were responsible for dichoptic suppression, that dichoptic suppression was affected by contrast and spatial frequency.

In further developing understanding about dichoptic suppression, Arvind et al demonstrated that with closeness in timing of presentation of a dichoptic stimulus increased levels of dichoptic suppression occurred [73]. Experiments were performed using dichoptic mfVEP virtual reality goggles on a number of normal volunteers. They found that increasing the separation of presentation of a checkerboard stimulus decreased the effects of interocular suppression, thus increasing recording amplitudes. At a presentation speed of 1.66 times/s there was minimal interocular suppression, at around 5%, this was deemed the ideal stimulus speed so that sufficient amplitude generation could be achieved for clinical applications. As part of the experiments they demonstrated there was similar suppression between orthogonal and checkerboard stimuli, this finding supports the presence of dichoptic suppression as orthogonally oriented gratings don't appear to have an effect on dichoptic suppression, as shown by Lennestrand[71].

Baker et al. demonstrated the separation of two paths in cross orientation masking that preceded the pathway to binocular summation[110]. The research demonstrated the presence of an ipsiocular pathway that was "spatially broadband, immune to contrast adaptation and has a suppressive weight that tends to decrease with stimulus duration"[110]. The second pathway appeared to be" interocular in nature which was spatially tuned, desensitizes with contrast adaptation and has a suppressive

weight that increases with stimulus duration"[110]. Based upon their findings they concluded the ipsiocular effect occurs at the Lateral geniculate nucleus (LGN) or retina and the interocular effect at the visual cortex. As both these pathways were part of cross orientation suppression, they could also play a significant part in interocular suppression. Keeping this in mind, the nature of the interocular suppression path having a "suppressive weight that increase with stimulus duration"[110] may refer to the temporal characteristics of dichoptic suppression and thus the dependence of DS on temporal separation of stimuli. Conversely Messe[111] found that cross orientation suppression (XOS) in monocular form is space/time scale dependent but XOS in its interocular form is scale independent. This could point towards different mechanisms underlying dichoptic suppression of mfVEP amplitudes and dichoptic suppression with XOS.

6.4 TARGETING OF NON-REDUNDANT PATHWAYS

Technologies such as short wavelength automated perimetry and frequency doubling perimetry both aim to target populations of RGCs that are affected earlier in the pathogenesis of glaucoma to aid in early diagnosis before demonstrable white on white defects appear. As mentioned before these systems target sub-populations with smaller overall representation in the RGC total population, namely the koniocellular and magnocellular cells. Research into these techniques reveals both physiological reasons and clinical research which points to their success. [112-115]

The above principles have been utilised in mfVEP research [48,49] in order to target non-redundant pathways in the hope of identifying the presence of glaucoma at an early stage. It follows from the above research findings that there is some benefit to altering stimulus characteristics to tailor to the sub-type of ganglion cell desired. Such stimulus characteristics take the form of colour, contrast and speed of presentation which can be adjusted to suit the RGC of interest.

Whilst the above thesis appears attractive it does over-simplify the complexity of the magnocellular, koniocellular and parvocellular RGC functions. The study of these cells is constantly evolving, indeed recent work demonstrated that there is increased sensitivity of all cells as eccentricity from the fovea is increased[116]. Hence the separation of the sub-populations is a complicated and should be

approached with care to avoid false assumptions, especially as redundancy as a concept in natural design is increasingly falling out of favour.

7 AIMS

This thesis was designed to answer several questions regarding the use of the dichoptic mfVEP in the detection of glaucoma, and its comparison with structural and other functional changes.

7.1 IS THERE AN INCREASE IN ASYMMETRY USING DICHOPTIC MFVEP VERSUS MONOCULAR?

Initial studies of dichoptic mfVEP stimulation showed there could be an increase in asymmetry when the technique was used versus monocular [75]. The mechanism was not fully elucidated but was suggested to come from a release of inter-ocular suppression.[76].

7.2 HOW IS INTEROCULAR SUPPRESSION RELATED TO ECCENTRICITY?

MfVEP dichoptic research has shown the benefit of dichoptic stimulation and the possible effects of interocular suppression/release. The modifiers of interocular suppression such as contrast levels, chromaticity and speed of presentation have not been studied and underlie the choice of the optimum stimulus for glaucoma detection.

7.3 WHAT ARE THE CHARACTERISTICS OF A NON-REDUNDANT PATHWAY SPECIFIC MFVEP STIMULUS?

Targeting of non-redundant pathways is a useful tool in glaucoma detection, the physiological parameters of RGC response underlie these tools. Using chromaticity (koniocellular), low-contrast (koniocellular and magnocellular) and higher speed of presentation (magnocellular) represent targeted modifications of mfVEP stimuli that could lead to earlier glaucoma detection.

7.4 WHAT IS THE MOST SENSITIVE STIMULUS FOR DICHOPTIC MFVEP GLAUCOMA DETECTION?

Combining the stimulus characteristics (speed of presentation/contrast/colour) and the modification of interocular suppression (using the above 3 characteristics) is need to elucidate the stimulus that maximises the benefits of dichoptic stimulation.

7.5 IS MFVEP DICHOPTIC STIMULATION MORE SENSITIVE THAN MONOCULAR? WHAT IS THE ROLE OF INTEROCULAR SUPPRESSION IN TARGETED STIMULI?

Arvind et al. addressed this question with their work on dichoptic mfVEP[75]. However the change in device design, from virtual reality goggles to frame-mounted LCD screens necessitated re-evaluation. Although the fundamental processes remain the same, the field of stimulation (16 degrees for goggles, 24 degrees for LCD screens), the different optics of the two devices and the altered ergonomics meant that this question needed to be addressed.

7.6 How do contemporary retinal imaging devices compare and how does disc imaging relate to mfVEP findings?

MfVEP is a functional imaging tool and without structural correlation, remains only part of the detection of glaucoma in a structure-function paradigm. The correlations between imaging devices and functional changes in glaucoma are fundamental to the detection of glaucoma and provide an avenue for assessment of the accuracy of current technologies.

8 Goals of this project

This project sought principally to assess the role of dichoptic suppression, as a phenomenon underlying dichoptic mfVEP, in the detection of early glaucoma. In order to understand the effects of dichoptic suppression, the parameters which drive DS need to be understood and defined. The role of non-redundant pathways and DS also needs to be delineated to assess the most appropriate stimulus for glaucoma detection. As the above relationships rely heavily on the structural and functional connections observed in glaucoma, further development of structural and functional assessment needs to be obtained. Finally, combining work on structure and function with mfVEP and DS, a clinical study investigating the efficacy of a novel dichoptic mfVEP should provide guidance on future directions in the detection of glaucomatous optic neuropathy.

Chapter 2 MATERIALS AND METHODS

Summary

This chapter describes the technologies used in this thesis which assess structural and functional changes in glaucoma. Methods of statistical analysis are detailed and the reasons for utilizing them. Recruitment of subjects for the trials and the studies in which they are involved are explained.

1 MATERIALS AND METHODS

The aim of this thesis is to further understand the nature of structural and functional relationships as they pertain to normal and glaucomatous eyes. These relationships guide the experimental design and analysis in identifying potential mechanisms for earlier detection of glaucomatous field loss.

This chapter outlines the materials and methods used throughout the thesis. Generally the functional testing was performed using Humphrey Visual Field (HVF) testing or multifocal Visually Evoked Potentials (mfVEPs) either monocularly or dichoptically and the structural testing was performed using Spectral Domain Optical Coherence Tomography (SD-OCT) or Heidelberg Retinal Tomography (HRT). Each individual chapter has outlines of materials and methods which generally parallel those described in this chapter.

1.1 SUBJECT RECRUITMENT

1.1.1 NORMAL SUBJECTS

Subjects for inclusion in the normal cohort (chapters 3, 4 and 6) were recruited through either the Macquarie University staff and student population through email contact or from 1 of 2 Sydney based glaucoma clinics through advertisements placed in these clinics. All subjects underwent basic ophthalmological assessment to ensure suitability for experimental inclusion which included visual acuity testing, stereoacuity testing (Titmus fly) intraocular pressure measurement and optic disc examination by the author or senior ophthalmologists. For normal patients to be included they had to have best-corrected visual acuity of 6/9 or better in both eyes, anisometropia (if any) less than 1.5 D, stereoacuity of 40 seconds of arc on Titmus fly stereogram, and normal ophthalmic examination results.

1.1.2 GLAUCOMA SUBJECTS

Glaucoma subjects were recruited via advertisements placed at 2 Sydney-based glaucoma clinics and circulated email referral (Chapters 5, 6, 7 and 8). All glaucoma patients had comprehensive medical and ophthalmic histories and examination recorded including Goldman applanation tonometry, fundoscopy, slit lamp examination and gonioscopy. The diagnosis of glaucoma was made by a

glaucoma specialist prior to the study based upon optic disc appearance with focal thinning of the neuroretinal rim matching visual field loss consistent with glaucoma including arcuate patterns or clusters, respecting the horizontal meridian on HVF. Each patient had the minimum requirements of stereopsis >100 seconds of arc and visual acuity >6/18 in the worse eye. Patients also had to be free of other ocular diseases affecting visual function besides glaucoma namely – diabetic retinopathy, macular degeneration, vitreous opacity and visually significant cataract.

1.1.3 HUMAN ETHICS

Human ethics approval was granted initially through University of Sydney (external HREC Approval number: 05-2009/11594) and subsequently inter-alia with Macquarie University (reference number: HE25SEP2009-D00139) under the title: "*Dichopticly measured Multifocal Visually Evoked Potentials in Normal and Diseased states*".

All human experimental work was conducted under the tenets of the Helsinki agreement with written and verbal informed consent. All participation was voluntary and no coercion or incentives were offered.

1.2 DATA ANALYSIS

1.2.1 STATISTICAL ANALYSIS

Statistical analysis was performed using SPSS (versions 17 and 19) and Graphpad Prism (version 5 and 6). A significance level of $p=0.05$ was set for all statistical testing with $p<0.05$ considered significant. T-testing was the predominant analysis tool used for statistical significance testing but ANOVA was used where appropriate as well as logarithmic and linear regression analyses. When analysing data, one standard deviation was used to provide a measure of the range of variability.

For chapters 7 and 8 correlation coefficients in the form of Spearman's Rho (r_s) were used to assess the relationship between structural and functional measures. For comparative purposes only, strong correlation was defined as $r_s = 0.7\text{-}1$, moderate as $r_s = 0.4\text{-}0.7$ and weak as $r_s < 0.4$.

As there is inherent symmetry between eyes[117] we used only one eye per patient in our correlation analyse so as to avoid spurious correlations.

1.2.2 ASYMMETRY ANALYSIS

As the genesis of this thesis was the research that dichoptic mfVEP enhances asymmetry between eyes in early glaucoma, analysis of asymmetry and dichoptic suppression was integral to quantifying and understanding whether this asymmetry is real and clinically relevant. We used a number of formulae to quantify these terms:

1) Relative asymmetry coefficient (RAC) which quantifies the difference in amplitude between each eye (a negative RAC meaning left amplitude is larger, a positive RAC meaning right amplitude is large) (Equation 2-1).

$$\frac{amplitude_{right\ eye} - amplitde_{left\ eye}}{amplitude_{right\ eye} + amplitde_{left\ eye}}$$

Equation 2-1 - Formula for calculating asymmetry using Relative Asymmetry Coefficient (RAC)

2) Dichoptic (interocular) suppression which quantifies the degree of suppression when changing from monocular to dichoptic testing conditions (Equation 2-2).

$$\frac{Am - Ab}{Am} x100\%$$

Equation 2-2 - Dichoptic (interocular) suppression, Am = monocular amplitude, Ab = dichoptic amplitude in uV for an individual segment or sector.

1.2.3 STRUCTURAL AND FUNCTIONAL ANALYSIS

Analysis of the relationship between structure and function is fundamental to this thesis and is integral to understanding how these technologies work in mapping glaucomatous damage. The

interplay of structure, which is essentially the retinal location as judged by co-ordinates of eccentricity and relation to RNFL arcuate bundles, and function, which is the measurement of the function of these retinal locations, requires structure-function maps to aid analyses. These are detailed below.

1.2.3.1 HVF AND RNFL

The structure-function map of Garway-Heath[118] was used to relate sectors of the RNFL to the Humphrey visual field output(Figure 2-1).

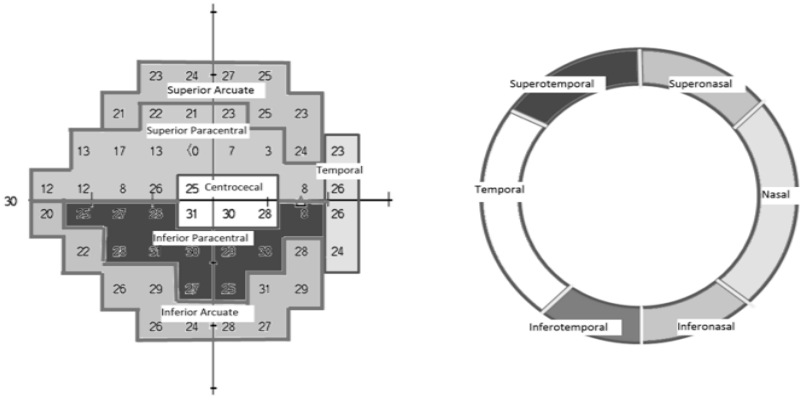

Figure 2-1 - Structure-function relationship used for the present study based upon the map derived by Garway-Heath et al

1.2.3.2 MFVEP AND RNFL

For mfVEP structure/function analysis the map below was used to average the amplitudes for each segment creating 4 averaged amplitudes for each eye as previously used in other papers[46,104].

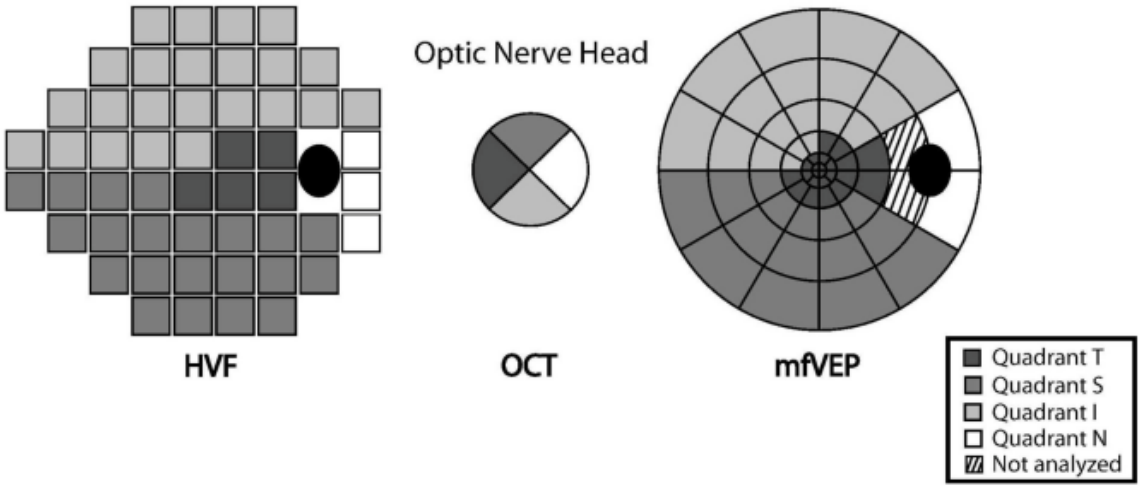

Figure 2-2 - MfVEP structure function map based on the work of Laron and Hood.

The above map (Figure 2-2) is sourced from Laron et al.'s [103]study examining patients with multiple sclerosis and is based upon work by Hood et al[102]

1.3 FUNCTIONAL TESTING

1.3.1 DESIGN AND TESTING OF NOVEL DICHOPTIC MFVEP

As this thesis used an untested and novel design of the dichoptic mfVEP, there was a need for trial and verification of the setup. The design was the outcome of discussion with stakeholders involved in mfVEP research, namely Professor Graham, Associate Professor Klistorner and Dr Arvind.

In designing the current dichoptic mfVEP setup several design considerations had to be addressed in order to overcome the difficulties of the previous dichoptic mfVEP recording device, the Virtual Reality (VR) goggle setup. The VR goggles were the first published mfVEP system that enabled true dichoptic recording without the need for polarizing shutters or alternating displays [73] . Whilst the VR goggles enabled true dichoptic recording, stimulated to eccentricity of 16 degrees, were light and portable and demonstrated excellent reproducibility and sensitivity in glaucoma detection[75] there were however several problems which prevented the VR goggles from proceeding to widespread clinical use. The first of these was the difficulty in pupil monitoring which is essential in binocular recording conditions as the problems with binocular vision such as microtropia and latent strabismus may only manifest during recording conditions and therefore affect the results. Pupil monitoring, in the goggles, was addressed using small patient oriented cameras but difficulty with luminance in visualizing the pupils meant pupil monitoring was not feasible. The second limitation of the design was the limited degree of stimulation, at 16 degrees of eccentricity this somewhat limited the scope of the setup to detect peripheral glaucomatous defects. In designing the current dichoptic setup, Prof. Graham, A/Prof Klistorner with the assistance of Dr Yabai He (Senior research fellow MQ Photonics Research Centre; Department of Physics, Macquarie University, Sydney, NSW 2109, Australia), sought to address the design challenges of the VR goggle dichoptic recording system.

In order to overcome the difficulty of pupil monitoring, the new setup consisted of two mounted LCD screens (response time 2 ms; Flatron L1954TQS monitor; LG, Englewood Cliffs, NJ) on each side of the subject reflected through centrally located semitransparent mirrors to project a stimulus of 0° to 24° of eccentricity simultaneously to each eye. Mounted behind the mirrors are two infrared cameras, which continually monitor pupil position. Four infrared light-emitting diodes are placed around a lens holder to illuminate the eyes (Figure 2-3). The distance from the subject's cornea to screen is 30cm.

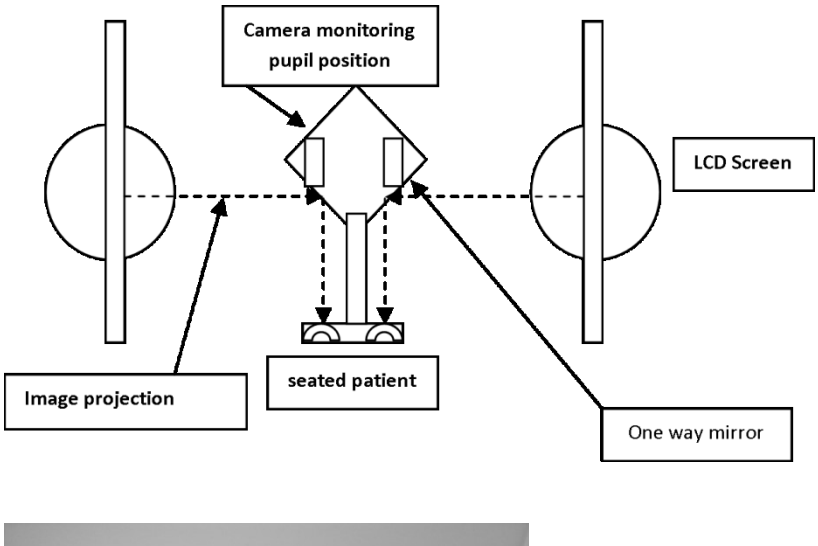

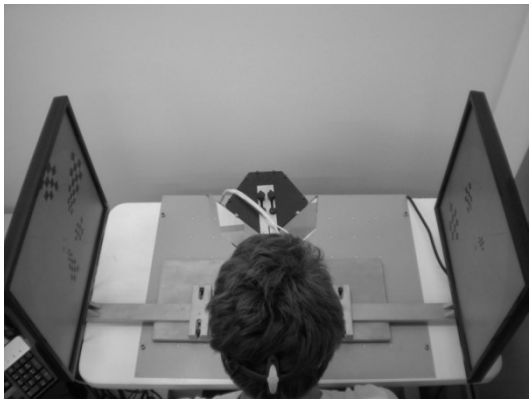

Figure 2-3 - Dichoptic design and setup. Schematic displaying parallel LCD screens, patient facing cameras, dichoptically presented images (top). Live patient seated at testing rig (bottom).

Stimuli are presented simultaneously (dichoptically) to both eyes as outlined in the literature review. Similar to monocular mfVEP, a central fixation target is presented that consists of rotating and slowly changing letters. The stimulus arrangement and the fixation target are identical for both eyes, which helps to fuse the images. The patient, therefore, perceives a single binocular image of the dartboard

stimulus. The stimuli were driven by pseudorandom binary sequences as outlined in the literature review.

1.3.2 STIMULUS PARAMETERS

Two main parameters were altered to target different retinocortical pathways namely magnocellular, parvocellular and koniocellular. These two parameters were stimulus type (which are characterised by their contrast and colour) and the temporal separation between stimulus onset/offset.

1.3.2.1 CONTRAST/COLOUR

There were three stimulus types:

- Low Luminance contrast Achromatic (LLA) consisting of darker grey checks (40 cd/m^2) on a lighter grey background (125 cd/m^2) (Michelson contrast 52%) , Figure 2-4

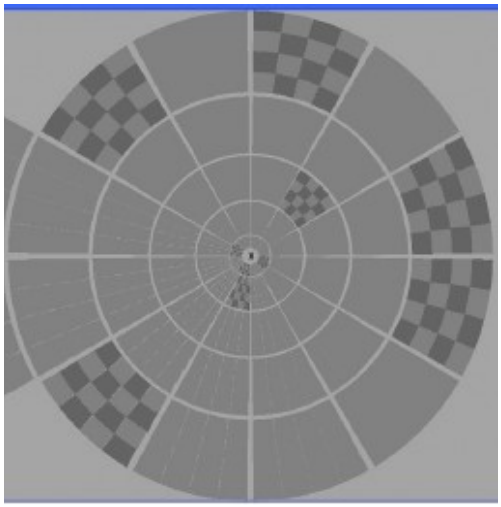

Figure 2-4 - Low contrast stimulus

- High Luminance contrast Achromatic (HLA) consisting of black and white checks (Michelson contrast 99%) on a grey background (mean luminance of black and white) (Figure 2-5).

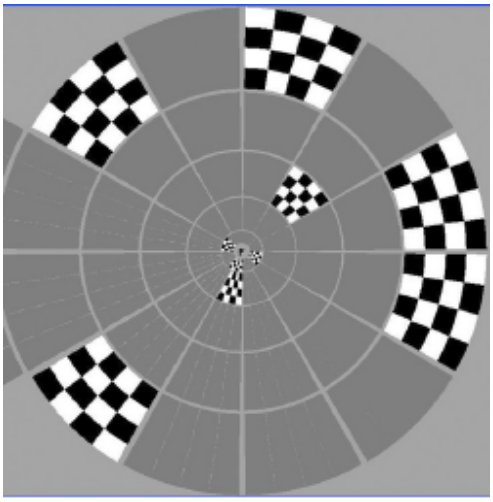

Figure 2-5 - High contrast stimulus

- Low luminance chromatic - Blue on yellow (BonY) consisting of blue checks on a yellow background, the luminance of the blue check was 40 cd/m^2, and the luminance of the yellow background was 125 cd/m^2 (Michelson contrast 52%) (Figure 2-6).

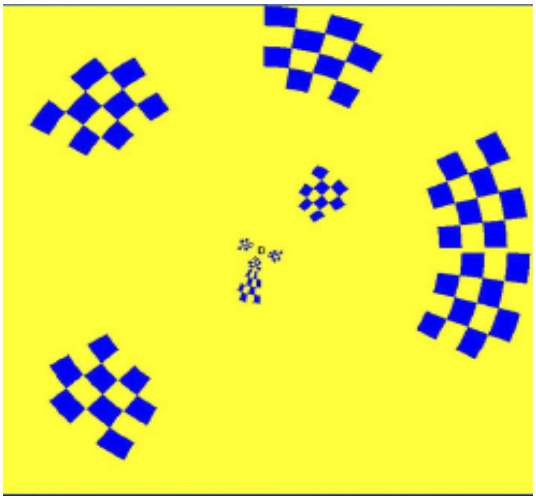

Figure 2-6 - Low contrast chromatic stimulus

1.3.2.2 TEMPORAL SEPARATION

Based upon work by the work by Arvind et al [73], dichoptic suppression using mfVEP is increased with decreasing separation between presentation of segments to corresponding retinal areas. Segments are presented in pattern on/off fashion as described earlier. For their clinical study [75], 18 frames/sequence was chosen as it provided a balance between dichoptic suppression and recording time, we used 18 frames/sequence for the majority of the clinical mfVEP work. However, in order to increase suppression (i.e. decreased separation between presentation of segments) we chose a

speed of 9 frames/sequence as this provided a balance between increased suppression and still maintaining detectable mfVEP amplitudes.

1.3.3 HUMPHREY VISUAL FIELD TESTING

The HVF machine used was the Zeiss Humphrey Visual Field Analyser (version 4.2.2 Model 750i) using SITA-standard 24-2 testing paradigm. Subjects were comfortably seated with one eye patched, optimally corrected for near whilst being observed for central fixation and attention. The testing paradigm works by presenting an ever decreasing intensity of white on white stimulation to 56 points in the visual field over 24 degrees of eccentricity with sensitivity of the patient judged by subjective responses. The parameters are assessed against a well-established age-matched normal database and a mean deviation (MD) score, in decibels, is produced by the software to represent generalised loss in the visual field. The software also calculates a pattern standard deviation (PSD) score which is based on the physiological hill of vision and the deviation of the subject's response from this norm. The preceding parameters are used to assess the severity of the change in visual field loss when compared to the normal database.

For quality control for HVFs an acceptable test was one with fixation losses<20%, false positives<15% and false negative errors <15%, all of which are established parameters for quality control. The tests were performed for normal and glaucomatous subjects in the above manner.

1.4 STRUCTURAL TESTING

1.4.1 SPECTRAL DOMAIN OPTICAL COHERENCE TOMOGRAPHY (SD-OCT)

In the experiments for this thesis SD-OCT is used to quantify the height of the RNFL and to provide indication of structural damage caused by glaucoma. SD-OCT scans were performed using Heidelberg Spectralis ® (version 1.6.4.0 HRA2/Acquisition module 3.0.7.0), circle scan, centered on the optic nerve head.

1.4.2 HEIDELBERG RETINAL TOMOGRAPHY

HRT scans were performed using HRT3 (version 1.6.2.0 ONH acquisition module 3.0.7.0) with a 15° scan diameter, 3 scans averaged for mean topography.

1.5 VALIDATION AND REPRODUCIBILITY OF DICHOPTIC MFVEP

Validation of the novel dichoptic mfVEP setup was performed using 23 normal (no history of eye disease, no intraocular surgery, no frank diabetes mellitus, average age (34), 14 males) subjects using dichoptic stimulation alone. Subjects were selected and recordings performed under the tenets of the declaration of Helsinki. Each subject underwent testing, with correction for near, using an 18 frames per sequence (139 seconds per run, 3 runs, total testing time 7 mins) dichoptic stimulation. Validation of the technology was assessed by statistical analysis looking for discrepancies in amplitude values and for differences between eyes. A relative asymmetry coefficient value between eyes of less than 0.01 was considered to be reasonable, as this represented similar value to those in experiments by Arvind et al[75]. There was no significant difference between the average of right and left amplitudes (paired t-test, $p>0.05$) in the normal population. The average for right eyes was 616.1 +/- 125.9nV and left eyes 606.7 +/- 125.3nV and the average relative asymmetry coefficient between eyes was 0.0054+/-0.042.

Averaged amplitudes for the volunteers were symmetrical between eyes as is demonstrated in Figure 2-7.

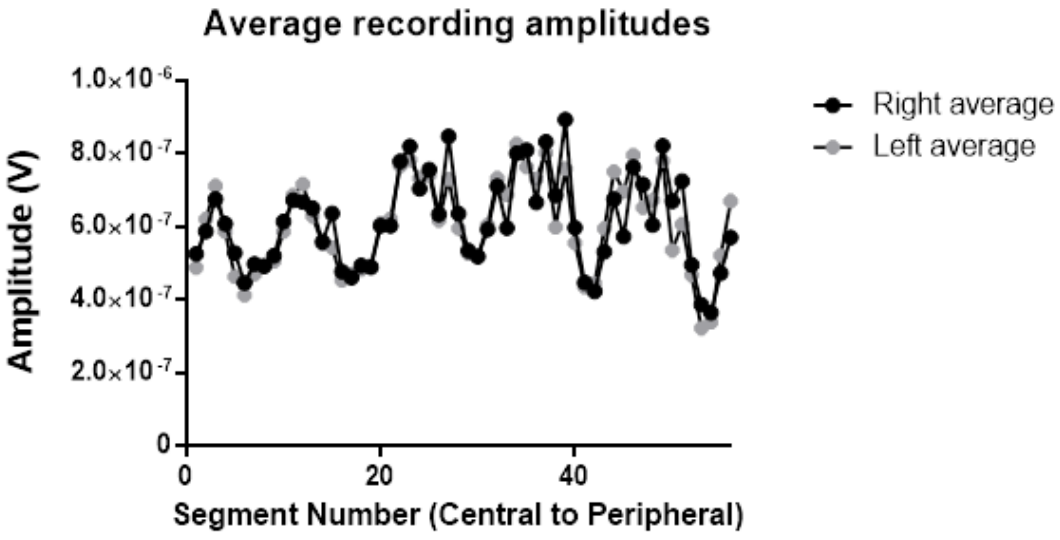

Figure 2-7 – Average amplitude profiles for 23 normal volunteers

There is reasonable agreement between eyes for each segment of the visual field as shown by the asymmetry plot (Figure 2-8), with the relative asymmetry (Equation 2-3) coefficient as calculated below:

$$\frac{AmpR - AmpL}{AmpR + AmpL}$$

Equation 2-3 - Relative asymmetry coefficient

The asymmetry plot demonstrates the characteristic fluctuations seen with mfVEP as the field moves peripherally and asymmetry naturally increases as the temporal-nasal amplitude difference becomes apparent[69].

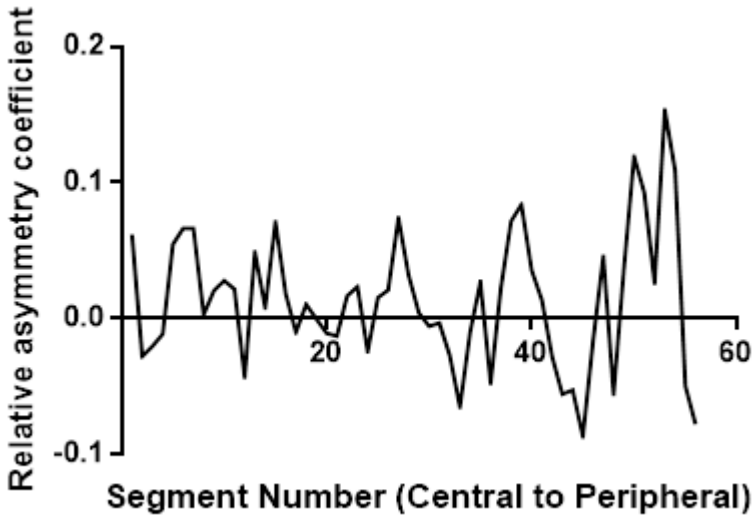

Figure 2-8 - Relative asymmetry coefficient from central to peripheral segments displaying characteristic fluctuating left and right asymmetry, increasing with eccentricity

Repeatability was assessed by examining a subset of 8 volunteers on repeat testing, repeat recordings were performed between 1 day and 3 months after the initial recording. There was an average of 15.8 +/- 5.5% average difference between repeat left eye recordings and 14.9 +/-4.0% average difference between right eye recordings, there was no statistical difference between the variation in repeat recordings (paired t-test, p=0.42). There was no statistical difference between left and right eyes for the averaged repeated recordings for the 8 subjects (paired t-test, p=0.36) (Figure 2-10)

The relative asymmetry coefficient was averaged at 0.0079+/-0.02 (Figure 2-9) for the 8 subjects over both recordings (RAC recording 1 = -0.011+/-0.03; RAC recording 2 = -0.0049+/-0.02) and there was no significant difference between the relative asymmetry coefficients between recordings (paired t-test, p=0.4). The lack of statistical significance points to the consistency of responses and the low variation of asymmetry in mfVEP recordings. Comparatively the repeat recording asymmetry displays a much smaller fluctuation between central and peripheral RAC, this most likely represents the use of repeat subjects in the recording thereby diminishing natural asymmetry trends.

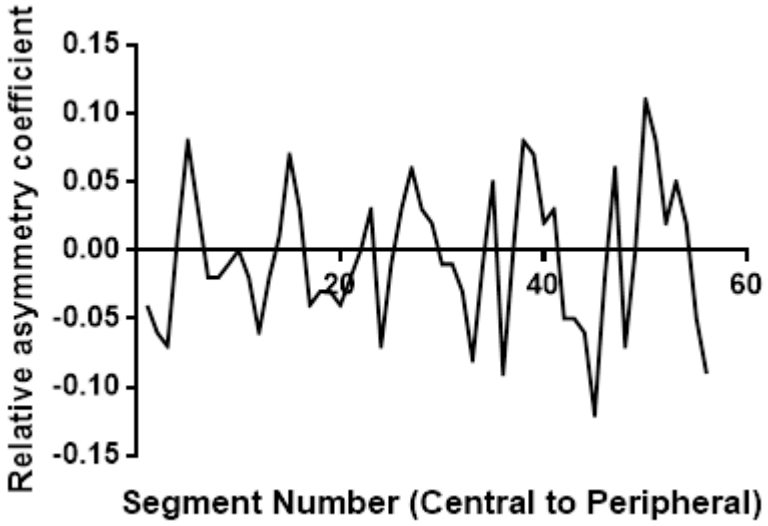

Figure 2-9 - Relative asymmetry coefficient averaged by segment for 8 repeat recordings

The graph (Figure 2-10) displays the close concordance of repeated right and left recordings for the 8 subjects.

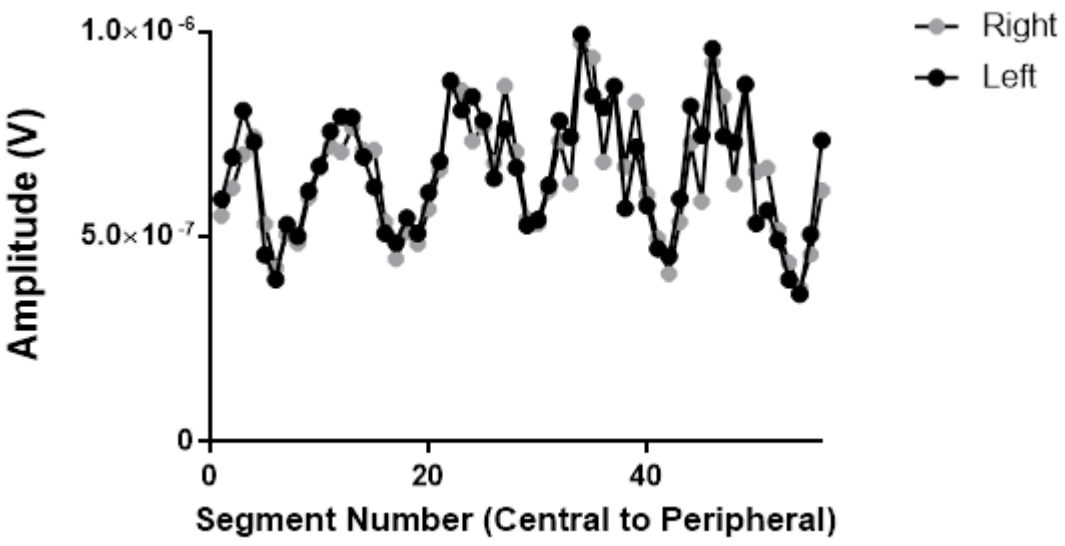

Figure 2-10- Averaged repeat recordings for 8 healthy volunteers (left vs. right eyes)

1.6 DESIGN CONSIDERATIONS

Neck position proved to be a challenging aspect of the dichoptic mfVEP design as the sensitive nature of the occipitally mounted electrodes meant that eletromyograms (EMGs) were a source of significant low frequency, high amplitude noise. This problem was persistent in the early design of the setup and necessitated good position of the patient, with the neck mildly flexed. The patient, similar to other electrophysiological recordings, had to be comfortable so as to avoid EMG noise as well as gross body movements.

1.6.1 DISEASE AND REFRACTIVE ERROR CONCERNS

In order to faithfully record dichoptic signals from a subject there were a few diseases that had to be identified before testing could take place. Namely the presence of amblyopia, high refractive error, anisometropia greater than 3D, high myopia >-6D and strabismus. These concerns were addressed by visual acuity testing and ensuring correction to 6/9 or greater, elimination of any patients with myopia >-6D and the ongoing monitoring of eye position during testing to identify any manifest strabismus or clear loss of fixation.

1.6.2 COMPARISON OF VR GOGGLES VERSUS MOUNTED SCREENS MFVEP RECORDING

Ultimately there were significant differences between the VR goggles and the mounted screens mfVEP recording systems in order to address the problems with the VR goggles. The main difference lay in the design of the retro-mirror mounted infrared cameras which allowed continuous and clear pupil fixation monitoring. This system allowed a fundamental redesign of dichoptic mfVEP recording and addressed the difficulties in pupil monitoring seen with the goggles setup. Other fundamental differences included the increase in eccentricity of stimulation from 16 degrees to 24 degrees, direct comparison/correlation with the monocular mfVEP recording system as the screen size, resolution, luminance and stimulation patterns were identical which was the basis for cross-over comparisons.

Chapter 3 DICHOPTIC SUPPRESSION OF MFVEP AMPLITUDE: EFFECT OF RETINAL ECCENTRICITY AND SIMULATED UNILATERAL VISUAL IMPAIRMENT

Published as:

Leaney, J., Klistorner, A., Arvind, H., Graham, S. L., *Dichoptic Suppression of mfVEP Amplitude: Effect of Retinal Eccentricity and Simulated Unilateral Visual Impairment.* Investigative Ophthalmology & Visual Science, 2010. **51**(12): p. 6549-6555.

Summary

Dichoptic mfVEP has been previously shown to possess advantages over monocular mfVEP in the detection of glaucoma through enhancing asymmetry between eyes through dichoptic suppression. To further understand the mechanisms underlying this phenomenon a study on normal subjects with simulated visual impairment was undertaken to assess potential influences on dichoptic suppression, namely degree of suppression and eccentricity.

1 INTRODUCTION

Multifocal Visually Evoked potentials have multiple applications in various fields of diagnostic ophthalmic medicine including multiple sclerosis and glaucoma[45,47] and provide a reliable and objective method for assessing neural damage to the optic pathways[53,119] The method of presentation typically involves a pseudo-random sequence of contrast reversing checkerboard patterns, scaled for eccentricity, presented monocularly to a subject with bipolar electrodes mounted over the occipital lobe[56]. The techniques for presenting and recording mfVEPs have developed over the last 16 years (since Sutter[58] first made inroads into presentation of multifocal stimuli), including the use of the multiple electrodes[56], EEG scaling and inter-eye asymmetry analysis[67,120], and introduction of pattern-pulse sparse stimulation[61,62,121,122]

However, the technique, as typically applied, is performed monocularly and requires 20-30 minutes of recording time. Monocular recording also results in unequal psychophysical conditions during recording of each eye. As was reported previously, asymmetry analysis of mfVEP amplitude is the most sensitive way to detect early changes. [8,9] However, towards the end of the test the patient may fatigue or lose attention, which may negatively affect recording of the second eye, producing artificial asymmetry and therefore false positive results. Simultaneous recording of both eyes would therefore be beneficial.

Dichoptic and binocular VEP recording has been described using full-field VEPs with pattern-reversal viewing [123] followed later by the use of pseudorandom binary sequences to independently stimulate each eye[74].

James et al demonstrated the feasibility of dichoptic independent mfVEP recording conditions [61] using liquid crystal polarising shutters. These alternately stimulate the two eyes, but reduce luminance substantially. They also described the benefits of temporal sparseness on recording.[62]. We demonstrated the feasibility of dichoptic mfVEP recordings using virtual reality goggles[73,75]. The advantage of using identical recording conditions for both eyes resulted in decreased inter-eye variability and reduced recording time[124]. Intrinsic to dichoptic recording is, however, a degree of mfVEP amplitude suppression as a result of having two competing images presented

simultaneously[125-127]. The degree of suppression was demonstrated to be related to the closeness, in timing, of the presentation of images to each eye, with increasing temporal separation resulting in increased amplitude[124].

When applied to a group of patients with early glaucoma, dichoptic stimulation demonstrated more extensive abnormalities (namely, larger inter-eye asymmetry) as compared to a monocular technique[75]. A few possible explanations for the observed trend were suggested including a tighter asymmetry among normals, additional cortical suppression of a relatively less-defined image from a glaucomatous eye or release of suppression in the contralateral eye, which may potentially increase inter-eye asymmetry [76]. Therefore, the phenomenon of dichoptic suppression of the mfVEP, despite negatively affecting magnitude of mfVEP, may be helpful in detection of early unilateral abnormalities.

Most frequently early glaucoma presents as a localised mid-peripheral visual field defect rather than diffuse reduction of sensitivity. Therefore, in the current study we aimed to investigate an effect of retinal eccentricity on the described phenomenon of dichoptic suppression of the mfVEP amplitude. The second aim of this study was to examine the relationship between degree of simulated unilateral visual impairment (using visual blur) and possible release of dichoptic suppression of the mfVEP amplitude in the contralateral eye as a probable mechanism for increased inter-eye asymmetry in early glaucoma. Since dioptric blur eliminates higher spatial frequencies of the mfVEP stimulus (which predominantly stimulate central field), it was expected to produce a wide range of amplitude reduction at different eccentricities in the blurred eye[128].

2 METHODS

2.1 DICHOPTIC SET-UP

We used a novel binocular VEP set-up for dichoptic mfVEP testing. Previous reports by Arvind[73,75] et al had described the use of virtual reality goggles. However, inability to monitor fixation during recording made the technology difficult to implement. The new setup consisted of 2 mounted LCD screens (LG Flatron, L1954TQS, response time 2 ms) on each side of the subject reflected through centrally located semitransparent mirrors to project a stimulus of 0 to 24 degrees of eccentricity

simultaneously to each eye. Mounted behind the mirrors were two infrared cameras, which continually monitored pupil position. Four infrared lights emitting diodes were placed around lens holder to illuminate eyes (Figure 2-3 (Methods, Chapter 2)).

Stimuli were presented simultaneously (dichoptically) to both eyes as described previously[124]. Briefly, the display to each eye consisted of a cortically scaled dartboard with 56 segments arranged in five concentric rings (1°-2.5°, 2.5°-5°, 5°-10°, 10°-16°, 16°-24°) and a central fixation target extending up to 0.5°. The stimulus in any segment consisted of a 4 x 4 Blue-on Yellow (BonY)[48] check pattern. Segment size was scaled according to the cortical magnification factor[129]. Corresponding to the size of the segments, the size of the individual checks also increased with eccentricity. Luminance of the blue check was 40 cd/m^2, luminance of the yellow background was 125 cd/m^2. A central fixation target was provided that consisted of rotating and slowly changing letters. These features—the ring arrangement and the fixation target—were identical for both eyes, which helped to fuse the images. The patient, therefore, perceived a single binocular image of the dartboard stimulus.

Pseudorandom binary sequences (PRBS) were used to drive stimuli at each test location, so that the presentation at each location was random and independent of other locations. Each binary sequence had a 50% probability of being 1 or 0 at any point of time. Element 1 was represented by two consecutive states: state *pattern on* lasting two frames of the screen (33.3 ms), when the stimulus pattern was displayed, and state *pattern off* lasting 16 frames (266.4 ms), when the whole segment was diffusely illuminated with an intensity of the mean luminance. Element 0 consisted of a pattern off state for 18 frames. The average rate of presentation at each segment was 1.66 times/s. Presentation of the stimulus to the corresponding segment of the second eye was always shifted by nine frames; therefore, the minimum separation between stimuli to corresponding areas of the visual fields of both eyes was seven frames (116.7 ms). Three runs were recorded, each lasting 139 seconds. Technique described in detail elsewhere.[73,75] Monocular recordings were performed using the same set up with one eye covered.

2.2 RECORDING

Four gold cup electrodes (Grass, West Warwick, RI) mounted in an occipital cross-electrode holder were used for bipolar recording. Two electrodes were positioned 4 cm on either side of the inion: one electrode was in the midline 2.5 cm above the inion, and one electrode was 4.5 cm below the inion. Electrical signals were recorded along four channels as the difference between superior and inferior, left and right, and obliquely between left and inferior and right and inferior electrodes. A ground electrode was placed on one ear lobe. Cortical responses were amplified 100,000 times and band-pass filtered (1–20 Hz). Uniquely designed software correlated the responses with the stimulating PRBS and attributed the calculated signals to the respective segments of the visual field. This software also scaled the responses to the background EEG to reduce the inter-individual variability, described elsewhere[130]. For every segment, the largest peak-to-trough amplitude for each wave within the interval of 60 to 200 ms was determined for each channel. The wave of maximal amplitude from each segment in the field from the four channels was automatically selected, and the software created a combined topographic map[131].

2.3 SUBJECTS

8 subjects (average age 30.2+/-7.9 years) were recruited for the study. All had best-corrected visual acuity of 6/6 or better in both eyes, anisometropia (if any) less than 1.5 D, stereoacuity of 40 seconds of arc on Titmus fly stereogram, and normal ophthalmic examination results. Written informed consent was obtained and the experiments were conducted under the tenets of the declaration of Helsinki. There were 5 males and 3 females. “A hole in the card” test was used to assess ocular dominance with 7 right eyes and 1 left eye dominant.

All subjects underwent monocular and dichoptic mfVEP recordings in random order. Both eyes were optimally corrected for distance with near correction, if needed, for all recordings.

To simulate reduced visual input in one eye, lenses of +4D and +6D over distance correction were placed in front of the subject’s right eye before performing additional dichoptic recordings. This effectively induced +1D and +3D respectively of blur for near.

2.4 ANALYSIS

The coefficient of dichoptic suppression of the VEP amplitude was calculated as the difference between the averaged monocular amplitude (Am) and the averaged dichoptic amplitude (Ab), divided by the monocular amplitude (Equation 4-1). To investigate the effect of retinal eccentricity the amplitude of all segments within each ring of the stimulus was also averaged and coefficient of dichoptic suppression was calculated for each ring.

$$\frac{Am - Ab}{Am} x100\%$$

Equation 3-1 Dichoptic suppression formula, Am = monocular amplitude, Ab = binocular amplitude

Statistical analysis was performed using SPSS® software. The p value < 0.05 was considered significant. Where appropriate, correction was applied to correct for an increase in type 1 errors (Bonferroni or Tukey).

3 RESULTS

The dichoptic recording set-up allowed simultaneous acquisition of mfVEP from both eyes in all subjects. A typical example presented in Figure 3-1.

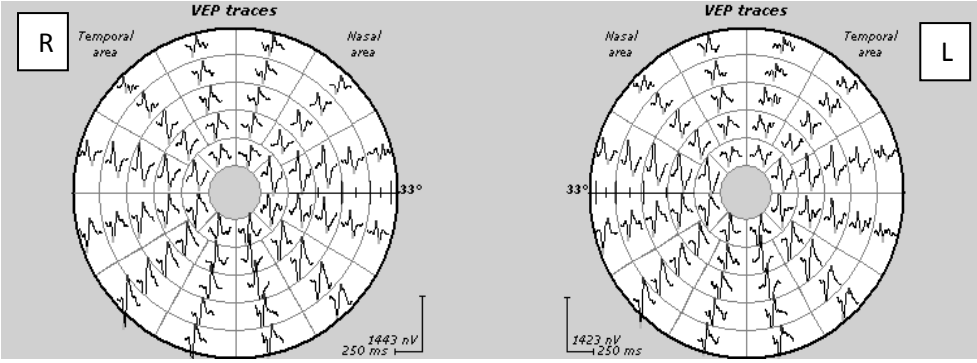

Figure 3-1 - Typical result of dichoptic recording.

3.1 DICHOPTIC SUPPRESSION VS ECCENTRICITY.

The average dichoptic suppression of the mfVEP amplitude across the entire field was 19.8+/- 4.9%. When analysed ring-wise, dichoptic amplitude suppression was significant at all eccentricities (paired t-test, p<0.0001, with Bonferroni correction adjusted p value =0.01) (Table 3-1).

Average Dichoptic Suppression (%)				
Ring 1	Ring 2	Ring 3	Ring 4	Ring5
34.3+/-5.9% p<0.0001	25.5+/-5.4% p<0.0001	17.0+/-5.0% p<0.0001	14.5+/-6.0% p=0.0006	12.8+/-8.6% p=0.004

Table 3-1 - Average Dichoptic suppression at different eccentricities.

The central part of the visual field, however, demonstrated significantly greater suppression as compared to more peripheral areas ($p<0.0001$, one-way ANOVA)

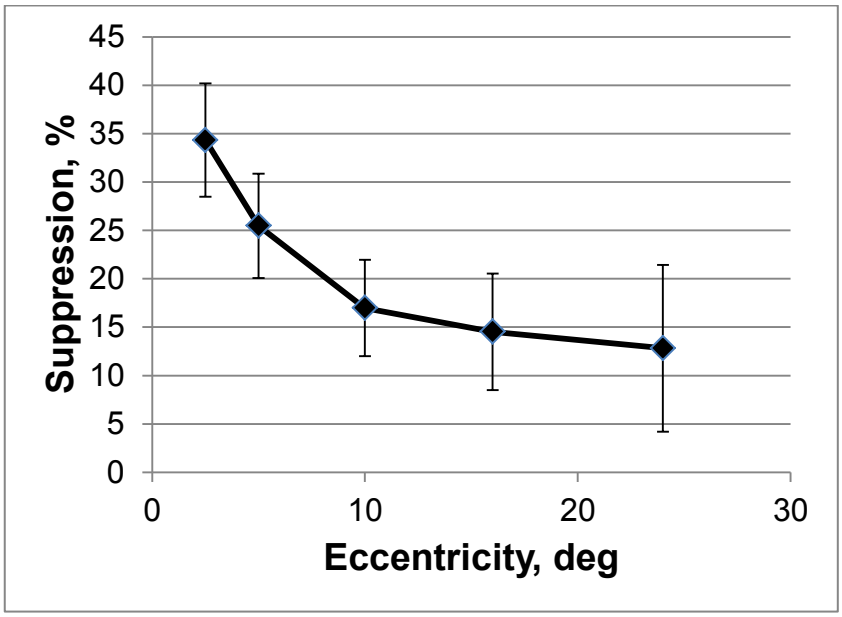

Figure 3-2 - Suppression versus eccentricity for dichoptic recording. There is a clearly non-linear relationship between suppression and distance from centre with a much steeper gradient within the central 10 degrees of eccentricity and flattening of the curve at the periphery.

The pattern of dichoptic suppression declined smoothly with eccentricity toward an asymptotic value of around 10% (Figure 3-2). Dichoptic suppression dropped from 34 % at 2 degrees to 17% at around 10 degrees and changed little beyond that eccentricity. Post-hoc analysis (Turkey t-test) demonstrated significant differences for ring 1 and 2 between each other and remaining rings ($p<0.01$ for all), while there was no significant difference between rings outside 10 degrees of eccentricity.

3.2 Effect of dioptric blur on dichoptic recordings

Under dichoptic recording conditions the visual blur resulted in significant reduction of mfVEP amplitude of the blurred eye. Thus, introduction of +4D lens produced 19.6 +/-12.6% reduction of averaged mfVEP amplitude ($p=0.004$, paired t-test), while +6 D yielded even larger reduction (38.7+/-5.1%, $p<0.0001$, paired t-test). All values considered significant with adjusted Bonferroni correction, $p=0.01$.

When analysed ring-wise, amplitude reduction was significant at all eccentricities (Table 3-2).

	Average reduction due to blur (%)				
Lens	Ring 1	Ring 2	Ring 3	Ring 4	Ring5
+4D	43.5+/-13.0 (p<0.001)	37.0+/-16.6 (p<0.001)	18.3+/-14.5 (p<0.01)	12.2+/-9.3 (p<0.01)	8.1+/-9.6 (p<0.05)
+6D	58.8+/-5.0 (p<0.00001)	56.6+/-7.0 (p<0.0001)	40.2+/-9.9 (p<0.0001)	27.7+/-5.4 (p<0.0001)	20.9+/-5.7 (p=0.0001)

Table 3-2 - Average reduction due to blur versus eccentricity showing significant suppression through all eccentricities

The pattern of amplitude reduction was eccentricity-dependant with the reduction significantly declining from centre to periphery for both levels of visual blur. An individual example is presented in Figure 3-3.

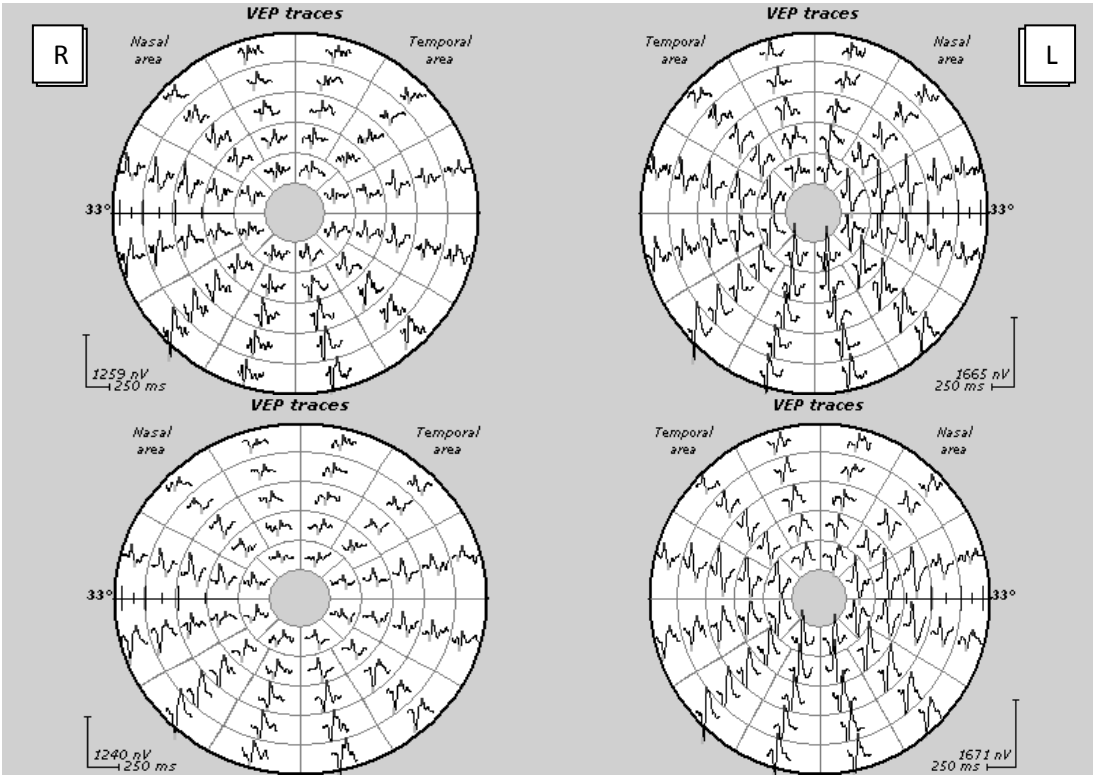

Figure 3-3 – An example of mfVEP dichoptic recording using +4D (top row) and +6D (bottom row) lenses to induce blur in right eye

With blurring, the contralateral eye demonstrated significant amplitude increase, which was proportional to the degree of blurring. The averaged amplitude of the contralateral eye increased by 9.3+/-5.0% (p=0.003) following the +4D lens and by 16.7+/-9.3% (p=0.002) when the +6D lens was applied. Bonferroni correction applied, p = 0.01 for significance.

Ring-wise analysis demonstrated amplitude increase in the contra-lateral eye at all eccentricities for both levels of blurring. It was statistically significant in 3 central rings for both blurring conditions and additionally in ring 4 for the +6D lens (Table 3-3). The pattern of amplitude increase again demonstrated strong relations to retinal eccentricity with central part of the visual field showing maximum amplitude increase, which gradually diminished towards periphery.

	Mean Release of Suppression (%)				
Lens	Ring 1	Ring 2	Ring 3	Ring 4	Ring5
+4D	17.6+/-9.5% (p<0.01)	14.2+/-4.5% (p<0.01)	7.8+/-4.4% (p<0.01)	4.6+/-10% (p=0.25)	3.1+/-12.1% (p=0.52)
+6D	31.6+/-17.0% (p<0.001)	23.8+/-12.7% (p<0.001)	12.3+/-8.1% (p<0.01)	8.9+/-10.7% (p < 0.05)	6.2+/-11.1% (p=0.13)

Table 3-3- Release of suppression in the left eye with right eye +4D/+6D lens applied

There was highly significant correlation (r=0.95, p<0.0001) between degree of amplitude reduction caused by visual blur in one eye and extent of amplitude increase in the contralateral eye (Figure 3-4). Examples of this amplitude reduction in one eye and amplitude increase in the fellow eye can be seen in Figure 3-5, demonstrating a relationship between eccentricity and the degree of change.

Latency values were analysed at different eccentricities and at all 4 dichoptic settings (monocular/dichoptic/+4D/+6D) and there was found to be no significant difference. (p>0.05, one-way ANOVA)

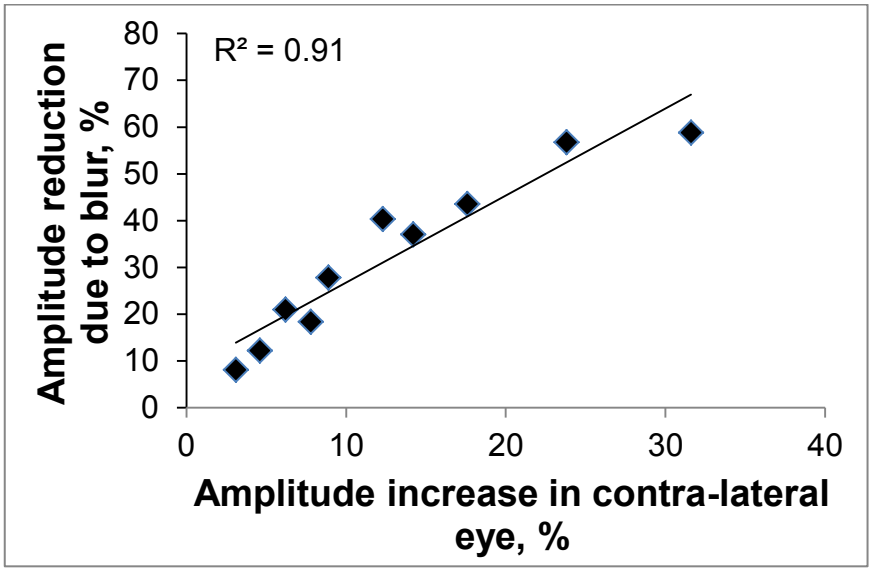

Figure 3-4 Relationship between amplitude reduction due to blur and release of suppression in the contralateral (left) eye. The degree of suppression in the blurred eye is directly proportional to the release of suppression in the fellow (unblurred) eye.

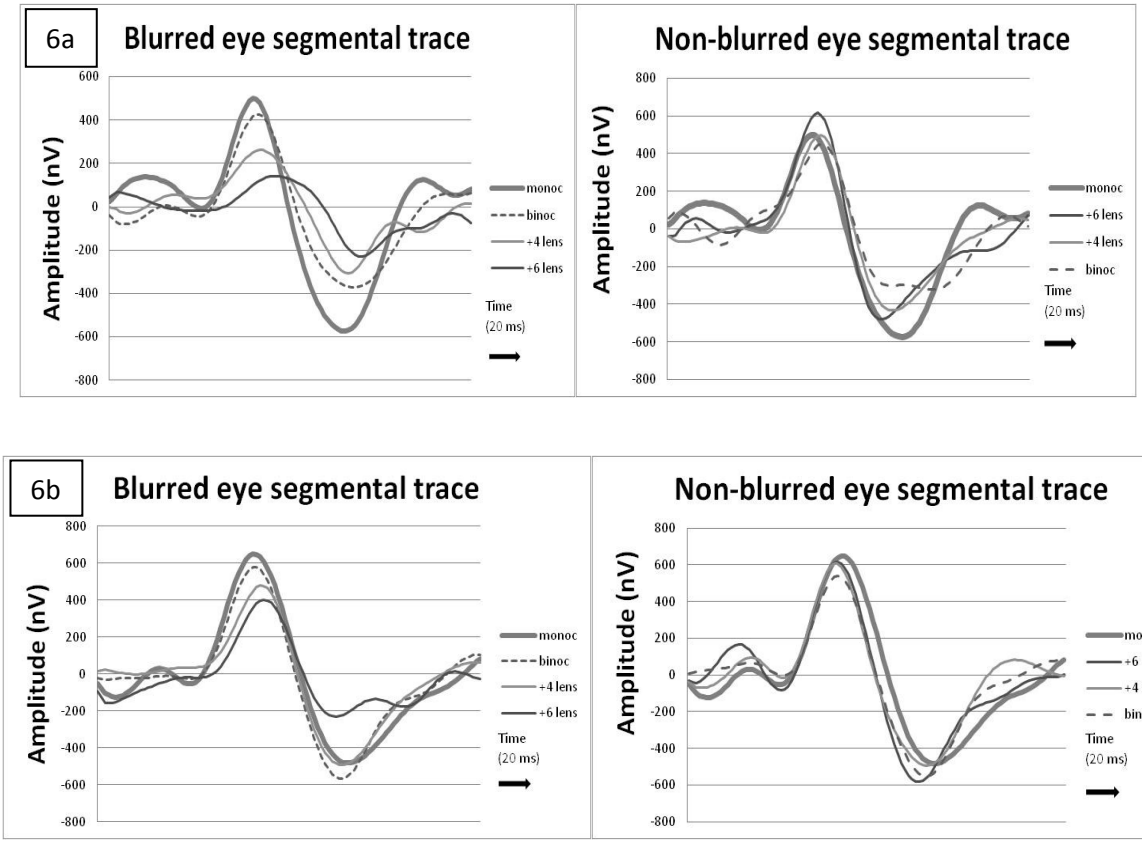

Figure 3-5- Example of segmental traces from a typical subject, note the decrease in amplitude from monocular, dichoptic and blurring and the subsequent increase in corresponding sector in the non-blurred(contralateral) eye. This is the basis for an increase in asymmetry between scotoma and a healthy corresponding segment. 6a represents an inferior segment, eccentricity 2.5-5°, 6b represents a superior segment, eccentricity 5-10°. The effect is greater for the more central location

4 DISCUSSION

Dichoptic stimulation has been explored in various forms previously[62,75,124] and has been shown to be a robust and repeatable method for recording mfVEPs. The technique benefits from shorter testing time and identical psychophysical setting for each eye. It has previously demonstrated superior capability in detection of abnormalities in early glaucoma as compared to monocular recording[75]. However, the additional defects detected by dichoptic recording tended to be more central, rather than the arcuate defects classically expected in glaucoma. We hypothesised that release of interocular suppression by early unilateral visual loss may contribute to enhanced asymmetry and better detection. Therefore, in the current study we investigated the degree of interocular suppression induced by dichoptic stimulation at various eccentricities of the visual field and tested the hypothesis that possible release of suppression in contralateral eye could result in greater inter-eye amplitude asymmetry in unilateral disease.[76]

There are two main findings in this study, both of which have not been reported before. Firstly, there is a strong dependence of the magnitude of suppression of the mfVEP amplitude elicited by dichoptic stimulation on retinal eccentricity. While average suppression across the whole tested field was under 20%, it reached almost 35% in central region and fell to 12% at around 20 degrees of eccentricity. It was suggested earlier that interocular suppression may have cortical origins. Thus, both inhibitory interactions between adjacent ocular dominance columns in the striate cortex[132] and low temporal resolution of binocular neurons[133] were proposed as possible mechanisms of interocular suppression[124].

The variable degree of suppression across the visual field, however, may also be, at least in part, related to temporal characteristics of neurons in the anterior visual pathway. There are two major pathways, parvocellular and magnocellular, which are anatomically segregated up to the major input layer (4C) of the striate cortex, but converge in higher visual areas[134]. One of the characteristic features of the functional dichotomy between parvocellular and magnocellular neurons is a functional difference in temporal properties of two types of neurons. Parvocellular neurons are slow with sustained response to light (low-pass filter with 5-10Hz corner frequency), while the

magnocellular pathway is more transient with band-pass temporal characteristics, having maximal sensitivity at about 20Hz[135]. The distribution of parvocellular and magnocellular neurons across the retina is also different. Whilst the central visual field is dominated by P-cells, the relative number of magnocellular neurons increases with retinal eccentricity by a factor of 10[136]. While the majority of cells in layer 4C are almost completely monocular, neurons in other (higher) layers of striate cortex tend to be binocular[137]. Therefore, the change in the relative contribution of parvo/magnocellular neurons into the binocular neurons at higher levels of striate cortex may result in increase of their temporal resolution in the more peripheral part of the visual field and lead to a reduction of dichoptic suppression with eccentricity. Further studies (by using targeted stimuli) are needed to explore the potential role of each pathway in mechanism of cortical suppression.

Secondly, the study not only confirmed the existence of the phenomenon of the release of amplitude suppression, but more importantly, demonstrated a strong relationship between the degree of mfVEP amplitude reduction caused by visual impairment in one eye and release of amplitude suppression in contralateral eye.

The use of refractive blur was intended to simulate disruption of normal visual function monocularly. The loss of amplitude due to blur is most likely derived from loss of edge definition of the high frequency spatial elements, which predominate the central field as stipulated by Winn et al[128]. Due to the variable effect of blur on central and peripheral vision, it produced a wide range of amplitude reductions (varying from 8% to 59% at different eccentricities and using different lens strength). This allowed us to study the mechanism of the release of dichoptic suppression of mfVEP amplitude in the contralateral eye quantitatively. The high degree of correlation between reduced visual input to one eye and release of amplitude suppression in the contralateral eye implies that both mechanisms may operate at the same level of the visual pathway. It also showed that release of amplitude suppression occurs across the whole visual field provided suppression itself is large enough. It is noteworthy that as amplitude reduction due to blur in one eye approached 60% (which is comparable to the level of background noise), the release of suppression in fellow eye reached it maximum value (increase of about 30%), coming close to an amplitude of a monocular recording. The central-peripheral

differences in the release of interocular suppression may explain the central clustering of defects we found earlier among subjects with glaucoma.[75]

The averaged dichoptic suppression over all eccentricities found in this study was considerably larger than that found by Arvind et al[124] using virtual reality goggles. The reason for this difference most likely lies in the difference between the monitors used (liquid crystal on silicon technology, used in the Arvind et al study has much faster response time than the LCD monitor used here). In addition Blue-on-Yellow stimulation used in the current study (as opposed to achromatic black/white stimulation employed previously) may also contribute to an increase of suppression since temporal sluggishness of koniocellular pathway is well known[138,139].

It should be noted that one limitation of the current study is the fact that the use of a lens to create a monocular visual impairment may not adequately mimic a real scotoma as a lens-induced blur reduces mostly high frequency spatial elements.

5 CONCLUSION

The study demonstrated that dichoptic stimulation results in eccentricity-dependent suppression of mfVEP amplitude. It also revealed that factors affecting visual performance of one eye (monocular blur or possibly a monocular pathological process) not only have a negative effect on dichoptic mfVEP amplitude of the affected eye, but also promote release of dichoptic suppression in the fellow (unaffected) eye. This phenomenon supports our earlier hypothesis[76] that unilateral loss leads to a relative increase in inter-eye asymmetry and therefore may potentially be utilised for early detection of unilateral pathological processes.

Chapter 4 STIMULATION SPEED, BUT NOT CONTRAST DETERMINES DEGREE OF DICHOPTIC SUPPRESSION OF MFVEP

Prepared for submission as:

Leaney, J., Klistorner, A., Graham, S. L., *Stimulation speed, but not contrast determines degree of dichoptic suppression of mfVEP.* Documenta Ophthalmologica

Summary

The study explores stimulation speed to gain deeper understanding about factors that can be adjusted to alter levels of dichoptic suppression. The finding that dichoptic suppression is influenced by speed of presentation but not contrast aids understanding of the types of retinal ganglion cells involved and potential targets in the non-redundant pathways involved in glaucomatous optic nerve pathogenesis.

1 INTRODUCTION

Crucial to the development of a sensitive and specific mfVEP stimulus is the selection of contrast levels which facilitate glaucoma detection. Arvind et al [50] showed in monocular mfVEP that both low luminance contrast (LLC) and blue on yellow (BonY) were superior to high luminance contrast (HLA) for detection of glaucoma. Furthermore they demonstrated that the chromatic component of the BonY was not responsible for the increase in sensitivity in glaucoma rather that the low luminance component was the most important factor. The authors proposed that both the LLA and BonY stimuli were more magnocellular specific [50] and thereby targeted the non-redundant pathways which have been suggested to increase detection of glaucoma [140]. In terms of magnocellular pathway targeting, the dichoptic mfVEP has the advantage of interocular suppression being mediated by the temporal frequency of the stimulus[73]. Previous dichoptic mfVEP research has demonstrated that temporal frequency modulates the degree of interocular suppression in normal subjects [62]. In increasing temporal separation between stimulation of corresponding segments, the degree of interocular suppression is decreased. Indeed Arvind et al., using virtual reality goggles, noted there to be no interocular suppression with a separation of 166.7ms between stimulation of the corresponding segments in each eye. Based upon these findings, in the development of a mfVEP stimulus for glaucoma testing, there is a need to investigate contrast levels and temporal frequency on interocular suppression profiles. While minimising suppression has the advantage of larger amplitudes, facilitating some interocular interaction may be a valuable strategy to detect increased asymmetry where one eye has early damage, as in early focal glaucomatous loss.

2 BACKGROUND

The phenomenon of dichoptic suppression (DS) of mfVEP amplitude has recently been reported by Arvind et al[75]. Amplitude reduction was induced when both eyes were stimulated simultaneously using virtual reality goggles. The effect of amplitude reduction was attributed to inhibitory interactions between adjacent ocular dominance columns in the striate cortex[109] and low temporal resolution of binocular neurons[141].

It was shown that DS is dependent on stimulation frequency with higher rate of stimulation producing larger DS[75]. We also recently demonstrated the eccentricity dependant character of DS[142].

When applied to a group of patients with early glaucoma, dichoptic stimulation produced more extensive abnormalities (namely, larger inter-eye asymmetry) as compared to a monocular technique[75]. A few possible explanations for the observed trend were suggested including a tighter asymmetry among normals, additional cortical suppression of a relatively less-defined image from a glaucomatous eye or release of suppression in the contralateral eye, which may potentially increase inter-eye asymmetry [76]. Therefore, the phenomenon of dichoptic suppression of the mfVEP, despite negatively affecting magnitude of mfVEP signal, may be helpful in detection of early unilateral abnormalities in glaucoma.

It is well established that visual information is processed along three major retino-geniculo-cortical pathways: parvocellular, magnocellular and koniocellular[134]. The parvocellular pathway, which constitutes about 80% of the total population of retinal ganglion cells is responsible for processing of high contrast, low temporal and high spatial frequency information while the magnocellular pathway conveys information about low contrast and low spatial frequency achromatic images and has higher temporal resolution[105,106]. The distribution of parvocellular and magnocellular neurons across the retina is also different. Whilst the central visual field is dominated by parvocellular RGCs, the relative number of magnocellular neurons increases with retinal eccentricity by a factor of 10 [107]. The third, koniocellular pathway, conveys blue-on/yellow-off colour signals to the brain and has projections from the central and peripheral retina.[143,144] The koniocellular pathway has characteristics similar to parvocellular cells in processing high contrast, low temporal and high spatial frequency information.[143,144]

It has been suggested that by using stimuli that preferentially target the magnocellular pathway it may be possible to identify glaucomatous visual field defects earlier.[55] This is thought to be due to lower functional redundancy of cells subserving the magnocellular pathway,[140] since it constitutes,

on average, only about 10% of the ganglion cell population.[25,26]Therefore, preferential stimulation of magnocellular pathway may be beneficial.

In this current study we investigated whether by manipulating the speed of presentation and contrast levels we could determine which stimulus parameters were responsible for suppression, and aim to bias DS toward either magno or parvocellular activity.

3 METHODS

3.1 DICHOPTIC SETUP

The setup for dichoptic testing has been described previously[142]. Briefly, it consists of two mounted LCD screens (response time 2ms, Flatron L1954TQS monitor, LG, Englewood Cliffs, and NJ) on each side of the subject reflected through centrally semitransparent mirrors to project a stimulus of 0^o to 24^o eccentricity simultaneously to each eye. Mounted behind the mirrors are two infrared cameras which are to monitor pupil position (Figure 2-3 (Methods, Chapter 2)). The current design is based on the previous setup except the monitor main support is inverted to sit superiorly to assist with attaining appropriate neck positioning. The design is based on that used by Arvind et al[73].

Dichoptic presentation was achieved with separate stimulation for each eye and has been described previously[142]. Briefly, the display to each eye consisted of a cortically scaled dartboard with 56 segments arranged in five concentric rings (1°–2.5°, 2.5°–5°, 5°–10°, 10°–16°and 16°–24°) and a central fixation target extending up to 0.5°. Segment size is scaled according to the cortical magnification factor. Corresponding to the size of the segments, the size of the individual checks also increases with eccentricity. The stimulus consisted of a 4x4 check pattern. The main features –ring arrangement and fixation target – are identical for both images thus enabling fusing of the images.

There were 4 different types of stimuli, recorded dichoptically and monocularly. There were 2 luminance contrasts – Low Luminance contrast Achromatic (LLA) consisting of darker grey checks (40 cd/m^2) on a lighter grey background (125 cd/m^2, Michaelson contrast 52%); High Luminance contrast Achromatic (HLA) consisting of black and white checks (Michaelson contrast 99%) on a grey background (mean luminance of black and white).

At each stimulus location the stimuli was driven by pseudorandom binary sequences (PRBSs) enabling the presentation to be random and independent of other locations. The presentation has been described previously[142], each binary sequence had a 50% probability of being 1 or 0 at any point in time.

In order to test the effects of temporal closeness on interocular suppression, two temporal separations were used for each stimulus. “Fast” stimulation consisted of 2 elements - Element 1 was represented by two consecutive states: pattern on, lasting two frames of the screen (33.3 ms), when the stimulus pattern was displayed, and pattern off, lasting 7 frames (116.7 ms), when the whole segment was diffusely illuminated with an intensity of the mean luminance. Element 0 consisted of the pattern-off state for 9 frames. The average rate of presentation at each segment was 3.33 times/s. The presentation of the stimulus to the corresponding segment of the second eye was always shifted by 4 frames; therefore, minimum separation between stimuli to corresponding areas of the visual fields of both eyes was either 2 (33.3ms) or 3 frames (50.0 ms). Three runs were recorded, each lasting 69 seconds. Each run lasted 69 seconds and 6-8 runs were recorded per stimuli.

“Slow” stimulation consisted of 2 elements - Element 1 was represented by two consecutive states: pattern on, lasting two frames of the screen (33.3 ms), when the stimulus pattern was displayed, and pattern off, lasting 16 frames (266.4 ms), when the whole segment was diffusely illuminated with an intensity of the mean luminance. Element 0 consisted of the pattern-off state for 18 frames. The average rate of presentation at each segment was 1.66 times/s. The presentation of the stimulus to the corresponding segment of the second eye was always shifted by 9 frames. Therefore there was a minimum of 7 frames between stimulation of corresponding areas of the visual field. Each run lasted 139 seconds and 3-4 runs were recorded per stimuli.

Monocular recordings were performed using the same equipment setup with one eye covered. The order of the recordings was randomised as was the eye chosen as the monocular eye. Two recording sessions were necessary as the total testing time was over two hours. The “fast” recordings were

performed in a separate session to the “slow” recordings. In total there were 2 speeds (slow and fast) and 2 stimuli (HLA and LLA) recorded dichoptically and monocularly giving 8 different recording conditions.

3.2 RECORDING

Four gold cup electrodes (Grass, West Warwick, RI) mounted in an occipital cross-electrode holder were used for bipolar recording. Two electrodes were positioned 4 cm on either side of the inion: one in the midline 2.5 cm above the inion and one 4.5 cm below the inion. Electrical signals were recorded along four channels as the difference between superior and inferior and between left and right, and obliquely between the left and inferior and right and inferior electrodes. A ground electrode was placed on one ear lobe. Cortical responses were amplified 100,000 times and band-pass filtered (1–20 Hz). Custom designed software correlated the responses with the stimulating PRBS and attributed the calculated signals to the respective segments of the visual field. This software also scaled the responses to the background EEG to reduce the interindividual variability, described elsewhere[75]. For every segment, the largest peak-to-trough amplitude of each wave within the interval of 60 to 200 ms was determined for each channel. The wave of maximum amplitude from each segment in the field from the four channels was automatically selected, and the software created a combined topographic map.

3.3 SUBJECTS

Twelve subjects (average age, 29.5+/- 6.5 years, 9 male) participated in the study. All had best-corrected visual acuity of 6/6 or better in both eyes, anisometropia (if any) less than 1.5 D, stereoacuity of 40 sec arc on Titmus fly stereogram, and normal ophthalmic examination. Written, informed consent was obtained, and the experiments were conducted according to the tenets of Declaration of Helsinki.

All testing was performed in a random order within each temporal spacing setting. The monocular eye to be tested was also chosen randomly. All subjects were optimally corrected for near distance viewing.

3.4 ANALYSIS

Analysis was performed using amplitude values at 56 points over 24 degrees of eccentricity for each testing type (low contrast/high contrast/slow/fast stimulation). These values were then averaged to produce total amplitude in volts for each testing condition (i.e. full field average amplitude) or amplitudes for each of the 5 rings of eccentricity (i.e. eccentricity dependent amplitude) for each of the testing conditions.

The averaged amplitudes and dichoptic suppression values, for each testing condition and eccentricity, were analysed using GraphPad Prism 6 (Version 6.02 for Windows) and Microsoft Excel (Version: 14.0.612.5000). We used paired t-test when comparing the stimuli and one-way ANOVA for ring-wise analysis of suppression and amplitude profiles, Bonferroni, ANOVA repeated measures or Tukey multiple comparison tests were used where appropriate. The coefficient of dichoptic suppression of the VEP amplitude was calculated as the difference between the averaged monocular amplitude (Am) and the averaged dichoptic amplitude (Ab), divided by the monocular amplitude (Equation 4-1). To investigate the effect of retinal eccentricity the amplitude of all segments within each ring of the stimulus was also averaged and the coefficient of dichoptic suppression was calculated for each ring.

$$DS = \frac{Am - Ab}{Am}$$

Equation 4-1 - Dichoptic suppression (DS) equals Monocular amplitude minus Binocular amplitude divided by Monocular Amplitude

4 RESULTS

4.1 AMPLITUDE PROFILES

4.1.1 MONOCULAR STIMULATION

The highest amplitude was recorded at high contrast slow (HCS) stimulation, while the lowest amplitude was with low contrast fast (LCF) stimulation. Generally amplitude increased when contrast increased and stimulation become slower. Average amplitudes for each type of stimulation was 500+/-54nV for LCF, 604+/-62nV for high contrast fast (HCF), 668+/-61nV for low contrast slow (LCS) and 832+/-107nV for HCS.

There was a significant ($p<0.01$) difference between the averaged amplitude of each of the 4 stimulus types (Figure 4-1). (One-way ANOVA (repeated measures, Tukey multiple comparison test)).

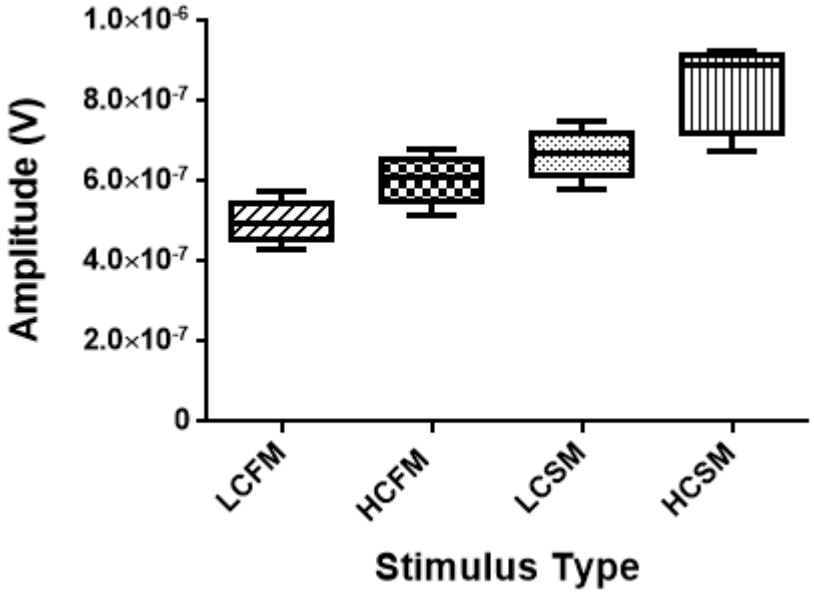

Figure 4-1 - Averaged amplitudes for monocular stimuli (note all are significantly different ($p<0.01$(One-way ANOVA (repeated measures)) (note LCFM = LCF monocular)

The pattern of amplitude at different eccentricities remained the same for all stimulus types, the curves were shifted up or down with change of contrast and speed (Figure 4-2).

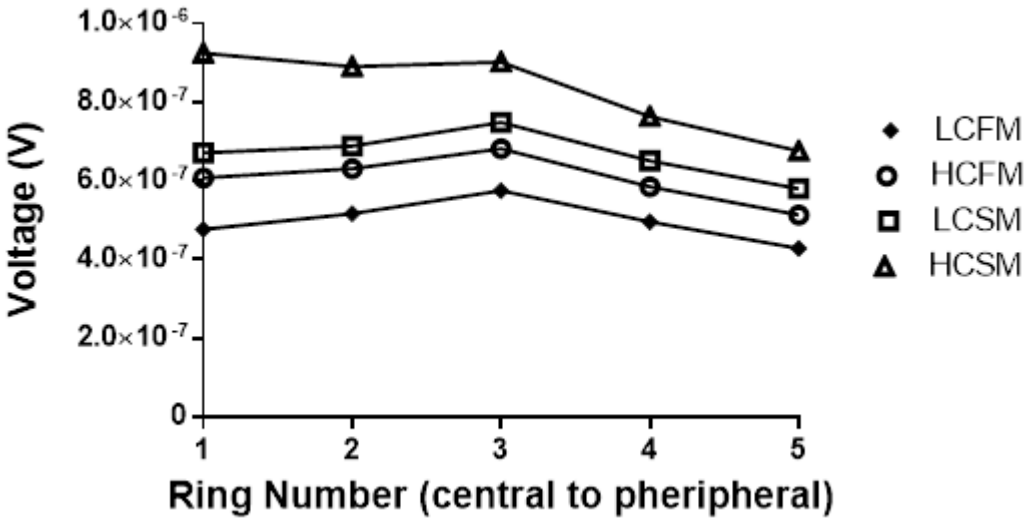

Figure 4-2 - Averaged voltage ring-wise for monocular stimuli. HCS is noticeably larger, especially centrally; LCF has the smallest amplitude throughout.

4.1.2 DICHOPTIC STIMULATION

A typical example of dichoptic recording of multifocal VEP is shown in Figure 4-3.

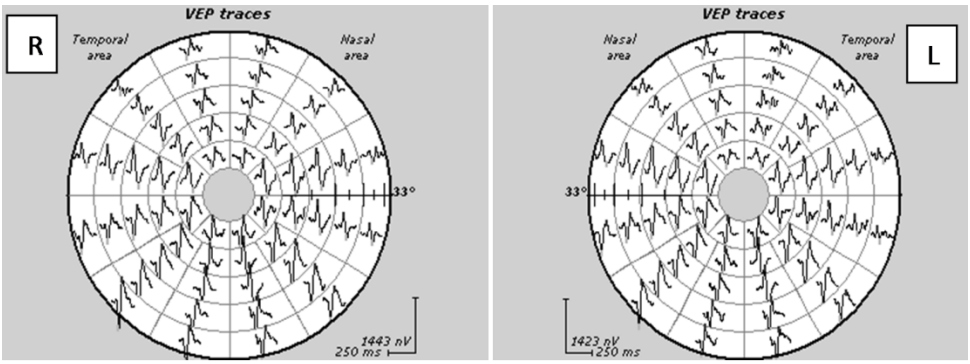

Figure 4-3 - Typical normal dichoptic mfVEP traces showing almost identical traces between eyes

Similar to monocular recording, the highest amplitude of dichoptic mfVEP was recorded at HCS stimulation while lowest at LCF stimulation. Generally amplitude increased when contrast increased and stimulation become slower. Thus, under similar temporal frequency of stimulation amplitude was higher for high contrast stimulation as compared to low contrast stimulation. Likewise, for a similar level of contrast, amplitude was higher for slow stimulation as compared to fast stimulation. Average amplitudes for each type of stimulation were 383+/-37 nV for LCF, 454+/-43 nV for HCF, 582+/-67 nV for LCS and 713+/-59nV for HCS. (Figure 5)

All averaged amplitudes were significantly different (One way ANOVA (repeated measures Tukey multiple comparison correction), p=<0.05)) (Figure 4-4).

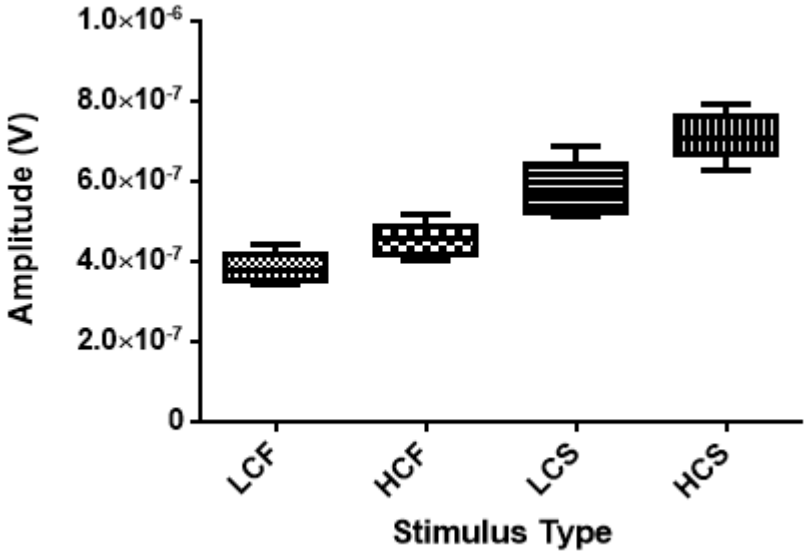

Figure 4-4 - Averaged amplitudes for dichoptic stimuli (note all are significantly different (p<0.01) except for LCF and HCF (p>0.05), One-way ANOVA (repeated measures))

There was again a similar profile of amplitude with eccentricity for all modes of stimulation, however, the central responses were more depressed as compared to monocular recordings in keeping with the known characteristics of DS (Figure 4-5).

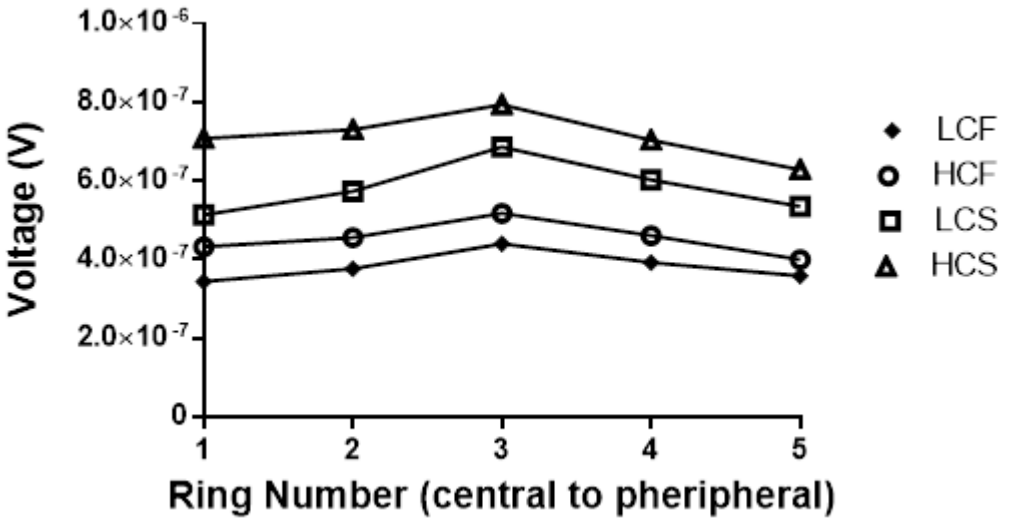

Figure 4-5 - Averaged voltage ring-wise for dichoptic stimuli. HCS has the largest amplitudes throughout with diminishing amplitudes from LCS down to HCF and then LCF with the smallest amplitude profile. Note central responses relatively lower than with monocular recording

4.2 DICHOPTIC SUPPRESSION.

DS, which represents the amount of amplitude reduction under dichoptic conditions as compared to monocular stimulation, demonstrated a different pattern of frequency and contrast dependency. Average dichoptic suppression was similar for both contrast conditions when fast stimulation was employed, (demonstrating 23.0+/-11.6% amplitude decrease for LC and 24.3+/-6.4% for HC). Dichoptic suppression for slow stimulation was also similar for both contrasts, but at a much lower level; 12.2+/-10.4% and 13.3+/-7.8% for LC and HC respectively (Figure 4-6). ANOVA demostrated significant difference in DS between different speeds of stimulation ($p<0.001$, One-way ANOVA (repeated measures) Tukey Post-hoc analysis) however, revealed there was no significance for stimulation with similar speed of presentation, but different contrast.

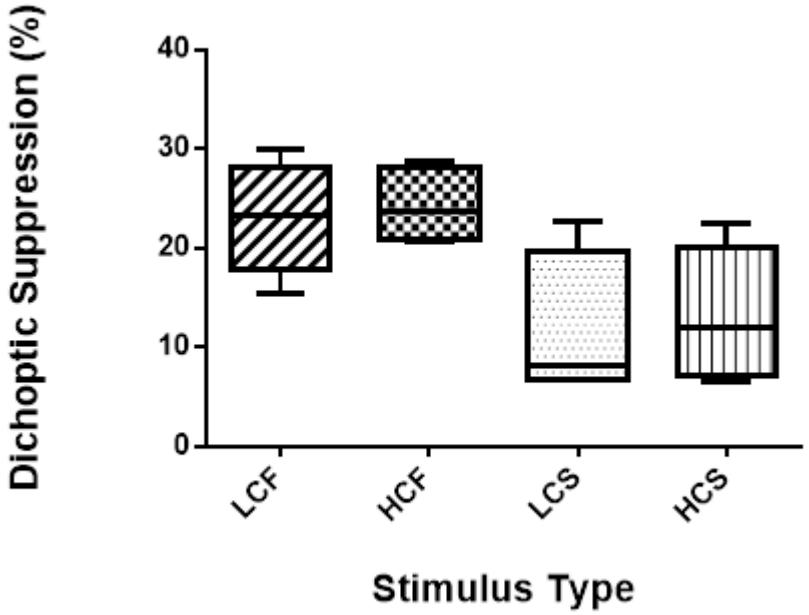

Figure 4-6 - Averaged amplitudes for dichoptic suppression for the four stimulus types (note there is no difference between dichoptic suppression at the same presentation speed)

When analysed for eccentricity effect the DS profiles of low contrast and high contrast recordings were very similar for the fast mode of stimulus presentation. It demonstrated the largest DS in the central part of the visual field which significantly declined towards the periphery. There was a significant difference between ring 1 and ring 5 ($p=0.033$) for LC and between ring 1 and between rings 4 ($p=0.025$) and 5 ($p=0.038$) for HC (One-way ANOVA) but no difference with respect to eccentricity between stimuli of the same presentation speed.

A similar profile of DS (large central suppression declining toward periphery), although of a lesser magnitude, was also present at slow stimulation mode. LCS differed significantly between ring 1 and rings 3 ($p=0.003$), 4($p=0.001$) and 5 ($p=0.001$). HCS differed significantly between ring 1 and rings 3 ($p=0.001$), 4($p<0.001$) and 5 ($p<0.001$). There was however no difference between LCS and HCS at any eccentricity ($p>0.05$, one-way ANOVA). (Figure 4-7)

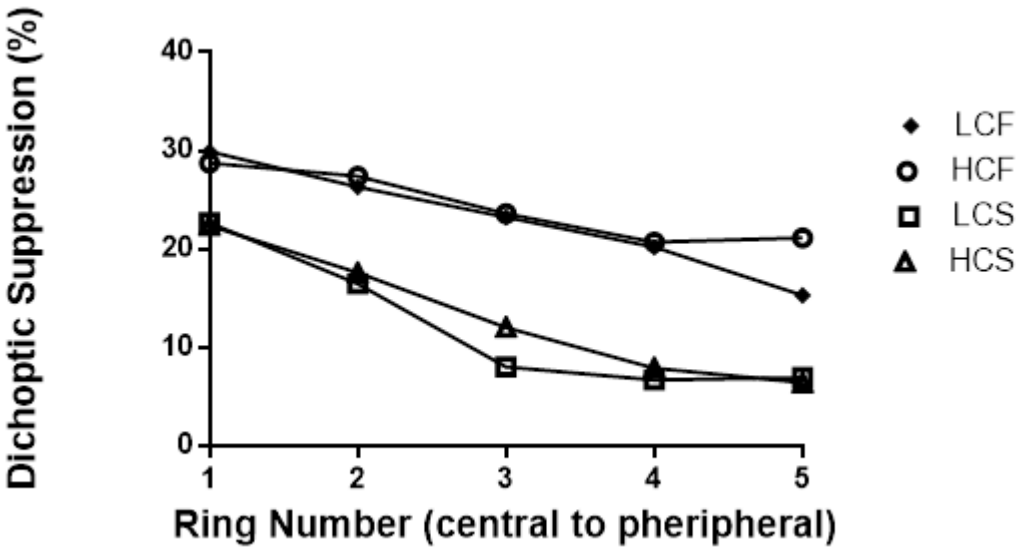

Figure 4-7 - Dichoptic suppression profile for 4 stimuli. There is no difference between stimuli of the same presentation speed.

5 DISCUSSION

We have recently[142] described the phenomenon of the mfVEP amplitude suppression under dichoptic conditions of stimulus presentation. We demonstrated that DS is critically dependent on speed of presentation (inter-eye stimulus interval) and it increases with stimulation frequency[73]. We also have shown an eccentricity-dependent nature of DS with significantly larger suppression in central retina and gradual reduction towards periphery. Contrast characteristics of DS, however, remain largely unknown[142].

In this study we sought to further characterise DS by assessing the combined effects of altering contrast levels and speed of presentation in order to investigate potential for biasing DS response towards either the parvocellular or magnocellular pathway.

The magnocellular and parvocellular pathways of the anterior visual pathways have distinctly different spatial and temporal properties and are segregated from the retina through the LGN and up to the entry level of striate cortex (layer 4C). Parvocellular neurons are slow with sustained response to light (low-pass filter with 5–10-Hz corner frequency), whereas the magnocellular pathway is more transient with band-pass temporal characteristics having maximum sensitivity at approximately 20 Hz[106]. Spatial distribution of magnocellular and parvocellular neurons is also different with ratio of parvo/magno increasing with retinal eccentricity by as much as 10 fold.

Based on the abovementioned properties of magnocellular and parvocellular pathways we expected to see differences in magnitude of DS. Since parvocellular neurons are slower we expected to see higher DS for high contrast stimulation, while for low contrast stimulation we expected to see a lesser increase in DS at a high speed of stimulation since it mainly targets the fast magnocellular neurons. We also expected to see changes in the retinal distribution of DS at high/low contrast or fast/slow stimulation speed since the proportion of magnocellular/parvocellular neurons varies significantly across the retina.

The study revealed that the amplitude of monocular mfVEP is significantly affected by both the speed of presentation and contrast of the stimulus. Amplitude was generally larger for higher

contrast and slower temporal frequency of stimulation, i.e. for fixed level of the stimulus contrast the amplitude was larger for slower stimulation and for fixed level of the stimulation rate the amplitude was larger for higher contrast of the stimulus. This tendency was preserved at all eccentricities of the stimulated visual field. Similar results were obtained for dichoptic stimulation.

We confirmed previous finding that dichoptic suppression is dependent on temporal characteristics of stimulation. This effect was observed at all eccentricities. Contrary to our expectations, however, the magnitude of DS did not relate to contrast characteristics of the stimulus. DS was observed to increase similarly between slow and fast stimulation for both low and high contrast stimuli. Furthermore, the DS eccentricity profile was identical for both (high and low contrast) types of stimulation, indicating similar retinal distribution of elements underlying the DS.

We believe that the most likely explanation for the observed result is the convergence of the magnocellular and parvocellular neurons at the supragranular layer of the striate cortex [25], which causes a balancing of M-cell and P-cell properties. Neurons in the cortical entry layer 4C remain clearly separated into magnocellular (4Cα) and parvocellular (4Cβ) sub-layers, but better respond to diffuse (flash) stimulation and the majority of them are monocular (therefore not optimally stimulated by pattern mf VEP), while the majority of higher order neurons (layer 2/3, 5 and 6), better respond to grating (better stimulated by pattern mfVEP) and are binocular (therefore having potential for generating DS), but they have mixed magno/parvo input.[145-147] We acknowledge the effects of contrast in binocular rivalry [148] and that there are similar physiological processes in suppression and rivalry. Even though we were unable to demonstrate an effect of contrast on DS levels, we still believe there may be an effect but that the mfVEP stimulus presentation effectively has a mean luminance effect rather than the contrast between gratings as used in binocular rivalry studies.

The above reasons could be the explanation for the apparent loss of M or P-cell specificity in mfVEP dichoptic suppression, while temporal dependence of the magnitude of DS on speed of presentation may simply reflect the nature of slow temporal resolution of high order cortical neurons.

We previously demonstrated a beneficial effect of DS in early detection of unilateral abnormalities in glaucoma. Increased asymmetry of mfVEP amplitude in glaucoma patients, however, was mainly restricted to the central part of the visual field since stimulation rate was slow. Fast stimulation used in the current study resulted in significant DS in the periphery. However, whether or not it will result in early glaucoma detection remains to be seen. The potential increase in DS appears to be related to speed of presentation only, which likely reflects the RGC population shift from centre where the dominant population are parvocellular RGCs (lower temporal resolution, higher DS) to more peripheral locations where the dominant population are magnocellular RGCs (higher temporal resolution, lower DS). The change in DS as indicative of RGC population change can be used to target peripheral magnocellular RGC dense areas but shifting the contrast appears to not add significant advantages.

The implications for the use of DS in glaucoma detection are that the stimuli choice needn't be limited by contrast in order to maximise DS. The findings add further information to the ongoing understanding of the role of subpopulations of RGCs in visual processing of the human visual system.

Chapter 5 COMPARISON OF LOW LUMINANCE CONTRAST (LLA) AND BLUE ON YELLOW (BONY) STIMULATION WITH FAST AND SLOW PRESENTATION IN THE DETECTION OF GLAUCOMA

Pilot Study (unpublished data)

Summary

This study incorporates the two preceding chapters into a clinical pilot study comparing degree of inter-eye asymmetry in four stimulus conditions to identify a sensitive stimulus for use in a larger clinical study. The study further investigates the thesis that faster stimulation increases dichoptic suppression and targeting of the koniocellular RGC pathway could increase rates of detection in early unilateral glaucoma.

1 AIMS

1) Using dichoptic mfVEP, to investigate whether colour of the stimulus or speed of presentation altered sensitivity of detection of glaucoma by assessing inter-eye asymmetry and amplitude profiles
2) Decide upon the optimum stimulus for use in a larger study investigating the early detection of glaucoma using dichoptic mfVEP

2 BACKGROUND

For the detection of glaucoma, dichoptic mfVEP using VR goggles[75] utilized a High Luminance Achromatic (HLA) stimulus (Michelson contrast of 99%) and a slow stimulation speed (18 frames/seq, 1.66 frames/sec) in order to minimise interocular suppression. The mfVEP stimulus has three major properties which can be altered to target the desired retino-ganglionic-cortical pathway namely, stimulus contrast, chromaticity and speed of stimulus presentation. These properties have been manipulated by research groups to target either normal pathways or demonstrate defects in disease states. [48,50,121,122]

Recent work by the same group[50] demonstrated that a Low Luminance Achromatic (LLA) stimulus was superior over HLA for detection of early glaucoma using monocular mfVEP. In the same paper, Arvind et al., showed that Low Luminance Achromatic (LLA) and Blue on Yellow (BonY) were comparable in their sensitivity for early glaucoma detection. They concluded from these findings that the low-luminance component of the LLA and BonY stimuli provided the extra sensitivity in early glaucoma and not chromatic properties or pattern-onset mode of presentation. These findings suggested that the stimulus types that would likely be useful in glaucoma detection would be either LLA or BonY, with the chromatic component seeming to not add a significant advantage over achromatic[50]. Despite these findings, the inclusion of a blue on yellow stimulus in these experiments was felt necessary as the koniocellular cells could respond differently under conditions of dichoptic suppression.

The speed of stimulus presentation, i.e. the interval between stimulus on and off states, is the third defining factor in deciding on stimulus type. Many studies have shown[62,73,149] that there is a close

relationship between speed of stimulation and interocular suppression, with Arvind et al.[73] finding that a 1.66 frames/sec speed adequately minimised dichoptic suppression whilst still maintaining a reasonable testing time.

As we sought to maximise dichoptic suppression, to utilise the enhanced inter-eye asymmetry[75] thought to be integral to the mechanisms by which dichoptic mfVEP was more sensitive than monocular alone, we hypothesised that a faster stimulus might be appropriate. This needed to be examined in a population of well-characterised glaucoma patients in order to identify the most appropriate stimulus for use in a larger clinical study.

3 METHODS

Recording and experimental conditions have been described previously. Briefly the setup consisted of two mounted LCD screens (response time 2 ms; Flatron L1954TQS monitor; LG, Englewood Cliffs, NJ) on each side of the subject reflected through centrally located semitransparent mirrors to project a stimulus of 0° to 24° of eccentricity simultaneously to each eye. Mounted behind the mirrors were two infrared cameras, which continually monitored pupil position. Four infrared light-emitting diodes were placed around a lens holder to illuminate the eyes. Stimuli were presented simultaneously (dichoptically) to both eyes, as described previously. The display to each eye consisted of a cortically scaled dartboard with 56 segments arranged in five concentric rings (1°–2.5°, 2.5°–5°, 5°–10°, 10°–16°, and 16°–24°) and a central fixation target extending up to 0.5°. The stimulus in any segment consisted of a 4x4 check pattern. Segment size was scaled according to the cortical magnification factor. Corresponding to the size of the segments, the size of the individual checks also increased with eccentricity. A central fixation target was provided that consisted of rotating and slowly changing letters. These features—the ring arrangement and the fixation target—were identical for both eyes, which helped to fuse the images. The patient, therefore, perceived a single binocular image of the dartboard stimulus.

Pseudorandom binary sequences (PRBSs) were used to drive the stimuli at each test location, so that the presentation at each location was random and independent of other locations. Each binary sequence had a 50% probability of being 1 or 0 at any point of time. There were 4 different types of

stimuli, recorded dichoptically. There were 2 stimuli – Low Luminance contrast Achromatic (LLA) consisting of darker grey checks (40 cd/m^2) on a lighter grey background (125 cd/m^2, Michelson contrast 52%); Blue on yellow (BonY) consisting of the blue checks (40 cd/m^2Commission Internationale d'E´clairage (CIE) coordinates, 0.15, 0.06) on a yellow background (125 cd/m^2CIE coordinates, 0.46, 0.49).

At each location the stimuli were driven by pseudorandom binary sequences (PRBSs) enabling the presentation to be random and independent of other locations. The presentation has been described previously[142], each binary sequence had a 50% probability of being 1 or 0 at any point in time.

In order to test the effects of temporal closeness on interocular suppression, two temporal separations were used for each stimulus. "Fast" stimulation consisted of 2 elements - Element 1 was represented by two consecutive states: pattern on, lasting two frames of the screen (33.3 ms), when the stimulus pattern was displayed, and pattern off, lasting 7 frames (116.7 ms), when the whole segment was diffusely illuminated with an intensity of the mean luminance. Element 0 consisted of the pattern-off state for 9 frames. The average rate of presentation at each segment was 3.33 times/s. The presentation of the stimulus to the corresponding segment of the second eye was always shifted by 4 or 5 frames, alternating between sequences of 9 frames (i.e. 4 frames separation followed by 5 frames, followed by 4 and so forth); therefore, the minimum separation between stimuli to corresponding areas of the visual fields of both eyes was 2 frames. Each run lasted 69 seconds and 6-8 runs were recorded per stimuli.

"Slow" stimulation consisted of 2 elements - Element 1 was represented by two consecutive states: pattern on, lasting two frames of the screen (33.3 ms), when the stimulus pattern was displayed, and pattern off, lasting 16 frames (266.4 ms), when the whole segment was diffusely illuminated with an intensity of the mean luminance. Element 0 consisted of the pattern-off state for 18 frames. The average rate of presentation at each segment was 1.66 times/s. The presentation of the stimulus to the corresponding segment of the second eye was always shifted by 9 frames. Therefore there was a

minimum of 7 frames between stimulation of corresponding areas of the visual field. Each run lasted 139 seconds and 3-4 runs were recorded per stimuli.

3.1 RECORDING

Four gold cup electrodes (Grass, West Warwick, RI) mounted in an occipital cross-electrode holder were used for bipolar recording. Two electrodes were positioned 4 cm on either side of the inion: one in the midline 2.5 cm above the inion and one 4.5 cm below the inion. Electrical signals were recorded along four channels as the difference between superior and inferior and between left and right, and obliquely between the left and inferior and right and inferior electrodes. A ground electrode was placed on one ear lobe. Cortical responses were amplified 100,000 times and band-pass filtered (1–20 Hz). Uniquely designed software correlated the responses with the stimulating PRBS and attributed the calculated signals to the respective segments of the visual field. This software also scaled the responses to the background EEG to reduce the interindividual variability. For every segment, the largest peak-to-trough amplitude of each wave within the interval of 60 to 200 ms was determined for each channel. The wave of maximum amplitude from each segment in the field from the four channels was automatically selected, and the software created a combined topographic map

3.2 PATIENT SELECTION

5 patients for the LLA and BonY comparison study (fast and slow stimulation) and 4 further patients on just BonY fast and BonY slow were selected. All had early glaucoma (average MD, worse eye = -4.32+/-2.56dB), stereopsis >100s, average age 71.1+/-4.7years, 4 males and were recruited for the study through a Sydney based glaucoma practice. This made a total of 5 patients on the full protocol plus 4 patients comparing BonY fast and slow. Patients had asymmetric disease (average difference between eyes = 3.43+/-2.38dB).

Written informed consent was obtained, and the experiments were conducted according to the tenets of the declaration of Helsinki. Only binocular recordings were made and the order of the recordings was randomised.

3.3 PATIENT CHARACTERISTICS

5 subjects underwent the full testing (fast/slow/BonY/LLA) protocol with a mean age of 73.4 +/- 6.34 years and a mean deviation of the worse eye of -5.55 +/- 1.89 dB. The 4 other subjects that were only tested using BonY fast and slow had a mean age of 68.0 +/- 5.29 years and a mean deviation of the worse eye of -3.39 +/- 2.40 dB.

3.4 STIMULUS ANALYSIS

Identification of a suitable stimulus was integral to be able to undertake the clinical study involving a selection of glaucoma patients and age matched normals. In choosing the stimulus we sought to identify if one colour or speed of stimulation enhanced the Relative Asymmetry Coefficient (RAC) (Equation 5-1) between normal and abnormal segments. RAC was calculated as:

$$RAC = \frac{Amplitude\ Right\ eye - Amplitude\ Left\ eye}{Amplitude\ Right\ eye + Amplitude\ Left\ eye}$$

Equation 5-1 - Relative Asymmetry Coefficient (RAC)

RAC was used as a surrogate marker of disease as each patient had asymmetry in the severity of glaucomatous field loss, as defined by HVF testing. The assumption lies in the belief that the higher the RAC, the higher the likelihood that a particular stimulus detected unilateral field loss. Patients were analysed in two groups – 5 patients varying stimulation speed and chromaticity (4 testing conditions) and 9 patients varying only stimulation speed in comparing fast BonY and slow BonY (2 testing conditions).

GraphPad ® (Prism 6 for Windows 2012) was used for all statistical analysis using t-testing wjth Bonferroni correction for multiple comparisons or ANOVA with Tukey correction where appropriate.

4 RESULTS

4.1 FAST VERSUS SLOW STIMULI

Stimulation speed had a negative effect on the stimulation amplitude, chromaticity notwithstanding (Figure 5-1). Fast stimuli produced smaller averaged amplitudes, compared with slow stimuli (paired t-test, $p<0.0001$).

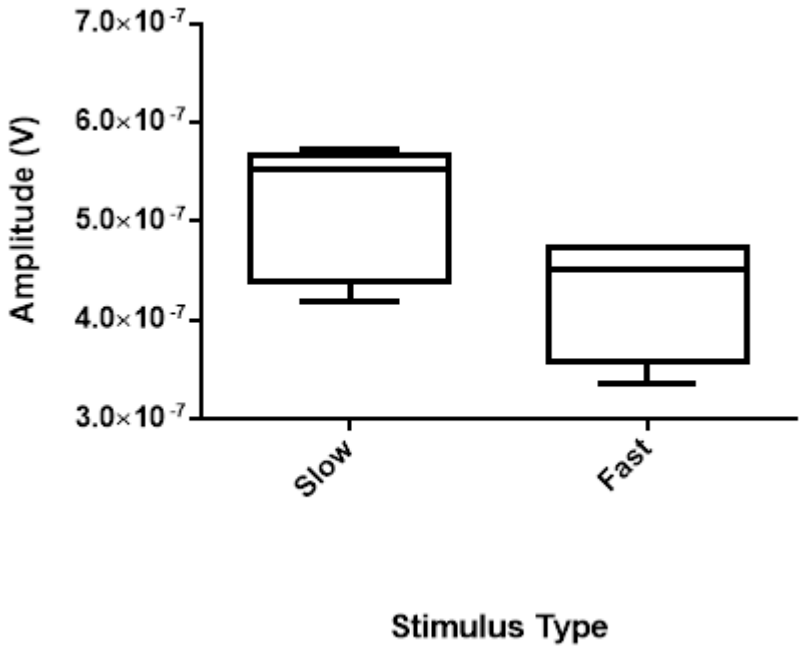

Figure 5-1 - Comparison of averaged amplitudes for fast and slow stimulation speed (both BonY and LLA included)

4.2 AMPLITUDE PROFILES

BonY fast and LLA fast had average amplitudes of 421+/-65nV and 424+/-60nV respectively. There was no significant difference (paired t-test, $p>0.05$) between the two stimulation types. BY slow and LLA slow had amplitudes of 520+/-67nV and 505+/-71nV respectively. In stimuli of the same speed there was no significant difference between BonY fast and LLA fast (paired t-test, $p = 0.39$), however there was a significant difference between BonY slow and LLA slow (paired t-test, $p = 0.009$, Bonferroni correction ($p=0.08$)) (Figure 5-2). In stimuli of the same chromaticity there was a significant difference (paired t-test, $p<0.0001$, Bonferroni correction ($p=0.08$)) between slow and fast stimulation, in keeping with the previous results on the effect of stimulation speed and amplitude (Figure 5-2).

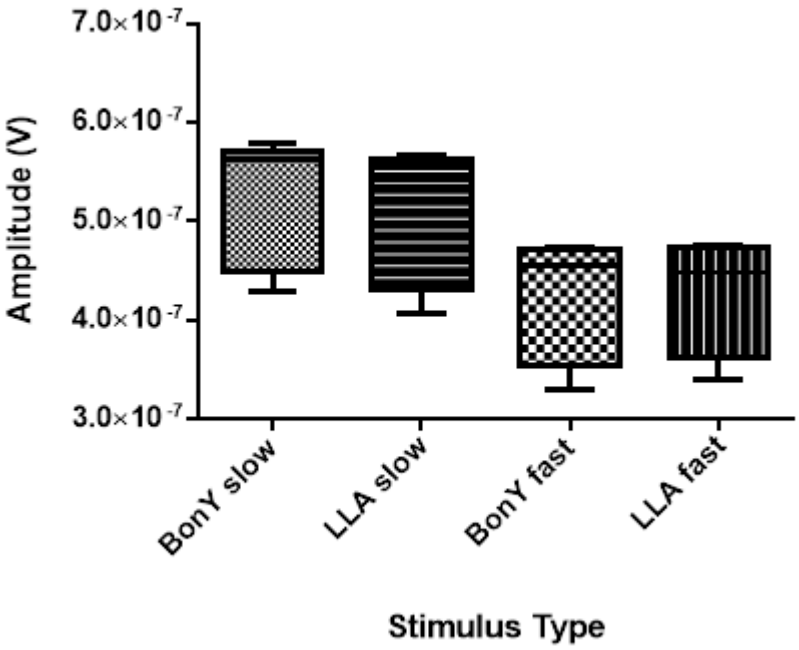

Figure 5-2 - Stimulus type versus averaged amplitude demonstrating the effect of stimulus speed and chromaticity on amplitude profiles

4.3 Effect of eccentricity on amplitude

All 4 curves follow a similar pattern from central to peripheral rings and noticeably there is no overlap between different stimulation speeds. There are demonstrably smaller signals (Figure 5-3) in the centre of the stimulus and larger signals peripherally, with the largest signals being mid-peripheral (ring 3).

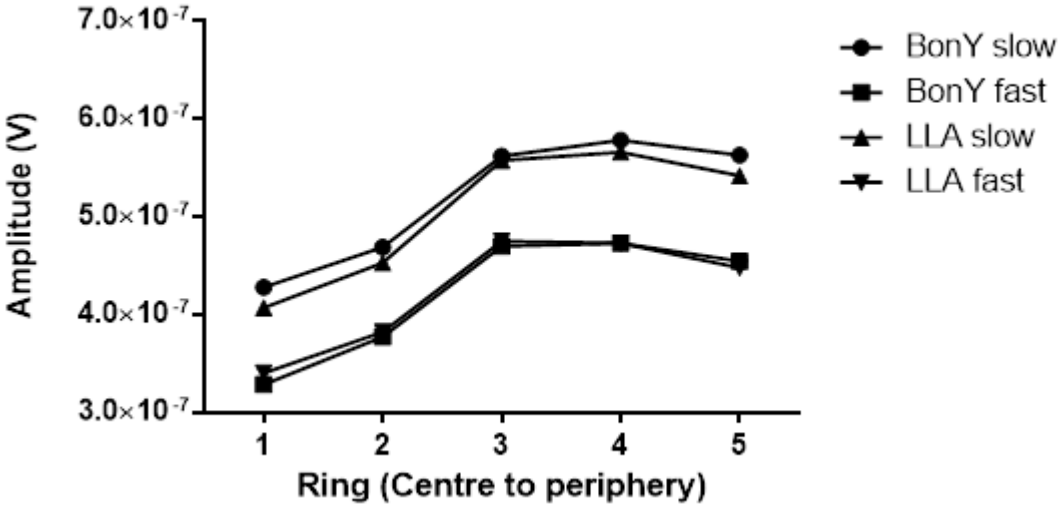

Figure 5-3 - Profile of stimuli with change in eccentricity demonstrating centrally smaller signals, increasing with increasing eccentricity

4.4 ASYMMETRY PROFILES

Of the stimulus conditions tested, the BonY fast had the highest RAC of the 4 stimuli with an RAC = 0.227+/-0.068, followed by BonY slow with an RAC = 0.214+/-0.073, then LLA fast RAC = 0.202+/-0.078 and LLA slow had the lowest RAC = 0.174+/-0.067. BonY fast was significantly different from from all other stimuli (1 way ANOVA, Tukey multiple comparison correction, $p<0.05$). When 4 more glaucoma patients were added to the analysis comparing BY fast and BY slow, the RAC was not significantly different; BonY fast average RAC, RAC=0.222+/-0.115, versus BonY slow, RAC=0.174+/-0.089 ($p=0.071$, paired t-test) as seen in Figure 5-4.

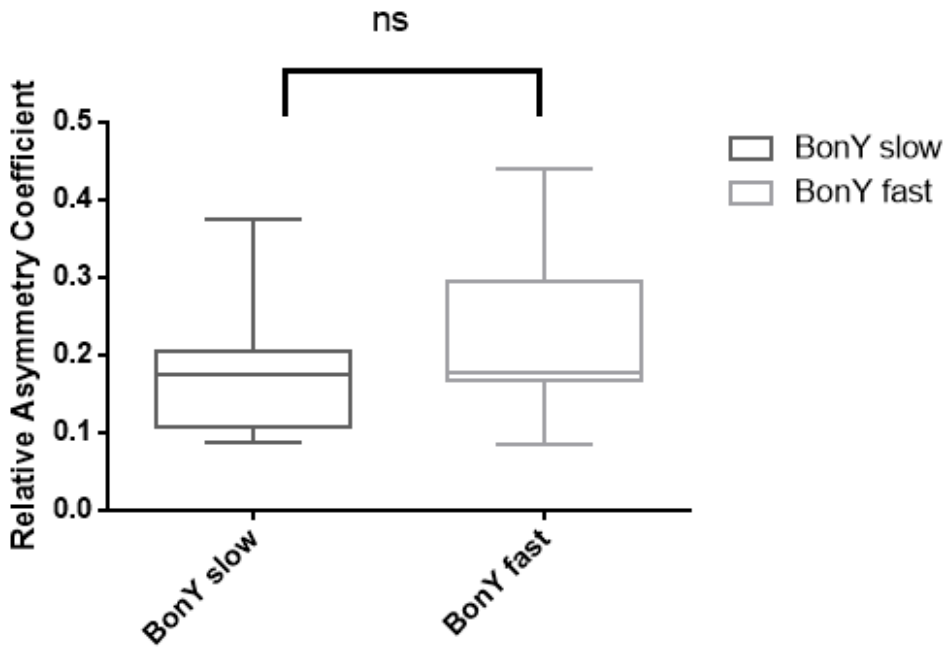

Figure 5-4 - Average RAC for BonY slow and BonY fast stimuli showing no significant difference

When the data were analysed with respect to eccentricity (Figure 5-5) there was a no significant difference between rings of BonY fast and BonY slow (ANOVA (Tukey post-hoc repeated measures) $p > 0.05$).

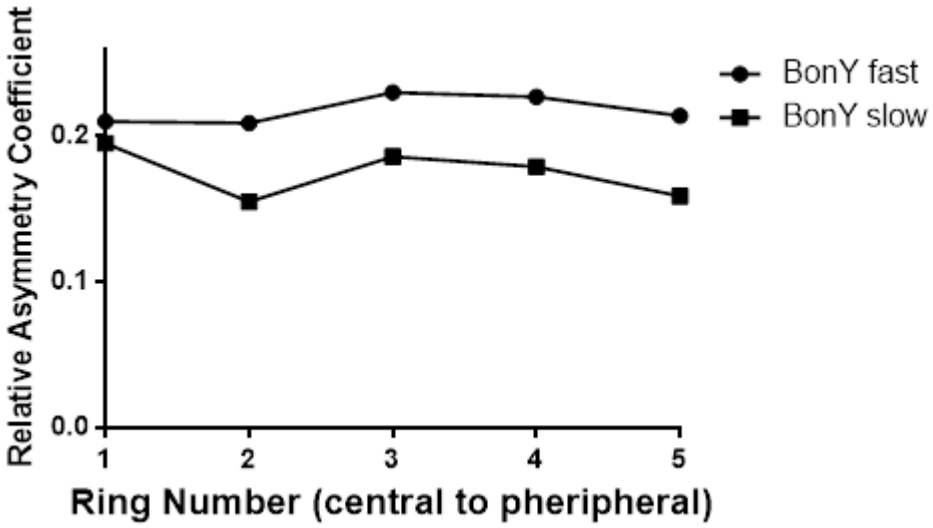

Figure 5-5 - Relative asymmetry coefficient for BonY fast vs. BonY slow versus eccentricity.

4.5 RECORDING TIME

For each of the fast stimuli average recording time is 6-8 runs of dichoptic stimulation which is approximately 10 minutes of testing time, for the slow stimulation this was approximately the same at 3-4 runs each of 2 minutes.

5 DISCUSSION

Detection of glaucoma with mfVEP can be optimised with the appropriate stimulus selection. As Arvind et al demonstrated[50], the difference in luminance between low contrast and high contrast can significantly affect glaucoma detection rates. In the detection of MS the use of dichoptic spatially sparse stimuli has been shown to be more sensitive and specific for quantifying progressive damage versus contrast reversal[150]. These findings built on work using temporally sparse dichoptic stimulation with liquid crystal polarizing shutters[62] and comparison of rapid contrast reversal, rapid pattern pulse presentation, and slow pattern pulse presentation[122]. Arvind further demonstrated, using dichoptic mfVEP goggles, the effects of closeness in timing on dichoptic suppression[73].

The use of a fast stimulation rate inevitably leads to lower amplitude generation resulting in a compromise between the need to maintain sufficient dichoptic suppression to increase asymmetry and sufficient amplitude generation to be safely above background noise levels, typically around 100-200nV. There is a reduction in signal size from BY slow to BY fast of 19% and similarly for LLA slow to LLA fast of 16%, however the size of the signals is still adequate to produce recordings with amplitudes greater than 300nV. However the advantage of fast stimulation is that the examination is completed in a shorter amount of time and with greater frequency of stimuli.

The aim of the experiments was to isolate a stimulus which had characteristics that would allow an increase in asymmetry of mid to peripheral glaucomatous defects. BonY fast had significantly more dichoptic suppression as evidenced by the smaller amplitudes compared to the slower stimuli. Fortunately the suppressive effects were not so pronounced that the recordings were clinically relevant and greater than background noise (i.e. above 300nV).

In these experiments the average asymmetry of BonY fast and BonY slow was not significantly different when tested using ANOVA repeated measures analysis. This outcome is likely to be due to variability driven by the differing visual field defects that exist between the subjects, the low number of subjects in the study and/or the inherent errors in recording mfVEP, especially peripheral rings where the amplitudes are often variable and lower than central rings.

The most likely case is that the peripheral suppression (and therefore potential for asymmetry) is similar for slow and fast stimulation owing to the declining effect of dichoptic suppression with increasing amplitude[142]. The inherent variability of mfVEP recordings and small sample size has meant that none of the 5 ring suppression figures have reached significance when comparing BonY fast and BonY slow. Additionally glaucoma is inherently a disease that varies with eccentricity as the arcuate pattern of the visual loss is encapsulated by multiple rings, we sought to ameliorate this difficulty by comparing the same patients (ie the same visual field defects) on different settings. This issue does complicate analysis and has been addressed as best as can be.

This project sought to focus on investigating the role of dichoptic suppression in asymmetry analysis in dichoptic mfVEP – thus identifying a stimulus that could maximise asymmetry was the goal of this chapter. Importantly, the asymmetry generated by BonY was significantly greater than the LLA stimulus types. Although there was no difference seen between BonY fast and BonY slow asymmetry values the experiment demonstrated non-inferiority of BonY fast versus BonY slow, so that BonY fast could still be useful for a larger clinical trial. Arvind et al[75] used a LLA stimulus for the original goggle dichoptic trial, which stimulated to 16 degrees of eccentricity – 24 degrees of eccentricity, as used here, incorporates a larger portion of the RGC population adding in the complicated effects of the interaction between konio-, magno- and parvocellular cells. These factors all play a role in determining appropriate stimulus choice for glaucoma detection.

Based upon previous work[142], the increase in asymmetry is generated from the dichoptic suppression present as a result of the dichoptic viewing conditions and the degree of dichoptic suppression, and hence asymmetry, is a function of the closeness in timing of stimulation of binocularly corresponding visual field segments[73]. It then follows that the fast stimulation should generate greater inter-eye asymmetry in glaucomatous patients. However it is unclear as to why the BonY has a higher RAC than the low contrast stimulus, whilst maintaining similar amplitudes. Potentially this could be explained through the recruitment of the koniocellular pathway which, although not registering an increase in overall amplitude, could contribute to the suppressive effects observed with dichoptic stimulation. The characteristics of the koniocellular RGCs are that they are small diameter axons [25], are

temporally sluggish, relay the blue-ON RGC [151] input and influence field properties of V1 cells in layer 2/3[25]. As koniocellular cells have a slower temporal responsiveness, they are likely to have contributed to the increased dichoptic suppression. Damage to this pathway has been suggested as a reason for the deficits seen with some glaucoma patients using SWAP testing. [152,153]

6 CONCLUSION

The temporal processing resolution of the koniocellular pathway may increase the degree of dichoptic suppression and account for the increase in asymmetry seen with this set of experiments. The above issues have formed the basis for the subsequent chapters to explore the utility of fast stimulation and the nature of dichoptic suppression in normal and glaucomatous patients.

Chapter 6 THE ROLE OF INTEROCULAR SUPPRESSION IN THE DETECTION OF GLAUCOMATOUS DEFECTS USING DICHOPTIC MFVEP FAST BLUE ON YELLOW STIMULATION

Prepared for submission as:

Leaney, J., Klistorner, A., Sriram, P., Graham, S. L., *The role of interocular suppression in the detection of glaucomatous defects using dichoptic mfVEP fast blue on yellow stimulation.*

Summary

Previous chapters have demonstrated the effects of eccentricity and presentation speed on dichoptic suppression. Hence, this study used the stimulus characteristics of fast, blue on yellow dichoptic and monocular mfVEP to explore the differences between monocular and dichoptic stimulation, comparing these technologies with the gold standard of Humphrey visual field testing. The finding that there was greater asymmetry in dichoptic stimulation versus monocular and that this asymmetry was accurate to the side of disease, demonstrated the sensitivity and accuracy of dichoptic mfVEP.

1 AIMS

1) To assess for a difference in detection of early glaucoma between monocular and dichoptic mfVEP using fast blue on yellow stimulus
2) To investigate whether the benefit of higher suppression for increased asymmetry is balanced by the increased degree of dichoptic suppression

2 INTRODUCTION

Detection of glaucoma at its earliest stages is crucial to early diagnosis and treatment, allowing subsequent visual loss to be arrested or slowed. Primary open-angle glaucoma is a prime example of the advantage of early detection. [15,16]. Glaucoma in its earliest stages is unilateral, subtle and often missed.[154]. Inter-eye asymmetry analysis has been shown to offer significant advantages in detection over analysis of amplitude traces alone even when part of large normative databases.[48,49,75]

The sensitivity of multifocal visually evoked potentials (mfVEP) for detecting glaucoma in its earliest stages has been demonstrated in a number of studies.[48,49,54] The development of a blue on yellow stimulus has afforded greater sensitivity in detection[48].

Further to the development of the blue on yellow stimulus, Arvind et al[73] published on the development of a true dichoptic mfVEP apparatus using virtual reality goggles. They demonstrated that dichoptic mfVEP has some advantages over monocular stimulation alone in glaucoma detection [75]. The increase in detection was theorised to originate from the tightness in asymmetry of the normals database and possible increase in asymmetry between normal and abnormal segments converging at the level of the binocular neurons of the same cortical locations [76,109]. We have demonstrated that suppression of one eye causes release of suppression of the fellow eye[142] and postulated that this may underlie the mechanisms of increasing asymmetry seen with dichoptic mfVEP stimulation[142].

As the amplitude generated in mfVEP dichoptic stimulation is at least partially dependent upon the speed of stimulus presentation[73], likely owing to the temporal processing of the three main types of retinal ganglion and the binocular neuron interactions at layer 4C of V1[109], an increase in stimulation speed may well cause an increase in asymmetry using dichoptic mfVEP. Previous work with VR

goggles[75] used a stimulus speed which was optimal for amplitude generation and minimised dichoptic suppression. We sought to explore whether there was a benefit to increasing the stimulus presentation speed over previous experiments and whether the increase in speed generated greater asymmetry and therefore more sensitive glaucoma detection using inter-eye asymmetry analysis.

3 METHODS

29 early glaucoma patients (average MD (worst eye) = -3.54) were recruited from two Sydney-based glaucoma specialty practices. Ethics approval was gained from the University human ethics department and the experiments were conducted in accordance with the tenets of the declaration of Helsinki.

All patients had comprehensive medical and ophthalmic histories and examination recorded including Goldman applanation tonometry, fundoscopy, slit lamp examination and gonioscopy. The diagnosis of glaucoma was made by a glaucoma specialist prior to the study based upon optic disc appearance with focal thinning of the neuroretinal rim matching visual field loss consistent with glaucoma including arcuate patterns or clusters, respecting the horizontal meridian on HVF. Each patient had the minimum requirements of stereopsis >100 seconds of arc and visual acuity >6/18 in the worse eye. Patients also were free of other ocular diseases affecting visual function besides glaucoma namely diabetic retinopathy, macular degeneration, vitreous opacity and cataract.

The normals database was constructed from 18 healthy age-matched normals having no history of ocular disease or eye surgery, excepting cataract, having best corrected visual acuity > 6/9, stereopsis>60 seconds of arc and normal ophthalmic exam results and testing (which included normal SD-OCT RNFL circumpapillary scan, HVF (white on white 24-2) with a Glaucoma Hemifield Test (GHT) within normal limits, IOP < 15mmHg and normal appearance of the optic disc.

3.1 MFVEP TESTING

All patients, both normal and glaucomatous, underwent mfVEP on monocular and dichoptic testing using a dichoptic mfVEP described previously[142]. Briefly the setup consisted of two mounted LCD screens (response time 2 ms; Flatron L1954TQS monitor; LG, Englewood Cliffs, NJ) on each side of the subject reflected through centrally located semitransparent mirrors to project a stimulus of 0° to 24°

of eccentricity simultaneously to each eye. Mounted behind the mirrors were two infrared cameras, which continually monitored pupil position. Four infrared light-emitting diodes were placed around a lens holder to illuminate the eyes (Figure 2-3 (Methods, Chapter 2)).

Stimuli were presented simultaneously (dichoptically) to both eyes, as described in chapter 2 methods. Briefly, the display to each eye consisted of a cortically scaled dartboard (Fig. 1A) with 56 segments arranged in five concentric rings (1°–2.5°, 2.5°–5°, 5°–10°, 10°–16°, and 16°–24°) and a central fixation target extending up to 0.5°. The stimulus in any segment consisted of a 4x4 blue-on-yellow(BonY)[48] check pattern. Segment size was scaled according to the cortical magnification factor.[155] Corresponding to the size of the segments, the size of the individual checks also increased with eccentricity. The luminance of the blue check was 40 cd/m^2, and the luminance of the yellow background was 125 cd/m^2. A central fixation target was provided that consisted of rotating and slowly changing letters. These features—the ring arrangement and the fixation target—were identical for both eyes, which helped to fuse the images. The patient, therefore, perceived a single binocular image of the dartboard stimulus. Pseudorandom binary sequences (PRBSs) were used to drive the stimuli at each test location, so that the presentation at each location was random and independent of other locations. Each binary sequence had a 50% probability of being 1 or 0 at any point of time.

Element 1 was represented by two consecutive states: pattern on, lasting two frames of the screen (33.3ms) when the stimulus pattern was displayed, and pattern off, lasting 7 frames when the whole segment was diffusely illuminated with an intensity of the mean luminance. Element 0 consisted of the pattern-off states for 9 frames. The average rate of presentation at each segment was 3.32 times/s. The presentation of the stimulus to the corresponding segment of the second eye was shifted by either 4 or 5 frames, the number of shifted frames alternating between stimulus presentations. The minimum separation between stimuli to corresponding areas of the visual fields of both eyes was either 2 (33.3ms) or 3 frames (50.0 ms). Three runs were recorded, each lasting 69 seconds.

Monocular recordings were performed with the same setup with one eye covered. Each patient underwent mfVEP testing in a random order for monocular and dichoptic testing with the three tests (binocular and 2 monocular) performed consecutively without breaks.

3.2 ANALYSIS

The aim of the analysis was to compare the sensitivity of the monocular and dichoptic mfVEP testing paradigms for detecting asymmetry between eyes that corresponded to glaucomatous damage. To assess if the correspondence between mfVEP field defects and glaucomatous damage was apparent, HVF, OCT and mfVEP were analysed and the location with worst defect identified. For HVF this was the location with the most significant (most number of points $p<0.02$) visual field defect. A visual field defect, as previously described[48], was defined as a scotoma with 3 or more abnormal points, with at least 2 points depressed by $p<0.02$ on the pattern probability plot. The cluster of abnormal points could not cross the horizontal meridian and points immediately above and below the blind spot could not qualify as part of the scotoma. Peripheral rim points could qualify as part of the overall scotoma, but at least 2 of the points qualifying as the nucleus had to be non-rim points.

To qualify as a glaucomatous field defect there had to be a corresponding significantly abnormal segment on OCT (OCT defect defined by Heidelberg Spectralis “outside of normal limits ($p<0.01$)” classification in one or more of 6 disc divisions (superotemporal (ST), inferotemporal (IT), inferior (I), inferonasal (IN), nasal (N), superonasal (SN), superior(S)). As this study was investigating the effects of dichoptic stimulation on disease asymmetry profile, the definition of the mfVEP abnormal location was the side identified by the Relative Asymmetry Coefficient (RAC). The RAC was negative in right sided disease and positive in left sided disease. As the patients studied had asymmetric disease this was used as an indicator of the side most affected by glaucoma.

A table summarising the comparison of the results was made to aid in establishing agreement of mfVEP recordings with HVF and OCT. If there was no agreement between the OCT and HVF, then the defect was not included in the analysis.

Further analysis was undertaken to discover any difference between dichoptic and monocular mfVEP. To do this we compared amplitude and asymmetry z-scores for both tests to elucidate the differences in glaucoma detection. Z scores were calculated for each segment (1 through to 56) (Figure 6-1) of each patient and an average z score for that eye was calculated. The z scores were then compared between the monocular and dichoptic tests. Amplitude and asymmetry were both analysed using z-scores and Student's t-test was used to assess the significance of any differences between dichoptic and monocular testing. No correction was made for multiple comparisons (ie Bonferroni or Tukey (ANOVA)) as there was no use of multiple t-testing. Instead t-testing was only used to assess the difference between 2 groups only.

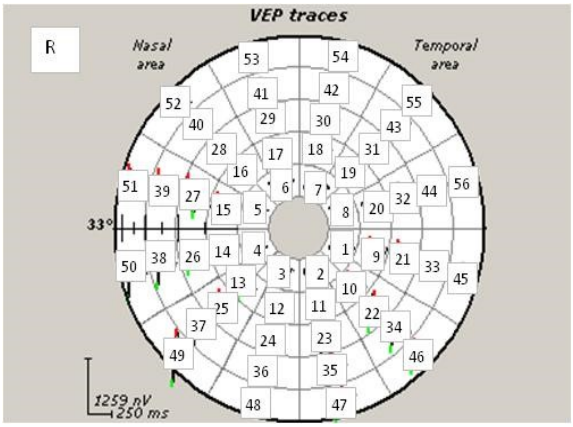

Figure 6-1 - MfVEP trace array showing segment distribution and numbering for a right eye

Averaged values for amplitude and averaged absolute values of asymmetry for each of the dichoptic and monocular tests were compared within groups of the normal and glaucoma patients. Absolute values of asymmetry were used as we were interested in the total value of asymmetry as this was considered important in analysing the effects of interocular suppression. If sign is retained for analysis, similar to work by Arvind et al[75]., the asymmetry would tend to balance out and the effects of increasing suppression/release of suppression would be less clear.

The normal patient asymmetry and amplitude values were used to calculate z-scores for amplitude and asymmetry for the glaucoma patients. The absolute magnitude of the z-score was used as an indicator of the accuracy of a test for assessing abnormality in the glaucoma population, the higher

the z-score, the higher the significance of the difference from the norm. The normals database was used to calculate average amplitude values and RAC values for each segment and to use the standard deviations of these values to calculate z-scores to calculate a p value. We used the formula below to calculate z-score for comparison of the monocular and binocular tests:

$$z = \frac{|x_n| - \lceil \mu_n \rceil}{\sigma_n}$$

x_n = asymmetry (or amplitude) value for specific patient at segment n (1≤n≤56)

μ_n = mean asymmetry (or amplitude) value for normal population at segment n (1≤n≤56)

σ_n =standard deviation of asymmetry (or amplitude) of normal population at segment n

Equation 6-1 - Z-score formula for calculating asymmetry z scores

where asymmetry is calculated as the relative asymmetry coefficient (RAC) is:

$$\frac{amplitude_{right\ eye} - amplitde_{left\ eye}}{amplitude_{right\ eye} + amplitde_{left\ eye}}$$

Equation 6-2 - Formula for calculating asymmetry using Relative Asymmetry Coefficient (RAC)

The absolute value was used for x_n and μ_n in equation 1 as asymmetry naturally has a sign to indicate the side of the imbalance between right and left eyes (negative indicating right sided disease, positive indicating left sided disease) but we sought to assess the magnitude of the deviation from the normal population values of asymmetry in order to identify which, if any, testing setup (dichoptic or monocular) was comparatively more sensitive. Hence the testing paradigm with the higher z-score should indicate which paradigm was the most sensitive to changes associated with glaucoma i.e. difference between fellow eyes.

Dichoptic suppression was calculated as follows (Equation 6-3):

$$\frac{Am - Ab}{Am} x100\%$$

Equation 6-3 - MfVEP dichoptic suppression, Am (Amplitude monocular), Ab (Amplitude binocular)

4 RESULTS

4.1 NORMAL POPULATION

Average amplitudes for the normals database were significantly higher for monocular testing. Average amplitude for monocular testing for right eyes was 734.5+/-184.4mV and for left eyes was 703.2+/-185.3mV. Average amplitude for dichoptic testing for right eyes was 600.6+/-153.7mV and for left eyes was 604.7+/-155.6mV. There was a significant difference between the averaged values of the right monocular and dichoptic values and the left monocular and dichoptic values (unpaired t-test, $p< 0.001$). There was no significant difference between right and left amplitudes of the monocular recordings (unpaired t-test, $p>0.05$). There was no significant difference between right and left amplitudes of the binocular recordings (unpaired t-test, $p>0.05$). The monocular and binocular recording amplitudes were significantly different (unpaired t-test, $p<0.0003$) (Figure 6-2).

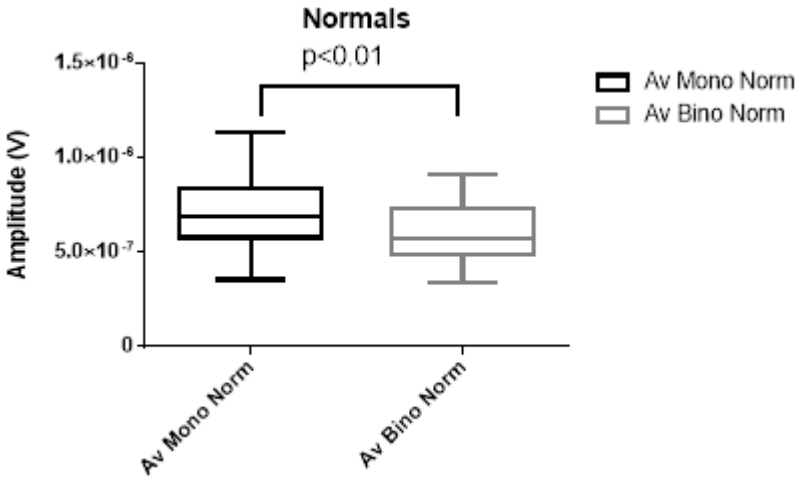

Figure 6-2- Normal population values for monocular and dichoptic (binocular) mfVEP recordings

The arithmetic means of the asymmetry values for the normal population were 0.071 +/- 0.019 for monocular recordings and 0.092+/-0.027 for binocular recordings. There was a significant difference between the monocular and binocular asymmetry values (Mann Whitney, $p<0.0001$ - two tailed) (Figure 6-3).

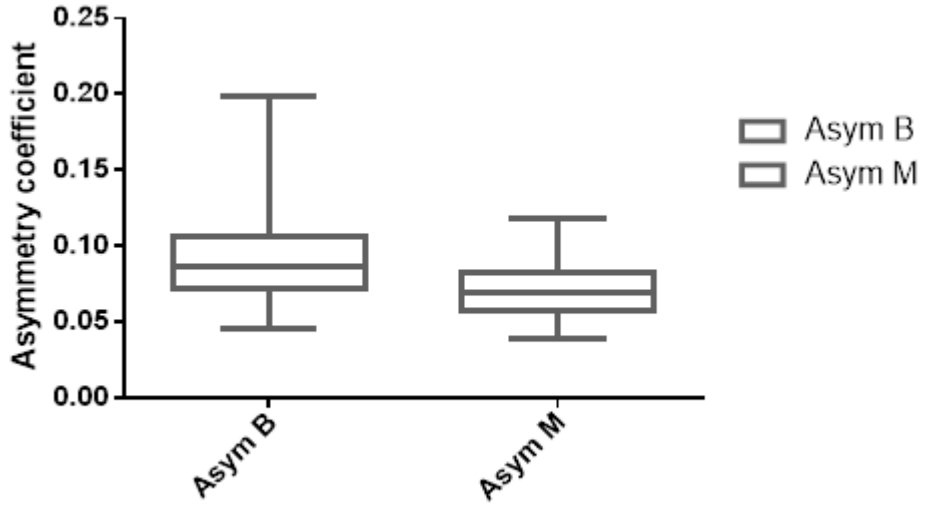

Figure 6-3 - Average asymmetry coefficient for normal patients on binoc and monoc recording settings.

4.2 GLAUCOMA POPULATION

In the 29 patients with early glaucoma the average amplitudes for monocular recordings were 685.3+/-185.0mV and for binocular recordings, 561.0+/-154.1mV. Monocular and binocular averaged amplitudes were significantly different (Mann-Whitney, p<0.001, 2 tailed) (Figure 6-4).

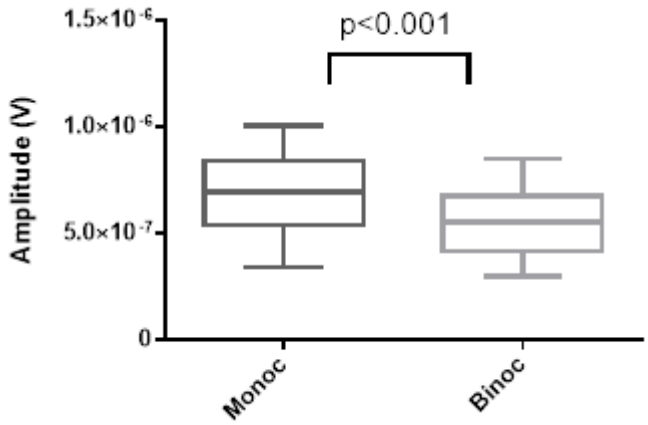

Figure 6-4 - Averaged amplitude for monoc and binoc recordings for glaucoma patients, note the significant difference between testing types

Z-score values for amplitudes in glaucomatous patients on monocular testing gave an average of z = 0.778+/-0.143, dichoptic z-scores gave an average z = 1.111+/-0.240. The difference between the 2 z-scores was significant. (Paired t-test, p<0.0001)

In the glaucoma population the average asymmetry was significantly higher for dichoptic than monocular recordings (0.227 vs. 0.146, Mann-Whitney, p<0.001) (Figure 6-5). When this is compared with the asymmetry found in the normals populations (RAC monocular = 0.071; RAC binocular = 0.092) there is a 2.05 times increase in asymmetry between normal and glaucoma using monocular testing compared to a 2.47 times increase between normal and glaucoma using binocular testing. This indicates that there appears to be an increase in asymmetry above those values naturally seen when going from monocular to binocular testing in normals.

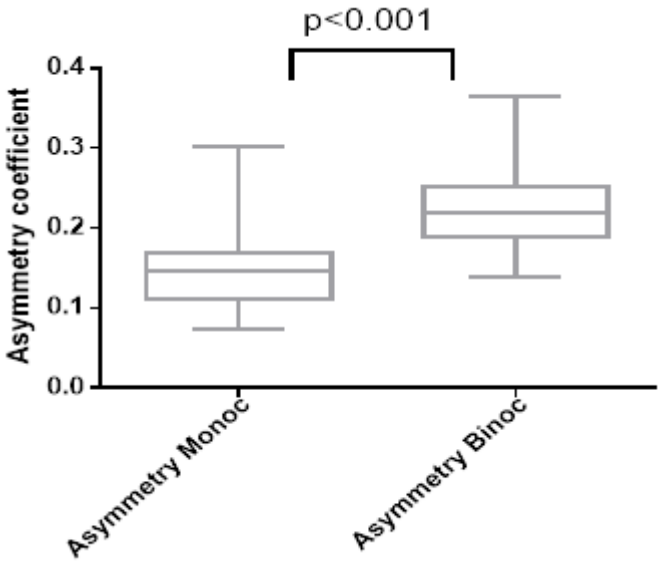

Figure 6-5 - Average asymmetry coefficient (RAC) for glaucoma patients on monocular and binocular testing

Similarly the z-scores for asymmetry analysis were significantly higher for dichoptic versus monocular testing (2.60+/-1.02 vs. 1.71+/-0.89, paired t-test, p<0.001) (Figure 6-6).

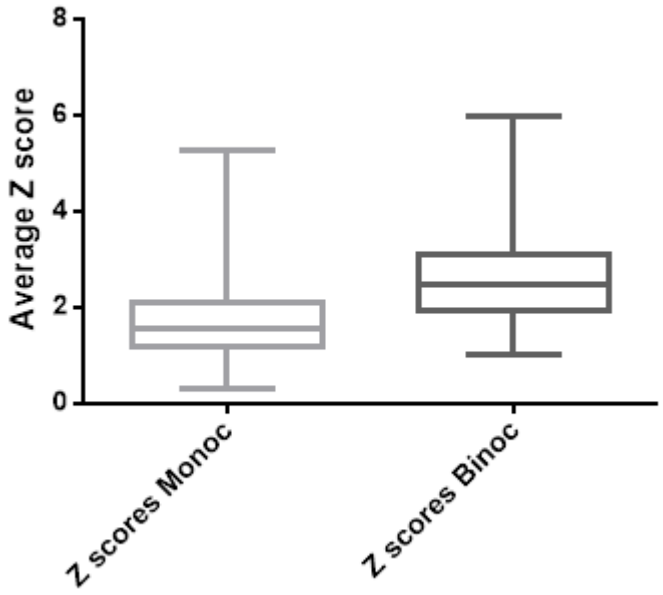

Figure 6-6 - Average z scores (asymmetry) comparing monoc and binocular recordings

4.3 ASYMMETRY ANALYSIS

Figure 8 demonstrates the effect of eccentricity on the asymmetry profiles. The monocular and binocular recordings of the normal population are similar in shape and value, with slightly higher asymmetry in binocular recordings, the lowest value for asymmetry for both curves being at ring 3.

For glaucomatous patients there is a marked difference between the monocular and binocular profiles with loss of the characteristic shape seen in the normal population. This is most likely a result of the fact that there is asymmetric and variable disease resulting in multiple scotoma locations (Figure 6-7).

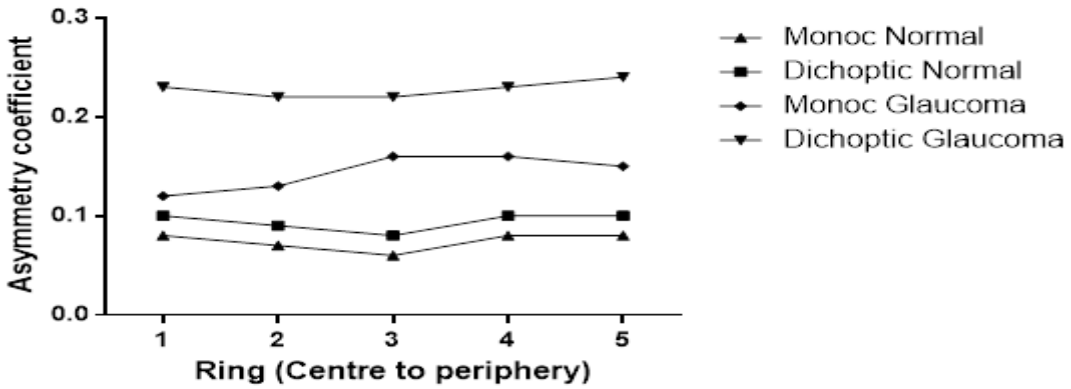

Figure 6-7 - Comparison graph of asymmetry profile ring wise (central to peripheral) for monocular/binocular recordings in normal and glaucomatous patients

4.4 DICHOPTIC SUPPRESSION

There appears to be an increase in asymmetry for dichoptic versus monocular recordings (Figure 8), however dichoptic suppression for normal and glaucomatous patients (Figure 6-8) shows a similar profile. The curves are not significantly different (unpaired t-test, $p>0.05$).

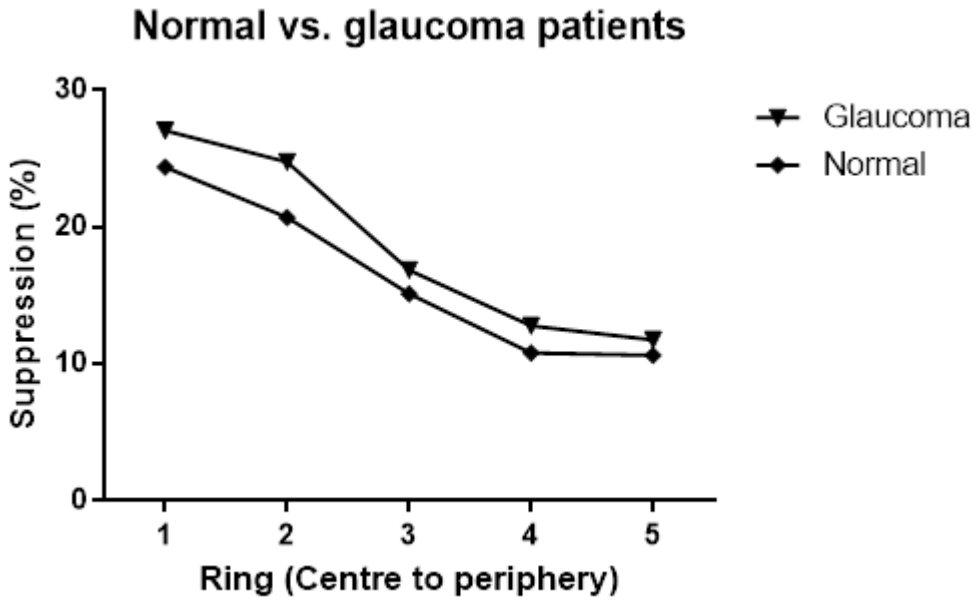

Figure 6-8 - Suppression versus ring number for normal and glaucomatous patients

When suppression curves are divided into the more affected eye and the less affected eye, there is a marked difference in suppression profiles, the glaucomatous side being far more dichoptically suppressed than the contralateral eye (Figure 6-9). As the suppression formula is indicative of the differential in amplitude between dichoptic and monocular testing, this analysis serves to highlight the effect of dichoptic interocular suppression on mfVEP amplitudes.

Interestingly there also appears to be a release of suppression seen in the central rings (rings 1 and 2) for the less affected glaucoma eyes with suppression values that are less than the normal population.

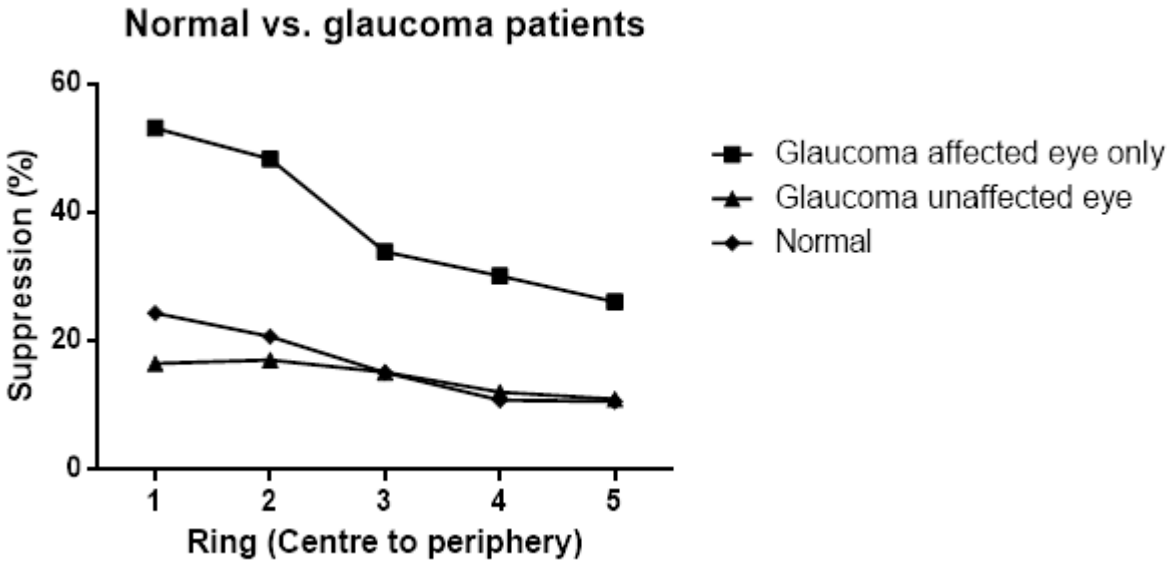

Figure 6-9 - Normal versus glaucoma patients with eyes separated into affected and unaffected (less affected) eyes, suppression versus ring number

4.5 CORRELATION OF STRUCTURE WITH FUNCTION

In order to assess whether the asymmetry and z-scores are indicative of actual disease, the worse defects were identified as described previously. In general the side with the greater asymmetry for binocular and monocular mfVEP was the same as that identified by HVF and OCT in 25/28 (89%) of the cases with monocular correct 3 times when dichoptic was incorrect and vice versa. This would indicate concordance and a degree of agreement with established technologies (Table 6-1).

Patient	Worst side HVF	Worst side OCT	Worst side mfVEP Monocular	Worst side mfVEP Dichoptic	MfVEP agree?	Which agrees with OCT/HVF
1	LS	L I	L	L	Y	BOTH
2	LS	LI	L	L	Y	BOTH
3	LS	LS	L	R	N	M
4	LS	LI	R	L	N	D
5	RS	RI	R	R	Y	BOTH
6	LI	LS	L	R	N	M
7	LS	LI	L	L	Y	BOTH
8	LI	LS	L	L	Y	BOTH
9	LI	LC	L	L	Y	BOTH
10	LS	LI	R	L	N	D
11	LI	RI	L	L	Y	Conflict
12	RI	RS	R	R	Y	BOTH
13	LI	LS	L	L	Y	BOTH
14	LI	LS	L	L	Y	BOTH
15	RI	RS	R	R	Y	BOTH
16	RS	RI	R	R	Y	BOTH
17	RS	RI	R	R	Y	BOTH
18	RI	RS	L	R	N	D
19	LI	LS	L	L	Y	BOTH
20	RS	RI	R	R	Y	BOTH
21	LS	LI	L	L	Y	BOTH
22	LS	LI	L	L	Y	BOTH
23	LS	LI	L	L	Y	BOTH
24	RI	RS	R	R	Y	BOTH
25	LI	LS	L	L	Y	BOTH
26	LI	LS	L	L	Y	BOTH
27	RI	RS	R	R	Y	BOTH
28	LS	LI	L	L	Y	BOTH
29	RS	RS	R	L	N	M

Table 6-1 - Most severe OCT, HVF and mfVEP defect by side with agreement or disagreement between technologies (L = left, R = right, S = superior, I = inferior)

5 DISCUSSION

This study aimed to provide insight into the mechanisms that underlie dichoptic suppression in mfVEP and whether these mechanisms could be manipulated to increase sensitivity in early glaucoma detection. As stipulated previously [76], a potential mechanism for increasing glaucoma detection in dichoptic mfVEP is the release of suppression (i.e. increase in recorded amplitude) on a normal segment when compared to a corresponding glaucomatous segment in the contralateral eye. By suppressing the already lower in amplitude segment, the relative difference between the two segments is increased and thus the inter-eye asymmetry.

For detection of glaucomatous damage to be useful and accurate the technology should provide a tangible benefit over existing technology. The dichoptic mfVEP, within the bounds of technical limitations, should increase the detection rate of glaucomatous defects versus established methods of visual field testing. Dichoptic mfVEP appears to generate increased asymmetry, and therefore increased levels of detection, between corresponding segments (i.e. contralateral cortical representations) versus monocular stimulation. If we believe that this increase in asymmetry is responsible for increased levels of detection, then the mechanism should lie within the cortical architecture supplying the visual fields. The mechanisms that can explain this phenomenon logically must lie in one of 4 cortical interactions:

a) V1 ocular dominance columns as this is the first point at which there is interaction between opposite retinotopically located visual field areas, as the retinotopic pathways are separate until then
b) Higher cortical centres, either dorsal or ventral steams through direct or indirect feedback to V1:
    a. Parvocellular pathways through to the dorsal (parietal) streams, specifically processing at V4 with mechanisms governing orientation
    b. Magnocellular pathways through to the ventral (temporal) streams, specifically V3/V3A with mechanisms governing stereoscopic depth processing
c) Feedback/feedforward interaction between LGN and V1.

As research by Sengpiel[109] et al has stipulated, interocular suppression lies at the level of the ocular dominance columns in V1. This is concordant with known cortical pathways and within the range of potential mechanisms to explain the increase in mfVEP asymmetry leading to increased sensitivity for glaucoma detection. To analyse these mechanisms we need to look closely at the change in electrophysiological profiles between normal subjects and glaucomatous subjects, to gain insight into the underlying processes.

Examining the normal cohort, amplitudes were reduced in dichoptic versus monocular stimulation by approximately 16%. The average asymmetry values were increased in dichoptic (RAC = 0.091) vs. monocular (RAC = 0.071), by 128%. In previous dichoptic mfVEP work[75], closer asymmetry of the normals database was considered a factor in increasing sensitivity to glaucomatous damage. This isn't apparent in these experiments; in fact the asymmetry coefficients are increased. This could be due to a number of factors - recording noise and error, the small size of the normals database or could be indicative of an underlying augmented increase in asymmetry seen with dichoptic stimulation particular to the current testing setup. If the last case is in fact true it could be related to the faster stimulation speed (9 frames per sequence versus 18 frames per sequence) and wider field of stimulation (24 degrees of eccentricity versus 16 degrees) compared to the previous mfVEP dichoptic stimulation used by Arvind et al [75].

In general, the amplitudes recorded in the glaucoma population were reduced compare with normal values (of the particular testing type – monocular or dichoptic), and were decreased 4.7% for monocular recordings ((normal-glaucoma)/normal) and 6.9% for dichoptic recordings. Demonstrating a slightly greater reduction in overall amplitude for dichoptic versus monocular recordings.

Dichoptic stimulation produced higher z-scores, versus monocular, across all points in the visual field. As dichoptic suppression is strongly influenced by the temporal separation of stimulus presentation at the level of the ocular dominance columns in layer 4c 3[109] the closeness in timing of the fast stimulation serves to increase suppression and proportionately increase asymmetry between normal and corresponding abnormal segments. We believe this is the mechanism underlying the increase in

detection seen with dichoptic stimulation in early unilateral glaucoma. This appears to be evident in figure 10 where there is a marked increase in suppression for glaucomatous eyes versus less affected contralateral eyes.

The preceding analysis points to an apparent increase in the detection of glaucomatous visual field defects as measured by z-score. The average amplitude of dichoptic recordings is reduced versus monocular, and despite this there is an increased asymmetry for both normal and glaucomatous subjects. The z-scores are increased as a result of the increased asymmetry and point to a higher sensitivity for detecting abnormal segments.

The aims of this paper are to assess whether there is an increase in the rate of detection of glaucomatous defects for dichoptic over monocular mfVEP, whether this is in fact representative of actual disease and to further understand the mechanisms that underlie this postulated increase in detection. On the first two points there does appear to be an increased magnitude of z-scores (a surrogate marker of glaucoma detection) and there does appear to be reasonable concordance between HVF and OCT and mfVEP defects. The mechanisms underlying these changes appear to lie with the release of suppression as seen in figure 10. Cortical mechanisms at the level of V1 underlying these processes enable the interactions between corresponding visual field segments, causing suppression and release of suppression thereby increasing asymmetry.

One of the weaknesses of this study was that it relied on SD-OCT as the sole measure of structural change – ideally disc photographs would provide the best reference for analysis of structural change. However a rejoinder to this weakness is the fact that we were comparing technologies (monocular and dichoptic mfVEP) rather than calculating sensitivity and specificity.

It is clear that these results would be strengthened by a larger normals database which would enable meaningful analysis of the individual defects and the correlation with field defects. Without this added information comparison with HVFs in terms of sensitivity is not likely to be accurate.

The above findings demonstrate for the first time the suppression – release of suppression interaction between glaucomatous and fellow eyes which appears to be the underlying mechanism

in dichoptic mfVEP asymmetry analysis in detecting glaucomatous field defects. We have demonstrated, on a novel dichoptic testing setup, that this increased rate of detection is real and is likely enhanced with increased speed of stimulation as increased speed of stimulation increases levels of dichoptic suppression [73].

6 CONCLUSION

In conclusion, there is a significant difference between the rates of detection, as measured by z-scores, between monocular and dichoptic asymmetry analysis using mfVEP. The increased dichoptic suppression in dichoptic mfVEP most likely enhances the dichoptic system for detecting early unilateral glaucomatous damage.

Chapter 7 CORRELATION OF DISC PARAMETERS WITH VISUAL FIELD INDICES USING SCANNING LASER AND SD-OCT AT DIFFERENT LEVELS OF GLAUCOMA SEVERITY

Published as:

Leaney, J., Healey, P., Lee, M., Graham, S.., *Correlation of structural retinal nerve fibre layer parameters and functional measures using Heidelberg Retinal Tomography and Spectralis spectral domain optical coherence tomography at different levels of glaucoma severity.* Clinical & Experimental Ophthalmology, 2012. **40**(8): p. 802-812.

Summary

In order to provide a basis upon which to explore the structural and functional changes in mfVEP, this study looked at the correlation between structural and functional parameters in optic nerve head imaging and Humphrey visual field testing technologies. The study thus provided a foundation upon which to explore structural and functional changes seen with mfVEP.

1 INTRODUCTION

Imaging of the mean retinal nerve fibre layer (RNFL) thickness with scanning laser ophthalmoscopy (SLO) or spectral domain optical coherence tomography (SD-OCT) are commonly used in the diagnosis and monitoring of glaucoma. It offers rapid, objective measurements of structural parameters relevant to glaucoma (Figure 7-1 - Case example demonstrating inferior wedge defect (shown with vertical arrows) correlating with a superior field defect (circled with ellipses).Figure 7-1) and are able to calculate regional and global changes over time. There is good evidence that both structural and functional change is a sign of glaucoma progression with structural change more often preceding functional change.[15,154,156]

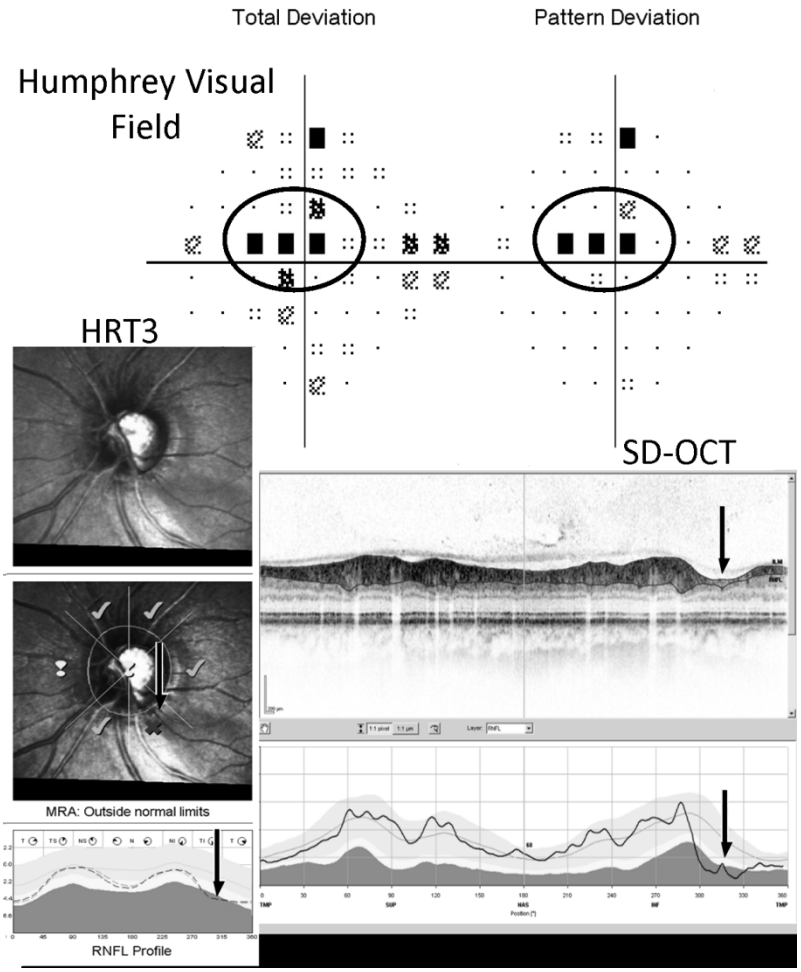

Figure 7-1 - Case example demonstrating inferior wedge defect (shown with vertical arrows) correlating with a superior field defect (circled with ellipses).

However, the relationship between mean RNFL thickness loss and visual field abnormalities in glaucoma has been reported to be inconsistent using current testing modalities.[83,85,87,157] A number of factors may contribute to this – the substantial variation in normal RNFL thicknesses, the disease processes involved in the pathogenesis of glaucoma which include many factors that affect the structure-function relationship[99,100], and the limitations of the instruments used to measure structural and functional status[85,87,157] .

Over the past decade, a number of models of glaucoma[95,96,98,99] have been developed to explain relationships between structure and function. These include the structure function topographical map described by Garway-Heath[158] among others[93,159].

The aims of the study were to investigate the structural correlation of SLO and SD-OCT, with functional measures as assessed by Humphrey Visual Fields (HVFs) using the well-established model of Garway-Heath. We sought to assess the effects of disease severity and optic disc size on the correlation strength and the strengths and limitations of each scanning technology with respect to the model.

2 METHODS

2.1 SUBJECT SELECTION

Participants were drawn from patients with open-angle glaucoma attending a large urban glaucoma practice in Sydney, Australia between September 2009 and June 2010. Those who had undergone one or more SD-OCT scans, two or more Heidelberg Retinal Tomography (HRT3) scans and two or more HVFs were eligible for inclusion. All patients had comprehensive medical and ophthalmic histories and examination recorded including Goldman applanation tonometry, fundoscopy, slit lamp examination and gonioscopy. The diagnosis of glaucoma was made by one of two glaucoma specialists prior to the study based upon optic disc appearance with focal thinning of the neuroretinal rim matching visual field loss consistent with glaucoma including arcuate patterns or clusters, respecting the horizontal meridian on HVF.

At the time of the original diagnosis neither of the glaucoma specialists was aware of the proposed study. In order to ensure the accuracy of the subject selection all written records were reviewed by a third clinician to ensure the patients had a recorded diagnosis of glaucoma and to check for any exclusion criteria. All subjects provided informed consent and the study was performed within the tenets of the declaration of Helsinki.

From an initial recruited pool of 220, 17 patients were excluded because they failed to meet the test quality parameters - for HVFs an acceptable test was one with fixation losses<20%, false positives<15% and false negative errors <15%. The patients had to have had at least 2 consecutive, acceptable HVFs as per the above criteria, in order to ensure a reproducible defect could be identified; for HRT3 an acceptable scan was considered to have a standard deviation < 40 μm; for SD-OCT the signal quality level had to be greater than 20.

Eyes were also excluded due to they had poor segmentation on OCT (lack of clear RNFL identification in all or part of the scan, or discontinuation of the segmentation line with abrupt loss of layer detection) or disc centration misalignment. HRT3 scans were manually inspected for artefact and

inaccurate optic disc margin placement. These exclusion criteria accounted for less than 10 scans out of the initial 220 total.

Patients were further excluded by identification of co-existing pathology, either in scan results or patient records. Co-existing pathology included disease that could possibly interfere with the glaucoma structure-function relationship such as cataract causing visual impairment, age related macular degeneration, visible diabetic retinopathy, vitreous opacity, disc drusen or branch retinal vein occlusion. In order to remove the inherent effects of inter-eye similarity, the eye with the worse disease, based upon Humphrey mean deviation, was selected. After exclusion using the above criteria, 169 eyes of 169 patients were included in the final data set.

The eyes were divided into early (MD>-4dB, N = 51), moderate (-10<MD<-4dB, N=60) and severe (MD<-10dB, N=58) disease. This division was made to facilitate 3 evenly size-matched groups so as to provide a meaningful spectrum of disease. This division is similar to the glaucoma staging system devised by Mills et al.[160]

2.2 TESTING SPECIFICATIONS

SD-OCT scans were performed using Heidelberg Spectralis ® (version 1.6.4.0 HRA2/Acquisition module 3.0.7.0), circle scan, centered on ONH. HRT scans were performed using HRT3 (version 1.6.2.0 ONH acquisition module 3.0.7.0) with a 15^{o} scan diameter, 3 scans averaged for mean topography and the HVF machine used was the Zeiss Humphrey Visual Field Analyser (version 4.2.2 Model 750i) using SITA-standard 24-2 testing paradigm. For an individual patient, all scans were performed within a 3 month period, for most patients all scans were performed on the same day.

2.3 ANALYSIS AND STATISTICS

RNFL measurements were divided into sectors (Superotemporal ($45\text{-}90^{0}$), Superonasal ($90\text{-}135^{0}$), Nasal ($135\text{-}225^{o}$), Inferonasal ($225\text{-}270^{0}$), Inferotemporal ($270\text{-}315^{0}$), Temporal ($315\text{-}45^{0}$)), according to the software of each machine. The Humphrey visual field was divided as per a structure-function model [158,161] (Inferior paracentral($41\text{-}80^{0}$), Inferior arcuate($81\text{-}120^{0}$), Temporal($121\text{-}230^{0}$), Superior arcuate($231\text{-}270^{0}$), Superior paracentral($270\text{-}310^{0}$), Centrocecal ($311\text{-}40^{0}$)) (Figure 7-2).

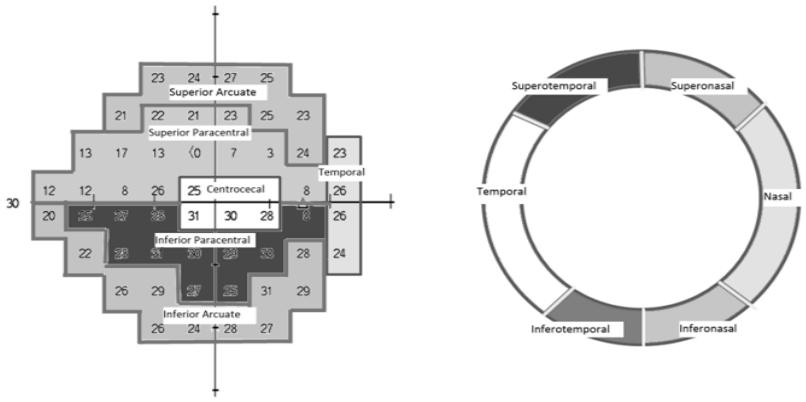

Figure 7-2 - Structure-function relationship used for the present study based upon the map derived by Garway-Heath et al[118,158]

There is a small difference of a few degrees between the division of the circumpapillary RNFL of the imaging modalities and that of the structure function map, but this was considered not likely to significantly affect the results. Mean threshold scores for each visual field sector (i.e. superotemporal, inferotemporal etc.) were determined by calculation of the arithmetic mean of the scores in decibels. Each sector thus had a single mean threshold score in dB calculated for the correlation analysis. Mean deviation scores were also converted from dB to a linear scale (1/Lambert) to provide a functional measure on a using the same scale as RNFL measurements[161]. In addition to the sectoral analysis, linear and logarithmic regressions were calculated for both Mean Deviation (MD(dB)) and Visual Field Index (VFI(%)) for the entire visual field so as to demonstrate overarching trends in the data and to calculate regression fit to global RNFL measures over the spectrum of disease. The effect of Disc Area (DA) on the correlation of structural and functional measures was assessed by dividing optic discs into small ($DA<1.85mm^2$, N=49), medium ($1.85mm^2 \leq DA \leq 2.25mm^2$, N=60) and large ($DA>2.25mm^2$, N=58) and calculating correlation coefficients within each group. These divisions allowed similarly sized groups to be used for analysis. Similar disc divisions have been used by Oddone et al [162] using HRT3.

The structure-function map of Garway-Heath was used[158] to relate sectors of the RNFL to the visual field (Figure 2). Analysis of the correlation between RFNL thickness and mean threshold, was

calculated using the bivariate correlation function in SPSS (version 19, IBM, NY) to determine Spearman's rho (r_s) coefficient. This was chosen because MD (dB) and VFI (%) were not normally distributed (one-sample Kolmogorov-Sminrnov test), consistent with many previous.[91,161,163] For comparative purposes only, strong correlation was defined as r_s = 0.7-1, moderate as r_s = 0.4-0.7 and weak as r_s < 0.4.

Each RNFL segment classification (normal/borderline/outside normal limits) was compared with the corresponding visual field area as per the structure function map. If the defect corresponded (e.g. superotemporal sector with inferior paracentral) with a scotoma (1 or more single points on HVF with p<0.5%) then this was considered to be a true positive correlation. A defect that corresponded to a normal visual field was considered a false positive. A normal RNFL segment that corresponded to a scotoma was considered a false negative.

3 RESULTS

Table 7-1 shows the baseline characteristics of the study sample.

Table 7-1 – Demographic data divided into disease severity categories

	Early	Moderate	Severe
	N = 51	N = 60	N = 58
Mean Age (years)	65.73 +/-11.70	69.85+/-11.45	67.05+/-13.41
Mean Optic disc area (mm2)	2.06+/-0.42	2.07+/-0.48	2.16+/-0.65
Mean MD of visual field (dB)	-1.83+/-1.46	-6.50+/-1.52	-16.92+/-5.79
Mean VFI (%)	95.45+/-3.87	85.07+/-6.86	53.03+/-10.00
Mean SD-OCT RNFL (micrometers)	76.77+/-12.40	66.19+/-12.87	53.94+/-10.00
Mean HRT3 RNFL (mm)	0.21+/-0.09	0.16+/-0.08	0.12+/-0.08
Mean HRT3 Rim area (mm2)	1.23+/-0.32	1.04+/-0.38	0.86+/-0.39

To gain an understanding of the correspondence between structural scanning parameters (RNFL and RA) and functional defects on HVF we explored the effect of disease severity and disc size on the goodness of fit, expressed as r-square, and the correlation strength, calculated as r_s, of structure with function.

3.1 LOGARITHMIC AND LINEAR REGRESSION

We analysed the linear and logarithmic regressions in terms of closeness of fit to either method of regression. Overwhelmingly, and in support of previous work,[91,161,163] a logarithmic regression model was the model of best fit. This, in turn, further supported the use of Spearman's Rho for the bivariate correlation analysis.

The graphs of visual function against RNFL thickness serve to demonstrate principally the wide variation when comparing functional measures with structural ones, especially with increasing disease severity. The graphs also demonstrate that the data appears to follow a logarithmic trend. The r-square values provide an indication of the amount of variation that could be accounted for in functional measures by the structural measures.

SD-OCT RNFL measures accounted for the most variation (i.e. had the largest r^2 values) regressed against MD (Figure 7-3, left graph) when compared with HRT3 RA and RNFL (Figure 7-3(middle and

right graphs). Similarly SD-OCT measures had a closer calculated fit to VFI (Figure 7-4 left graph) than either RNFL or RA (Figure 7-4 middle and right graphs).

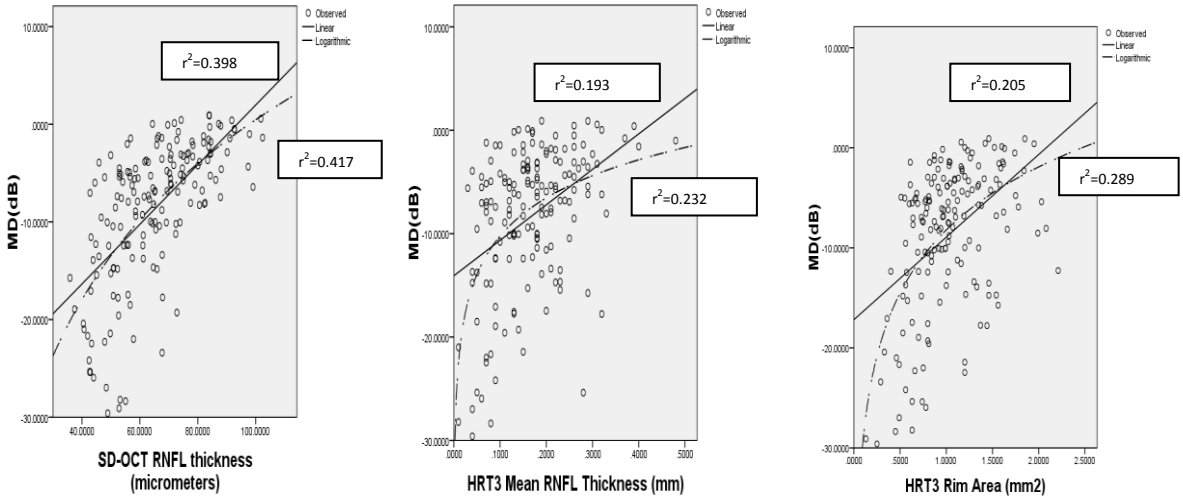

Figure 7-3 - Global Retinal Nerve Fibre Layer (RNFL) vs. Mean deviation (MD(dB)), linear (unbroken line) and logarithmic (dotted line) curve fitting, modelling fits a logarithmic approach: Left graph - SD-OCT (r^2=0.398(linear) vs 0.417(log)); Middle graph HRT3 RNFL (r^2=0.193(linear) vs 0.232(log)); Right graph HRT3 Rim area (r^2=0.205(linear) vs 0.289(log))

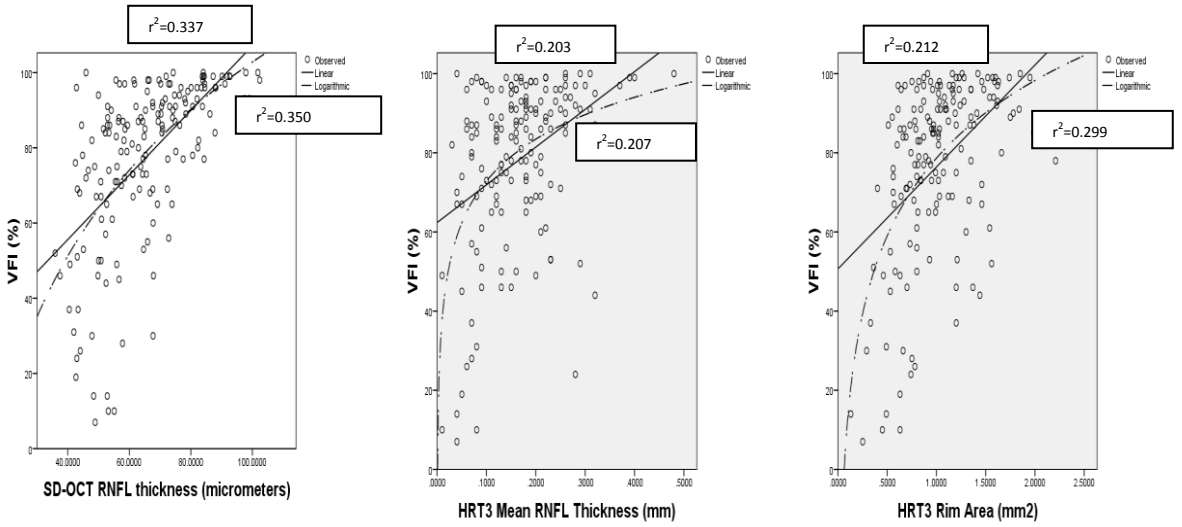

Figure 7-4 - Global Retinal Nerve Fibre Layer (RNFL) vs. Visual Field Index (VFI, %), linear and logarithmic curve fitting, modelling favours a logarithmic approach: Left graph- SD-OCT (r^2=0.337(linear) vs 0.350(log)); Middle graph HRT3 RNFL (r^2=0.203(linear) vs 0.207(log)); Right graph HRT3 Rim area (r^2=0.212(linear) vs 0.299(log))

When outliers were removed with robust linear regression, r^2 improved from 0.193 to 0.265 for RNFL against MD. Similarly the r^2 value for logarithmic regression increased to r^2=0.271 with outliers removed.

Recent work has noted a ceiling effect for VFI when MD is greater than -5dB[164] hence we analysed the data removing all values with MD>-5. When VFI was regressed against Spectralis RNFL there was a poorer fit to the data compared with the entire spectrum of disease with r^2=0.198 for linear and r^2=0.204 for logarithmic analysis. HRT RNFL regressed against MD was calculated as r^2=0.153 for linear and r^2=0.162 for logarithmic analysis. Similarly for HRT rim area regression obtained values were r^2=0.156 for linear and r^2=0.241 for logarithmic analysis.

3.2 MEAN THRESHOLD ANALYSIS

Previous work in structure-function analysis[118] has used conversion of threshold scores to 1/Lambert before calculating the arithmetic mean. To address this point all threshold scores were converted to 1/Lambert before averaging for each visual field sector. However, in our analysis, the strength of correlations was, equal to, or slightly weaker for both OCT and HRT3 using 1/Lambert hence we used only the arithmetic mean of threshold scores in units of decibels.

3.3 OCT ANALYSIS

3.3.1 MEAN THRESHOLD ANALYSIS

Both devices showed variable correlation strength across the 3 disease categories and visual field areas. SD-OCT tended to have the strongest correlations (Table 7-2) in the arcuate bundles and this was consistent over all stages of disease. The Nasal sectors demonstrated weak correlation strengths, most notably in early and moderate disease.

Table 7-2 - Table of correlations between OCT RNFL mean values and HVF sectoral scores in different disease severity divisions (*=p<0.05, **=p<0.01).

Disease Severity	Global	Temporal	ST	IT	Nasal	SN	IN
All	0.670**	0.282**	0.724**	0.716**	0.321**	0.562**	0.521**
MD>-4	0.417**	0.169	0.411**	0.603**	0.095	0.245	0.307*
-4<MD<-10	0.107	0.002	0.638**	0.529**	0.199	0.316*	0.245
MD<-10	0.444**	0.126	0.639**	0.560**	0.184	0.495**	0.346**

HRT3 rim area also had its strongest correlations in the arcuate bundles in severe disease. But in early and moderate disease severity, calculated correlation coefficients were generally smaller (Table 7-3).

Table 7-3- Table of correlations between HRT3 Retinal Nerve Fibre Layer (RNFL)/Rim area and HVF sectoral scores in different disease severity divisions (*=p<0.05, **=p<0.01).

Disease Severity	HRT3 Measure	Global	Temporal	ST	IT	Nasal	SN	IN
All	Rim Area	0.449**	0.467**	0.538**	0.518**	0.176*	0.309**	0.299**
	RNFL	0.421**	0.290**	0.514**	0.408**	0.287**	0.444**	0.387**
MD>-4	Rim Area	0.332*	0.229	0.202	0.335*	0.089	-0.030	0.000
	RNFL	0.243	0.155	0.193	0.265	0.188	0.187	0.188
-4<MD<-10	Rim Area	-0.056	0.260*	0.382**	0.277*	-0.144	0.052	-0.044
	RNFL	0.332**	0.056	0.203	0.225	-0.030	0.177	0.105
MD<-10	Rim Area	0.472**	0.455**	0.601**	0.408**	0.288*	0.468**	0.267*
	RNFL	0.481**	0.255	0.609**	0.320*	0.369**	0.604**	0.284*

HRT3 RNFL had its strongest correlations in the arcuate bundles, however HRT3 RNFL only had weak calculated correlation coefficients except in severe disease (Table 3).

Comparing the two HRT RNFL measures to OCT showed that OCT had calculated correlations that were consistently larger, excepting severe disease where the calculated HRT3 RNFL coefficients were similar to OCT.

Evaluation of all regression plots tends to show a spread of data particularly at the more severe end of the disease, indicating that the structure function relationship cannot readily be predicted even when there is substantial nerve fibre loss.

3.3.2 EFFECT OF DISC AREA

Division of patients into 3 disc size groups revealed moderate to strong correlation coefficients and significance for HRT3 RNFL, HRT3 Rim area and SD-OCT RNFL (Table 7-4).

Table 7-4 - Correlations for OCT between mean RNFL thickness and mean HVF scores for disc sizes (mm^2) over different segments (*=p<0.05, **=p<0.01)

Disc Area (DA)	Global	Temporal	ST	IT	Nasal	SN	IN
DA<1.85	0.713**	0.388**	0.716**	0.759**	0.381**	0.651**	0.554**
1.85<DA<2.25	0.564**	0.087	0.700**	0.582**	0.139	0.463**	0.469**
DA>2.25	0.668**	0.271*	0.736**	0.718**	0.410**	0.563**	0.520**

3.4 OCT

In the smallest disc size group, Global measures with MD demonstrated r_s values of 0.713 (OCT), 0.455 (HRT3 Rim area) and 0.499 (HRT3 RNFL). Sectorally the strongest correlations for OCT were IT (0.759) and ST(0.716). HRT3 showed a similar pattern with ST and IT having the highest r_s values (Table 7-5).

Table 7-5 - Correlations between HRT3 Rim area/RNFL and mean HVF scores at different disc sizes (mm^2) and at different segmental divisions (*=p<0.05, **=p<0.01)

Disc Area (DA)	HRT3 Measure	Global	Tempora	ST	IT	Nasal	SN	IN
DA<1.85	Rim Area	0.455**	0.423**	0.505**	0.448**	0.117	0.311*	0.173
	RNFL	0.499**	0.324*	0.457**	0.372**	0.261	0.463**	0.380*
1.85<DA<2.25	Rim Area	0.383**	0.405**	0.530**	0.454**	0.077	0.247	0.248
	RNFL	0.378**	0.258*	0.549**	0.314*	0.081	0.457**	0.352**
DA>2.25	Rim Area	0.521**	0.541**	0.554**	0.622**	0.239	0.295*	0.395**
	RNFL	0.504**	0.308*	0.503**	0.575**	0.440**	0.387**	0.480**

In the mid-size disc group, Global measures with MD showed similar values compared to the other disc size groups, but lower r_s values for OCT (0.564). OCT demonstrated moderate to strong correlations in IT, ST and SN while HRT3 Rim area showed moderate correlations and similarly HRT3 RNFL demonstrated moderate correlations in ST and IT.

In the largest disc group size MD correlated strongly with OCT and some HRT3 measures. Sectorally OCT had moderate to strong correlations with all except the temporal sector. HRT3 rim area showed moderate correlations in ST, temporal and SN sectors and RNFL closely correlated in ST and SN areas.

3.5 PERFORMANCE OF THE CLASSIFICATION SOFTWARE

Correspondence between RNFL defect and visual field defect was determined for each subject. If there were one or more corresponding segments this was assessed as a positive identification of field loss. Some subjects had scotomas that crossed several field areas, but for the purpose of this analysis we only included one positive sector per eye.

The correspondence of a flagged defect with a scotoma in the corresponding visual field area was calculated as 91% for OCT and 81% for HRT3. This figure represents those patients that have any scotomatous point ($p<0.5\%$) in their visual field and at least one correctly identified corresponding abnormal circumpapillary RNFL segment.

4 DISCUSSION

The aim of this study was to correlate both global and sectoral measurements derived from the two imaging technologies (HRT3 and SD-OCT) with related visual field sensitivities and scotomas, and also to examine their ability to correlate structural with functional defects over a wide range of disease severities and disc sizes.

This study used a large number (n=169) of well categorised glaucoma patients. It demonstrated that the strength of the structure-function relationship using VF threshold values is greater for SD-OCT than HRT3 for most sectors, and that it held across the spectrum of the disease to a varying degree. The strength of the relationship changed with different sectors (see below) and was notably weaker in the nasal and temporal sectors, particularly for SD-OCT.

The strongest correlations were found in superotemporal and inferotemporal sectors in OCT imaging, and is in agreement with previously published results by Horn et al[165] with SD-OCT (although Horn has used different sectoral classifications) and Miglior et al.[91] using time-domain (Stratus) OCT (Table 7-6). Compared to a previous correlation study of time-domain OCT[166] with MD and global OCT RNFL, we calculated a similar correlation coefficient, r_s = 0.670, compared to their value of 0.63.

Table 7-6 - Comparison of correlations between mean RNFL and mean HVF scores for sectoral analysis compared with 2 other studies (using SD-OCT and Stratus OCT)

Leaney (Spectralis)	n=169	Horn (Spectralis)	n=64	Miglior (Stratus)	n=68
Sector	MD=-8.6+/-7.3	Sector	MD=-6.9+/-6.0	Sector	MD=-10.4+/-7.5
Nasal	0.32	Nasal	0.75	Nasal	0.42
IN	0.52	IN	0.81	IN	0.57
IT	0.72	IN	0.68	IT	0.59
Temporal	0.28	R	0.47	Temporal	0.40
ST	0.72	Spectralis	0.57	ST	0.45
SN	0.56	SN	0.77	SN	0.57

In contrast to HRT measures, OCT correlation values did not appear to vary greatly across the 3 disease severity groups, this is contrast with a number of studies that have reported stronger correlations related to increasing disease severity. [87,167,168]

Global correlations, except in moderate disease, were generally higher across both tests than for individual sectors, excluding ST and IT sectors. This finding supports work by Leung et al using SD-OCT assessing diagnostic accuracy compared with HRT3.[83]

Compared to the findings of Moreno-Montanes et al. [166], HRT3 RNFL appeared similar in terms of correlation coefficients, with an r_s = 0.421 for global RNFL versus MD for our study versus their published value of r_s = 0.37. When divided into sectoral RNFL measurements, HRT3 RNFL r_s values were higher compared to previously published studies by Danesh-Meyer et al. which showed r values between 0.2 to 0.3[169]. This could represent improvements in software for the HRT3 versus HRT2. Another reason could be the increased standardisation of the contour line in HRT3 compared with HRT2.

HRT3 rim area correlations were similar compared to Saito et al[88] when MD was correlated with rim area; r_s =0.430 versus r_s =0.449 for this study. Their patients differed in disease severity, being comprised of patients at earlier stages of disease, and they had a smaller patient group.

Correlation of MD with OCT and HRT3 parameters appears to favour a non-linear approach, which has been seen in a few studies.[91,165] MD(dB) had a strong correlation with global OCT RNFL thickness and was improved with a logarithmic regression r^2=0.398 (linear) vs 0.417 (log) and appeared to trend towards an asymptotic value in concordance with other modelling.[165] Global OCT and HRT3 parameters demonstrated closer fits to MD(dB) versus VFI(%) except for Rim area which demonstrated slightly higher r^2 with VFI versus MD.

Dividing the patients into three disc sizes generally increased the significance and strength of the correlations. For OCT there were stronger correlations for both large and small discs when compared to medium sized discs. This difference could relate to the placement of the OCT circumpapillary measurement ring in relation to the neuroretinal rim and the geometry of small and large discs compared with medium discs. For HRT rim area and mean RNFL thickness, there appeared to be a demonstrable difference in correlation strength between discs sizes, with larger discs having the strongest correlations, followed by small discs then medium discs. This is in keeping with previous

studies demonstrating an effect of disc size on HRT diagnostic accuracy[170]. No appreciable difference in r_s values was found when comparing RNFL and rim area correlations. We do not believe that the above results relate to a variation in proportion of different disc sizes in the 3 glaucoma severity groups i.e. dependent on mean deviation. A one-way ANOVA on disc area (DA) versus stage of disease showed no significant difference between groups. There was a trend for smaller discs in early (DA mean = 2.06mm^2) and in moderate disease (DA mean = 2.07mm^2) and larger discs in severe disease (DA mean=2.16mm^2). The effect of disc size on OCT and HRT3 correlations appears to be minimal although other groups have found a significant effect for OCT[87] and HRT3[85,157,171]. It should be noted that OCT uses a set size circumpapillary ring which is not tailored to disc size whereas HRT uses an operator defined disc margin and an arbitrary 50µm addition to the height above the horizontal plane, however this wouldn't explain the change in correlation strengths for HRT3 and OCT.

Across all eyes and in all disease severities OCT showed, in general, stronger and more significant correlations than HRT3 for both rim area and RNFL. There were exceptions to this in the temporal disc sector for Rim area where HRT generally performed better than OCT and had similar correlation strengths for severe disease. In comparing OCT and HRT3 RNFL correlations HRT3 demonstrated stronger correlations in severe disease in most sectors but otherwise OCT showed closer correlations. Comparing HRT3 RNFL and rim area correlations showed that rim area correlated more closely in general with some exceptions in certain sectors and disease states.

Published data on the comparison of these technologies has favoured OCT[83,166,172] over HRT. This study has further confirmed that OCT analysis of RNFL thickness more closely follows a structure-function relationship, but not in all regions of the disc. One of the reasons that OCT demonstrates closer structure-function correlations versus HRT is the use of a circumpapillary scan which measures RNFL based upon direct visualisation rather than an arbitrary 50µm offset as with HRT. In addition OCT has previously demonstrated to have a stronger relationship with Mean Deviation[173] which could relate to the optics of the scanning method better representing the actual anatomical characteristics of nerve fibre layers.

A major strength of the study was that all patients had reproducible and reliable visual fields and HRT3 data as entry criteria, so that we were comparing the newer test with a well-established and categorised group.

The study limitations were that it was retrospective in nature, only collecting data from a consecutive series of patients tested routinely in the clinic meaning the investigators were reliant on past medical records alone and the study was limited to a single point in time. The structure-function map used in this study is still an approximation of the actual relationship between RGCs and thresholds and is subject to variability at different stages of disease[101,167]. We acknowledge other difficulties with structure-function analysis namely the inherent errors of each imaging technology, the wide spread of RNFL thicknesses even in the same disease category and continuing debate as to the relationship between structure and function[91,98,163]. We acknowledge that using regression as a means of assessing the relationship is also not ideal as it attempts to simplify a complex relationship to a single score, but it is useful for comparisons. In calculating the accuracy of the classification software we were biased towards glaucoma patients presenting with field loss rather than just abnormal discs. In contrast the initial diagnosis of patients was based somewhat on optic disc appearance, thus favouring structure over function in patient selection. However diagnosis was combined with structural and functional imaging and patients had at least 3 HVFs so there was a rigorous diagnostic paradigm which we feel addressed these imbalances between structure and function. It is also much less common to have a field defect without disc change and as our aim was to take consecutive patients at a glaucoma practice we used a definition of glaucoma that enabled ease of study design.

Finally, as we did not collect an age-matched normals database, the study is not suited to calculate sensitivity/specificity, so we cannot comment on this aspect.

Previous studies of HRT3 and SD-OCT [83] have been based on the agreement between imaging systems rather than the correlation of either modality with functional defects. This study demonstrates a number of findings not shown previously – the comparison of each modality to 2 different functional methods (thresholds and scotomas) in the same subjects, at different stages of

disease and RNFL sector, and in different sizes of optic disc. In terms of relevance to clinical practice, the strengths of both machines lie in the IT and ST areas, where correlation with glaucomatous damage was most convincingly demonstrated, and both systems correctly identified a high percentage of glaucoma cases.

5 CONCLUSION

The results of the present study indicate that the newer SD-OCT technology can provide evidence of a closer structure-function correlation. However the relationship is still not uniform for all subjects or RNFL location, and appears to vary at different stages of disease.

Chapter 8 STRUCTURAL AND FUNCTIONAL CORRELATIONS OF NOVEL AND CONVENTIONAL PERIMETRY TECHNOLOGIES

Summary

Correlation between structural and functional changes in a glaucoma disease detection technology is an indirect indicator of the accuracy of the technology for diagnosing glaucomatous disease. By measuring the correlation coefficients of dichoptic and monocular mfVEP against those of HVF, as established in the previous chapter, we provided insight into the strengths and weaknesses, in the detection of glaucoma, of monocular and dichoptic mfVEP both globally and segmentally.

1 AIMS

Compare the correlation of structure and function of monocular mfVEP, dichoptic mfVEP and Humphrey visual field technologies in early glaucoma to assess which technology better correlates structure with function using Spectral Domain OCT as the reference (structural) standard.

To analyse the correspondence, as measured by Spearman's Rho (r_s), of different functional measures, namely absolute amplitude versus asymmetry in the detection of glaucomatous changes

2 INTRODUCTION

The importance of understanding the structure-function relationship in glaucoma cannot be overstated as it is critical to diagnosis, expectant management and prognosis for the patient and clinician.

Previous studies have sought to better approximate the relationship between the structure of the retinal nerve fibre layer (RNFL) and certain functional measures such as Humphrey visual field testing (HVF)[94,98,174] and multifocal visually evoked potentials (mfVEP)[46,175] in optic neuropathies. Although there is a significant body of work on HVF and RNFL relationships, there are no recent studies looking at the structure and function relationship between mfVEP and RNFL measurements and certainly no studies looking at dichoptic mfVEP.

In this study we sought to compare the structure/function relationship between Spectralis OCT (SD-OCT) and HVFs, monocular and dichoptic mfVEPs using regression and correlation analyses. The study aims to provide deeper insight into the structure/function relationships and to see which technologies had the closest correspondence with structural change.

3 METHODS

3.1 SUBJECT SELECTION

Participants were drawn from patients with open-angle glaucoma attending a large urban glaucoma practice in Sydney, Australia between June 2011 and December 2011. All patients had comprehensive medical and ophthalmic histories and examination recorded including Goldman applanation tonometry, fundoscopy, slit lamp examination and gonioscopy. The diagnosis of glaucoma was made based upon optic disc appearance with focal thinning of the neuroretinal rim

matching visual field loss consistent with glaucoma including arcuate patterns or clusters, respecting the horizontal meridian on HVF.

All patients underwent Heidelberg Spectralis ®(SD-OCT) (version 1.6.4.0 HRA2/Acquisition module 3.0.7.0), circle scan, centered on ONH, Humphrey Visual Field (HVF) testing (version 4.2.2 Model 750i) using SITA-standard 24-2 testing paradigm and mfVEP. MfVEP testing utilised a fast (9 frames per sequence) sparse blue on yellow, pattern pulse stimulus. Subjects underwent both dichoptic and monocular mfVEP recordings in a randomly assigned order, optimally corrected for near and stereoacuity > 100 seconds of arc.

Patients were excluded by identification of co-existing pathology, either in scan results or patient records. Co-existing pathology included disease that could possibly interfere with the glaucoma structure-function relationship such as cataract causing visual impairment, age related macular degeneration, visible diabetic retinopathy, vitreous opacity, disc drusen or branch retinal vein occlusion. In order to remove the inherent effects of inter-eye similarity, the eye with the worse disease, based upon Humphrey mean deviation, was selected.

29 early glaucoma patients (average MD (worst eye) = -3.54) were recruited from two Sydney-based glaucoma specialty practices. Ethics approval was gained from the University human ethics department and the experiments were conducted in accordance with the tenets of the declaration of Helsinki.

3.2 MFVEP TESTING

All patients, both normal and glaucomatous, underwent mfVEP on monocular and dichoptic testing using a dichoptic mfVEP described previously[142]. Briefly the setup consisted

of two mounted LCD screens (response time 2 ms; Flatron L1954TQS monitor; LG, Englewood Cliffs, NJ) on each side of the subject reflected through centrally located semitransparent mirrors to project a stimulus of 0° to 24° of eccentricity simultaneously to each eye. Mounted behind the mirrors were two infrared cameras, which continually monitored pupil position. Four infrared light-emitting diodes were placed around a lens holder to illuminate the eyes (Figure 2-3 (Methods, Chapter 2)).

The display to each eye consisted of a cortically scaled dartboard (Fig. 1A) with 56 segments arranged in five concentric rings (1°–2.5°, 2.5°–5°, 5°–10°, 10°–16°, and 16°–24°) and a central fixation target extending up to 0.5°. The stimulus in any segment consisted of a 4x4 blue-on-yellow (BonY)[142] check pattern. Segment size was scaled according to the cortical magnification factor. Corresponding to the size of the segments, the size of the individual checks also increased with eccentricity. The luminance of the blue check was 40 cd/m^2 and the luminance of the yellow background was 125 cd/m^2. A central fixation target was provided that consisted of rotating and slowly changing letters. These features—the ring arrangement and the fixation target—were identical for both eyes, which helped to fuse the images. The patient, therefore, perceived a single binocular image of the dartboard stimulus. Pseudorandom binary sequences (PRBSs) were used to drive the stimuli at each test location, so that the presentation at each location was random and independent of other locations. Each binary sequence had a 50% probability of being 1 or 0 at any point of time.

Element 1 was represented by two consecutive states: pattern on, lasting two frames of the screen (33.3ms) when the stimulus pattern was displayed, and pattern off, lasting 7 frames when the whole segment was diffusely illuminated with an intensity of the mean luminance. Element 0 consisted of the pattern-off states for 9 frames. The average rate of presentation at each segment was 3.32 times/s. The presentation of the stimulus to the corresponding segment of the second eye was shifted by either4 or 5 frames, the number of shifted frames alternating between stimulus presentation. The minimum separation between stimuli to corresponding areas of the visual fields of both eyes was either 2 (33.3ms) or 3 frames (50.0 ms). Three runs were recorded, each lasting 69 seconds.

The technique is described in detail elsewhere[142]. Monocular recordings were performed with the same setup with one eye covered.

Each patient underwent mfVEP testing in a random order for monocular and dichoptic testing with the three tests (binocular and 2 monocular) performed consecutively without breaks.

3.3 ANALYSIS AND STATISTICS

All correlation and regression analysis was performed in GraphPad ® (Prism 6 for Windows 2012).

RNFL measurements were divided into 4 sectors (Superior (45-135°), Nasal(135-225°), Inferior(225-315°) and Temporal(315-45°)), according to the software of each machine. The Humphrey visual field was divided as per a structure-function model[103] (Figure 8-1). To avoid type 1 errors caused by multiple comparisons using both eyes[117], the worst eye of the two eyes was used for amplitude correlation calculations. For asymmetry analysis, only the difference between eyes is used (i.e. asymmetry) and thus no artificial increase in p values brought about by using both eyes. For these reasons a Bonferroni correction was not felt to be necessary.

Mean threshold scores for each visual field sector (superior, inferior, etc.) were determined by calculation of the arithmetic mean of the scores in decibels. Each sector thus had a single mean threshold score in dB calculated for the correlation analysis. For mfVEP structure/function analysis the map, seen with HVF below, was used to average the amplitudes for each segment creating 4 averaged amplitudes for each eye as previously used in other papers [46,104].

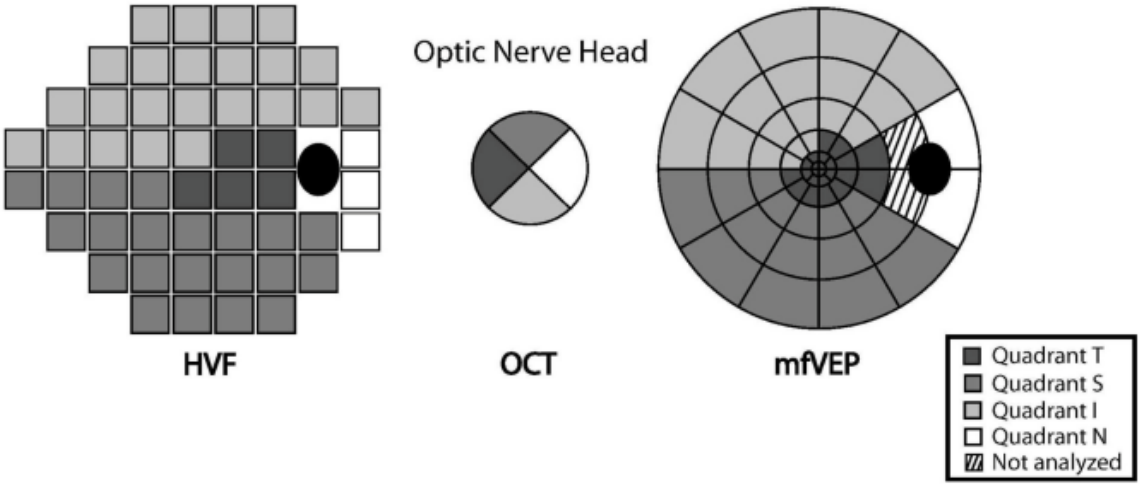

Figure 8-1 - MfVEP structure function map based on the work of Laron and Hood.

The above map (Figure 3) is sourced from Laron et al.'s [103]study examining patients with multiple sclerosis and is based upon work by Hood et al[102].

The structure-function map of Garway-Heath was used to relate sectors of the RNFL to the visual field (Figure 2). Analysis of the correlation between RFNL thickness and mean threshold was calculated using the bivariate correlation function in GraphPad to determine Spearman's rho (rs) coefficient. This was chosen because MD(dB) and VFI(%) were not normally distributed (one-sample Kolmogorov-Sminrnov test), consistent with many previous studies [91,161] . For comparative purposes only, strong correlation was defined as rs = 0.7-1, moderate as rs = 0.4-0.7 and weak as rs < 0.4.

4 RESULTS

Regression of the data using both linear and logarithmic analysis showed generally poor fit of the RNFL circle values and raw amplitudes of the mfVEP. HVF mean deviation and global RNFL thickness showed a closer fit using a linear model for regression analysis than for mfVEP.

Figure 8-2 shows correlation for monocular full field averaged mfVEP amplitude and SD-OCT values, there appears to be no correlation between these values.

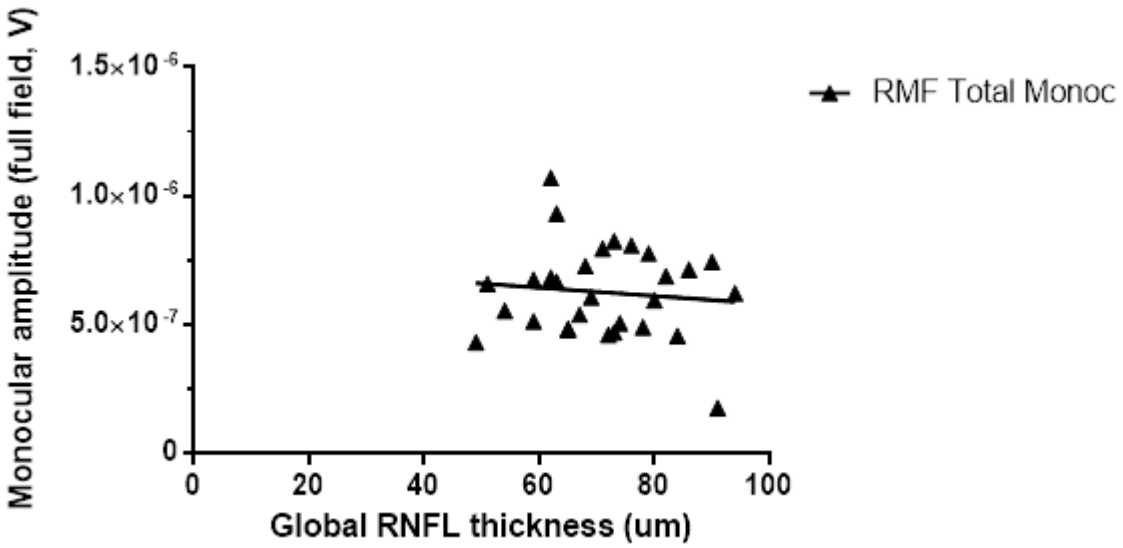

Figure 8-2 - Full field monocular (worst eye) mfVEP amplitude plotted against global RNFL thickness. Note the poor correlation of data for linear regression, r2 = 0.01.

Figure 8-3 shows the binocular mfVEP full field averaged amplitude values for dichoptic mfVEP, again showing limited correlation for raw amplitude values and global RNFL thicknesses.

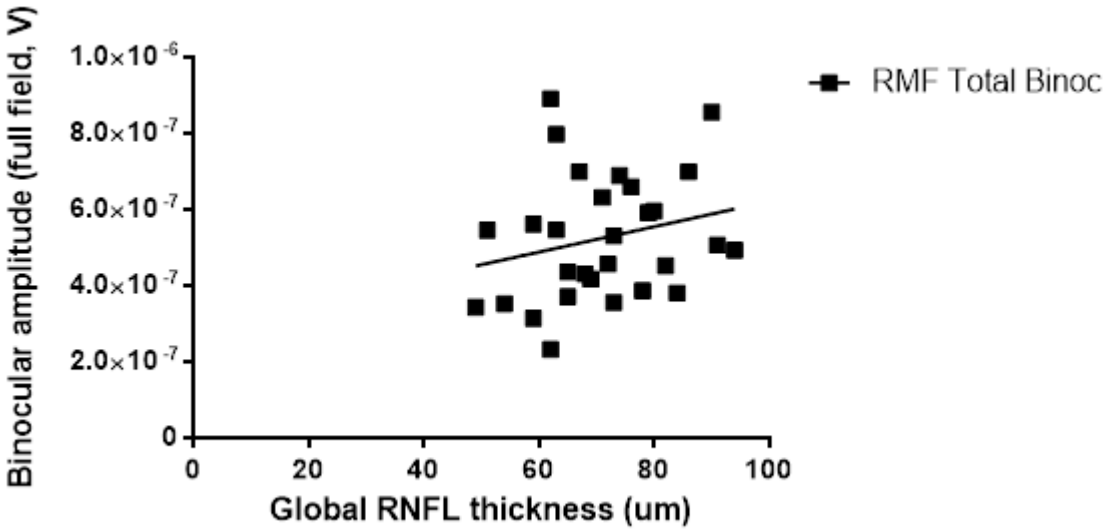

Figure 8-3 - Full field binocular (worst eye) mfVEP amplitude plotted against global RNFL thickness. Note the poor correlation of data for linear regression, r2 = 0.05

Figure 8-4 shows a slightly closer correlation between mean deviation for HVF and global RNFL values, with an appropriate trend for thicker RNFL values and lower MD values.

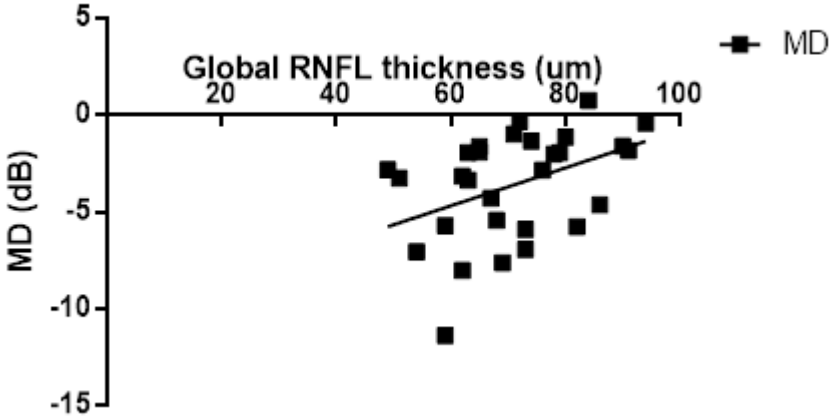

Figure 8-4 - Mean deviation of HVF plotted against global RNFL thickness. Note the higher r2 value = 0.17 for linear regression when compared to mfVEP.

Average amplitudes of mfVEP correlated poorly with the corresponding RNFL segment with r_s values below 0.3 for all sectors except binocular mfVEP for the inferior RNFL segment. This was demonstrated for both dichoptic and monocular mfVEP results (Table 8-1).

HVF averaged total deviation scores had much higher correlation coefficients compared with mfVEP. The highest were the inferior and superior segments with the corresponding visual field areas (Table 1). MD appeared to correlate more strongly with global RNFL versus PSD.

	Binoc	Monoc	HVF	
Temporal	0.047	0.168	0.073	
Nasal	0.182	0.049	0.216	
Inferior	0.417*	0.226*	0.706**	
Superior	0.263	-0.020	0.611**	
Global measures	0.274	-0.006	0.464*	MD
Global measures			-0.285	PSD

Table 8-1- Table of correlation coefficients (Spearman's Rho) for mfVEP (dichoptic and monocular) and HVF, segmentally and globally. Where global measures refers to entire field (i.e. total average amplitude in mfVEP or MD/PSD in HVF) (p values - * = p<0.05; ** = p<0.01)

Analysis of the data for intereye asymmetry for the field technologies (HVF, mfVEP) and RNFL asymmetry, as calculated by the Spectralis software system, showed a much closer relationship between structural and functional measures. Monocular intereye asymmetry was not as closely correlated to RNFL data as binocular intereye asymmetry (r^2 = 0.424 versus r^2 = 0.481) as can be seen in Figure 8-5 and Figure 8-6. HVF intereye asymmetry (difference between MD in each eye) appeared to follow a closer relationship with RNFL asymmetry values, r^2=0.522 (Figure 8-7).

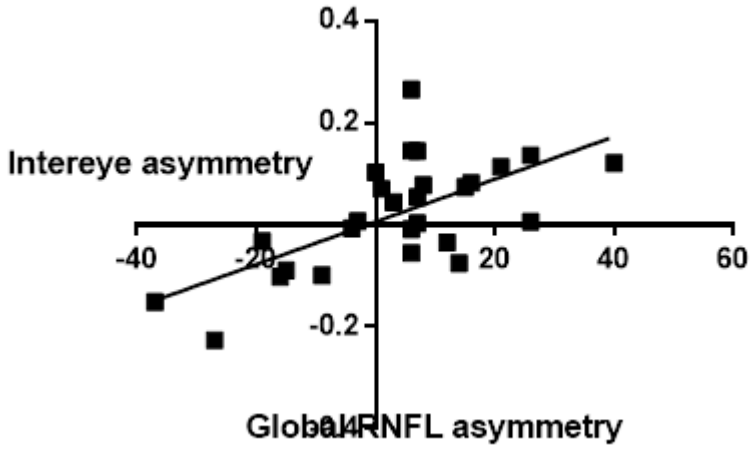

Figure 8-5 - Monocular intereye asymmetry plotted against global RNFL asymmetry. There is a strong correlation for linear regression (r2=0.4244) (2 outliers removed).

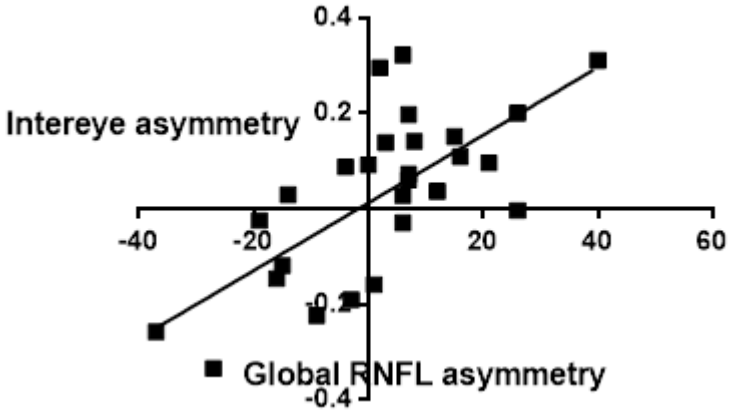

Figure 8-6 - Binocular intereye asymmetry plotted against RNFL asymmetry. For linear regression r2 = 0.4811 (1 outlier removed).

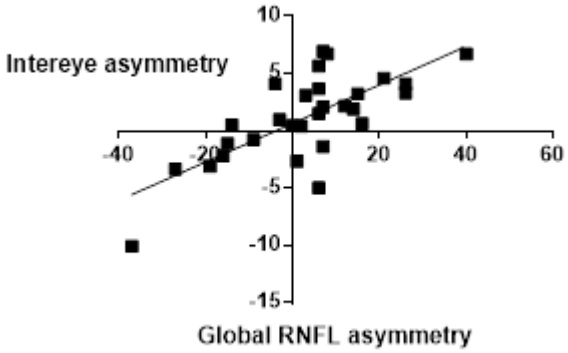

Figure 8-7 - HVF mean deviation asymmetry plotted against global RNFL asymmetry. For linear regression analysis r2=0.5218.

Compared to the amplitude profile correlation analysis, the asymmetry analysis demonstrated much stronger correlations for all technologies. Binocular mfVEP had correlations of 0.65 for inferior RNFL ring asymmetry coefficients (i.e. asymmetry of RNFL ring correlated with the corresponding mfVEP sectoral asymmetry) and 0.77 for the superior RNFL with global (RNFL versus total amplitude asymmetry) asymmetry calculated at r_s= 0.66. Monocular correlations were weaker than binocular but demonstrated the highest correlations in inferior and superior RNFL segments. Global asymmetry was calculated at r_s=0.43.

HVF asymmetry correlation coefficients were generally higher than mfVEP r_s values and demonstrated strong correlation values with the superior and inferior RNFL segments. Both MD and PSD asymmetry correlation coefficients were 0.68 and -0.61 respectively (Table 8-2).

	Binocular	Monocular	HVF	
Temporal	0.243	0.177	0.393*	
Nasal	0.480**	0.019	0.287	
Inferior	0.651**	0.588**	0.714**	
Superior	0.770**	0.7118**	0.848**	
Global measures	0.663**	0.434*	0.679**	MD
Global measures			-0.613**	PSD

Table 8-2 - Correlation coefficients (Spearman's Rho) for field technologies (mfVEP and HVF) with SD-OCT. Where global measures refers to entire field (i.e. total average asymmetry in mfVEP or average asymmetry between right and left MD/PSD in HVF) (p values - * = p<0.05; ** = p<0.01)

5 DISCUSSION

The aim of this paper was to use correlation analysis to compare HVF and mfVEP technologies and the correspondence to a commonly used structure/function relationship. Not surprisingly the mfVEP fared poorly when compared to the HVF in terms of correlation between sectoral values of amplitude readings and OCT RNFL values. This could be in part due to the nature of electrophysiological amplitude variations inherent in the normal population and without normalising the readings there is little scope for meaningful comparison. This aspect would be addressed by normalising the amplitude scores for the mfVEP testing and using these scores when comparing between HVF and mfVEP, however the limited size of the normals database means this is not particularly effective at this point in time.

In contrast and in keeping with previous work on asymmetry analysis,[99,176] there were strong correlations when analysing the inter-eye asymmetry scores and OCT sectoral RNFL measurements. Indeed the correlation coefficients for monocular and binocular mfVEP in table 2 were nearly the same as the HVF r_s values. This could indicate the strength of the mfVEP testing methods in early glaucoma, namely the strength of asymmetry analysis for detecting early defects. We have previously discussed the reasons why asymmetry analysis is an effective way to diagnose early glaucoma and the reasons why binocular mfVEP may offer advantages over monocular, namely tighter asymmetry between eyes in the normal database, recording of signals simultaneously[73,75] thereby increasing the homogeneity of the recording environment and reducing changes in testing environments when switching between eyes. For the aforementioned reasons binocular recordings appear to have similar asymmetry correlation coefficients when compared to HVF MD and HVF asymmetry analysis. For these same reasons the monocular mfVEP asymmetry analysis appears to have slightly lower asymmetry correlation coefficients. The amplitude correlations for the mfVEP is particularly disappointing and inconsistent with previous experience[48,75] – a possible explanation lies with the nature of the analysis performed and the numbers of patients involved meaning that for mfVEP, which has a wide variability, a critical number of patients was not reached to provide meaningful data. Addressing these issues could be an avenue to pursue in a larger clinical study.

In terms of segmental correlations the temporal and nasal sectors have the lowest correlation coefficients and for all three visual function tests and for asymmetry and amplitude analysis – this is consistent with previous

studies in HVF structure/function work[174,177] and with previous mfVEP studies[46,104,176]. These findings are most likely related to the pattern of glaucomatous defects (usually in the arcuate bundles) and due to the relative densities of the nasal/temporal RNFL bundles versus the larger and therefore more susceptible superior and inferior bundles.

It should be pointed out the limitations of the above study design namely that comparison of correlation coefficients does not provide a definitive link between cause and effect[117] and they may not be the most appropriate method for evaluating the effectiveness of a diagnostic tool, we have used an unconventional asymmetry tool in calculating the asymmetry of total measures (i.e. MD or PSD) between right and left HVF fields, we have used a structure-function maps that are widely accepted but are by no means a perfect representation of the complex relationship between retinal nerve fibre layer and visual field function. We have not used retinal photography to validate the optic disc pathology in the study so rely heavily on the reliability of the technologies rather than comparison to the gold standard of glaucoma diagnosis (i.e. trained physician, blinded optic nerve assessment).

6 CONCLUSION

This study aimed to provide a further understanding of the nature of structure/function correlations of mfVEP and OCT in glaucoma with HVF as an established standard to compare against. It was demonstrated that although amplitude is not strongly correlated to OCT changes, as compared with HVF, there are comparable correlation coefficients for asymmetry analysis for binocular and monocular mfVEP. In addition it was shown that binocular demonstrated superior correlation, versus monocular, in asymmetry and amplitude analyses.

Chapter 9 CONCLUSIONS AND FUTURE DIRECTIONS

1 CONCLUSIONS

This thesis sought to explore the hypotheses that stipulated a relationship between dichoptic suppression and stimulus presentation, that questioned whether dichoptic mfVEP could be optimised for early detection of glaucoma and that functional changes detected by mfVEP were consistent with functional HVF changes and structural retinal imaging changes. Fundamental to the hypotheses on glaucoma detection was whether altering dichoptic suppression through stimulus choice could increase the sensitivity of this emerging technology.

In addition this thesis sought to answer research questions concerning the structural and functional aspects of glaucomatous optic neuropathy and the relationship between HVF, retinal imaging technologies and mfVEP.

Dichoptic mfVEP is a clinically relevant tool in glaucoma detection and with correct stimulus selection, optimal detection of glaucoma can be achieved. Dichoptic suppression is an eccentricity and temporally-dependent phenomenon and increases rates of detection (through magnifying inter-eye asymmetry) by a suppression/release-of-suppression mechanism. Contrast appears to have little effect on dichoptic suppression, but adding a chromatic element to the stimulus causes significantly greater suppression and inter-eye asymmetry effects. Indeed, dichoptic mfVEP has clinical utility and in glaucoma patients appears to show greater sensitivity than monocular alone. In addition, both dichoptic and monocular mfVEP correlate favourably with HVF and OCT technologies. It was shown that the structure function relationship is complex in glaucoma and newer OCT imaging technology correlated more closely than HRT to HVF. Lastly, the structure function correlation in monocular and dichoptic mfVEP is greatly enhanced when inter-eye asymmetry is used to detect glaucomatous changes.

Chapter 3 sought to address the research questions related to the nature of interocular suppression and the mechanisms underlying increased asymmetry seen in previous dichoptic mfVEP experiments.

The study demonstrated that dichoptic stimulation results in eccentricity-dependent suppression of mfVEP amplitude. It also revealed that factors affecting visual performance of one eye (monocular blur or possibly a monocular pathological process) not only have a negative effect on dichoptic mfVEP amplitude of the affected eye, but also promote release of dichoptic suppression in the fellow (unaffected) eye. This phenomenon supports our earlier hypothesis[76] that unilateral loss leads to a relative increase in inter-eye asymmetry and therefore may potentially be utilised for early detection of a unilateral pathological processes.

Chapter 4 examined aspects of the hypotheses concerning stimulus selection for optimisation in glaucoma detection by altering stimulus speed and contrast, measuring the dichoptic suppression and amplitude characteristics of normal volunteers. This chapter primarily sought to address the questions as to whether magnocellular and parvocellular subtypes could be selectively stimulated to enhance the non-redundant pathways which are thought to be more susceptible to damage in early glaucoma. The research clarified the effect of eccentricity on dichoptic suppression, demonstrated that DS was a function of stimulus speed but not contrast levels and added further information on the effect of contrast and speed on ganglion cell populations' behaviour. The finding that stimulus speed but not contrast alters dichoptic suppression highlights the temporal dependency of dichoptic suppression and the points to the temporally sluggish binocular neurons as the slowest link in the retina to cortex chain.

Chapter 5 compared achromatic and chromatic stimuli at different presentation speeds to understand the relevance of dichoptic suppression and asymmetry in glaucoma patients. The studies addressed the research questions on fast stimulation use in dichoptic mfVEP and whether there was a role for fast stimulation over slower stimulation. The temporal processing resolution of the koniocellular pathway may increase the degree of dichoptic suppression and account for the increase in asymmetry seen with this set of experiments. Whilst there appeared to be no increase in inter-eye asymmetry with fast compared with slow BonY stimuli, the findings didn't rule out using fast stimulation for glaucoma detection in a larger clinical trial. The above issues have formed the basis

for the subsequent chapters to explore the utility of fast stimulation and the nature of dichoptic suppression in normal and glaucomatous patients.

Chapter 6 addressed two main hypotheses concerning the optimal detection of glaucoma using dichoptic mfVEP and the relationship between mfVEP changes, HVF and structural imaging technologies. Specifically it addressed the research questions concerning the sensitivity of dichoptic as compared with monocular, the use of fast stimulation in glaucoma detection, mechanisms for potential increase in asymmetry and combined these points into a relevant clinical experiment. This chapter found that there is a significant difference between the rates of detection, as measured by z-scores, between monocular and dichoptic asymmetry analysis using mfVEP. The increased dichoptic suppression in dichoptic mfVEP most likely enhances the dichoptic system for detecting early unilateral glaucomatous damage. Dichoptic mfVEP appears to have greater levels of sensitivity as compared to monocular testing and that the mechanism underlying this is enhanced dichoptic suppression, further increased by the use of a fast stimulation rate.

Chapter 7 explored the complex relationship between optic nerve structure and function and the confounding factors that exist in the relationship. This chapter addressed research questions relating to structural nerve head imaging, multiple conflicting technologies and the nature of the structure function relationship in glaucoma. In a head to head comparison, OCT structural RNFL values showed closer correlation to HVF decibel readings as compared to HRT. This is a significant finding as the two imaging technologies are the most commonly used and provide a large amount of the information that is instrumental in the diagnosis of glaucoma. Severity of disease appeared to influence correlation with structure/function but disc size had a minimal effect. Above all this chapter highlighted the inconsistencies in structure/function analysis and stressed the importance of utilising multiple sources of information in making a clinical diagnosis of glaucoma. Relying too heavily on any one piece of technology can lead to incorrect findings.

Chapter 8 answered a number of research questions but primarily highlighted the correlations between structural imaging using OCT and functional testing using HVF, monocular mfVEP and

dichoptic mfVEP. Using a small sample of patients, the raw amplitude values only provided limited correlations between structure and function. However, as has been one of the fundamental themes in this thesis, there was much closer correlation between glaucomatous disease when inter-eye asymmetry was used as a disease indicator. The finding that dichoptic mfVEP had closer correlation to structure and function than monocular and that HVF had superior correlations overall addressed research questions pertaining to the relevance of dichoptic mfVEP to glaucomatous disease.

Dichoptic mfVEP is an emerging technology with demonstrable benefits over monocular mfVEP in the detection of glaucoma. Dichoptic suppression, combined with correct stimulus selection, can target non-redundant pathways as evidenced by inter-eye asymmetry results. Dichoptic mfVEP shows good correlation to structural deficits and is indeed comparable to HVF results.

2 FUTURE DIRECTIONS

Whilst this thesis has continued work on the testing and understanding of dichoptic mfVEP and its clinical uses there is a significant body of work required for practical use of the technology to occur. Potential avenues of research are listed below:

1) Improving on the ease/cost of use of dichoptic mfVEP
    a. Simplifying the setup so as to lessen the need for a skilled operator
    b. Making the recording process as quick and efficient as possible
    c. Decreasing the setup and running cost of the setup
    d. Increasing the portability of the machinery
2) Further work on dichoptic mfVEP in glaucoma detection
    a. Large scale prospective cohort study comparing sensitivity and specificity of current technologies (HVF/FDT/SWAP) and dichoptic/monocular mfVEP in early disease detection over time
    b. Using targeted concentric stimuli, for instance high contrast central stimulus with low contrast peripheral stimulus
3) Further work on dichoptic mfVEP in other disease detection
    a. Detection of abnormalities in unilateral optic neuritis and other unilateral optic neuropathies
    b. Assessment of subtle amblyopia
    c. Assessment of non-organic visual loss
    d. Work on assessing eye dominance
4) Addressing the inherent limitations of mfVEP
    a. Software programming that could account for media opacities analogous to pattern standard deviation used in HVF testing
    b. Dual assessment with ERG testing such as PERG to quantify retinal macula function complementing mfVEP optic nerve evaluation

APPENDIX A – FINAL ETHICS APPROVAL LETTER

Klistorner
HE25Sep2009-D00139

MACQUARIE UNIVERSITY

Research Office
Research Hub, Building C5C East
MACQUARIE UNIVERSITY NSW 2109

Phone +61 (0)2 9850 8612
Fax +61 (0)2 9850 4465
Email ro@vc.mq.edu.au

Ethics
Phone +61 (0)2 9850 6848
Email ethics.secretariat@vc.mq.edu.au

18 September 2009

Associate Professor Alexander Klistorner
The University of Sydney
Campus of Sydney Eye Hospital
8 Macquarie Street
Sydney
NSW 2000

Reference: HE25SEP2009-D00139

Dear Associate Professor Klistorner

Title of project: Optimizing the detection of early glaucoma targeting specific visual pathways in combination with structural measures

The above application was considered by the Executive of the Ethics Review Committee (Human Research). In accordance with section 5.5 of the *National Statement on Ethical Conduct in Human Research (2007)* the Executive noted the final approval from the University of Sydney and your right to proceed under their authority.

Please do not hesitate to contact the Ethics Secretariat if you have any questions or concerns.

Yours sincerely

Dr Karolyn White
Director of Research Ethics
Chair, Ethics Review Committee (Human Research)

Cc: Dr Jennifer Batchelor, Department of Psychology, Faculty of Human Science

The University of Sydney

Human Research Ethics Committee
Web: http://www.usyd.edu.au/ethics/human

Gail Briody
Manager
Office of Ethics Administration
Telephone: +61 2 8627 8175
Facsimile: +61 2 8627 8180
Email: gbriody@usyd.edu.au

Marietta Coutinho
Deputy Manager
Human Research Ethics Administration
Telephone: +61 2 8627 8176
Facsimile: +61 2 8627 8177
Email: mcoutinho@usyd.edu.au

Mailing Address:
Level 6
Jane Foss Russell Building – G02
The University of Sydney
NSW 2006 AUSTRALIA

Ref: PB/PE

13 July 2009

Associate Professor Alexander Klistorner
Save Sight Institute
Sydney Eye Campus
Macquarie Street
SYDNEY NSW 2000
Email; sasha@eye.usyd.edu.au

Dear Professor Klistorner

Thank you for your correspondence dated 20 May 2009 addressing comments made to you by the Human Research Ethics Committee (HREC). After considering the additional information, the Executive Committee at its meeting on **26 May 2009** approved your protocol entitled ***"Optimizing the detection of early glaucoma targeting specific visual pathways in combination with structural measures"***.

Details of the approval are as follows:

Ref No.:	***05-2009/11594***
Approval Period:	***May 2009 to May 2010***
Authorised Personnel:	***Associate Professor Alexander Klistorner*** ***Dr Stuart Graham*** ***Dr Hemamalini Arvind***

The HREC is a fully constituted Ethics Committee in accordance with the *National Statement on Ethical Conduct in Research Involving Humans-March 2007* under *Section 5.1.29*

The approval of this project is **conditional** upon your continuing compliance with the *National Statement on Ethical Conduct in Research Involving Humans*. We draw to your attention the requirement that a report on this research must be submitted every 12 months from the date of the approval or on completion of the project, whichever occurs first. Failure to submit reports will result in withdrawal of consent for the project to proceed.

Chief Investigator / Supervisor's responsibilities to ensure that:

(1) All serious and unexpected adverse events should be reported to the HREC as soon as possible.

(2) All unforeseeen events that might affect continued ethical acceptability of the project should be reported to the HREC as soon as possible.

(3) The HREC must be notified as soon as possible of any changes to the protocol. All changes must be approved by the HREC before continuation of the research project. These include:-

- If any of the investigators change or leave the University.
- Any changes to the Participant Information Statement and/or Consent Form.

(4) All research participants are to be provided with a Participant Information Statement and Consent Form, unless otherwise agreed by the Committee. The Participant Information Statement and Consent Form are to be on University of Sydney letterhead and include the full title of the research project and telephone contacts for the researchers, unless otherwise agreed by the Committee and the following statement must appear on the bottom of the Participant Information Statement. *Any person with concerns or complaints about the conduct of a research study can contact the Manager, Ethics Administration, University of Sydney, on (02) 8627 8175 (Telephone); (02) 8627 8180 (Facsimile) or gbriody@usyd.edu.au (Email).*

(5) Copies of all signed Consent Forms must be retained and made available to the HREC on request.

(6) It is your responsibility to provide a copy of this letter to any internal/external granting agencies if requested.

(7) The HREC approval is valid for four (4) years from the Approval Period stated in this letter. Investigators are requested to submit a progress report annually.

(8) A report and a copy of any published material should be provided at the completion of the Project.

Yours sincerely,

Phil Beale

Associate Professor Philip Beale
Chairman
Human Research Ethics Committee

Encl. Approved Participant Information Statement
Approved Participant Information Statement – Control Subjects
Approved Participant Consent Form
Approved Revocation of Consent

REFERENCES

1. S Resnikoff ea. Global data on visual impairment in the year 2002. Bull World Health Organization 2004;82:844-51.
2. Kerrigan-Baumrind LA, Quigley HA, Pease ME, Kerrigan DF, Mitchell RS. Number of ganglion cells in glaucoma eyes compared with threshold visual field tests in the same persons. Invest Ophthalmol Vis Sci 2000;41:741-8.
3. Jonas JB, Gusek GC, Naumann GO. Optic disc, cup and neuroretinal rim size, configuration and correlations in normal eyes. Invest Ophthalmol Vis Sci 1988;29:1151-8.
4. MA Kass DH, EJ Higginbotham, et al.:. The Ocular Hypertension Treatment Study: a randomized trial determines that topical ocular hypotensive medication delays or prevents the onset of primary open-angle glaucoma. . Arch Ophthalmol 2002;120:701-13.
5. Wensor MD, McCarty CA, Stanislavsky YL, Livingston PM, Taylor HR. The prevalence of glaucoma in the Melbourne Visual Impairment Project. Ophthalmology 1998;105:733-9.
6. Dirani M, Crowston JG, Taylor PS, et al. Economic impact of primary open-angle glaucoma in Australia. Clinical & Experimental Ophthalmology 2011;39:623-32.
7. Sehu W, Lee, W.R. Ophthalmic Pathology: An illustrated guide for clinicians: Wiley; 2005.
8. Shaarawy T, Sherwood, M., Hitchings, R., Crowston, J.G. Glaucoma2009.
9. Schulzer M, Drance SM, Douglas GR. A comparison of treated and untreated glaucoma suspects. Ophthalmology 1991;98:301-7.
10. Kass MA, Heuer DK, Higginbotham EJ, et al. The Ocular Hypertension Treatment Study: a randomized trial determines that topical ocular hypotensive medication delays or prevents the onset of primary open-angle glaucoma. Arch Ophthalmol 2002;120:701-13; discussion 829-30.
11. Quigley HA, Enger C, Katz J, Sommer A, Scott R, Gilbert D. Risk factors for the development of glaucomatous visual field loss in ocular hypertension. Arch Ophthalmol 1994;112:644-9.
12. Flammer J, Orgül S. Optic nerve blood-flow abnormalities in glaucoma. Progress in Retinal and Eye Research 1998;17:267-89.
13. Tielsch JM, Katz J, Sommer A, Quigley HA, Javitt JC. Hypertension, perfusion pressure, and primary open-angle glaucoma. A population-based assessment. Arch Ophthalmol 1995;113:216-21.
14. Burgoyne CF, Downs JC, Bellezza AJ, Suh JK, Hart RT. The optic nerve head as a biomechanical structure: a new paradigm for understanding the role of IOP-related stress and strain in the pathophysiology of glaucomatous optic nerve head damage. Prog Retin Eye Res 2005;24:39-73.
15. Gordon MO, Beiser JA, Brandt JD, et al. The Ocular Hypertension Treatment Study: baseline factors that predict the onset of primary open-angle glaucoma. Archives of Ophthalmology 2002;120:714-20; discussion 829-30.
16. Heijl A, Leske MC, Bengtsson B, et al. Reduction of intraocular pressure and glaucoma progression: results from the Early Manifest Glaucoma Trial. Archives of Ophthalmology 2002;120:1268-79.
17. Leske MC, Nemesure B, He Q, Wu SY, Fielding Hejtmancik J, Hennis A. Patterns of open-angle glaucoma in the Barbados Family Study. Ophthalmology 2001;108:1015-22.
18. Perkins ES, Phelps CD. Open angle glaucoma, ocular hypertension, low-tension glaucoma, and refraction. Arch Ophthalmol 1982;100:1464-7.
19. Su WW, Cheng ST, Ho WJ, et al. Glaucoma is associated with peripheral vascular endothelial dysfunction. Ophthalmology 2008;115:1173-8.e1.
20. Rechtman E, Harris A, Rechtman E, Harris A. Choroidal blood flow regulation and possible implications to glaucoma.[comment]. Clinical & Experimental Ophthalmology 2008;36:111-2.
21. Wall M, Doyle CK, Zamba KD, Artes P, Johnson CA. The repeatability of mean defect with size III and size V standard automated perimetry. Invest Ophthalmol Vis Sci 2013;54:1345-51.
22. Ansari EA, Morgan JE, Snowden RJ. Psychophysical characterisation of early functional loss in glaucoma and ocular hypertension. Br J Ophthalmol 2002;86:1131-5.

23. Sample PA, Bosworth CF, Blumenthal EZ, Girkin C, Weinreb RN. Visual function-specific perimetry for indirect comparison of different ganglion cell populations in glaucoma. Invest Ophthalmol Vis Sci 2000;41:1783-90.
24. Wild JM. Short wavelength automated perimetry. Acta Ophthalmol Scand 2001;79:546-59.
25. Callaway EM. Local circuits in primary visual cortex of the macaque monkey. Annual Review of Neuroscience 1998;21:47-74.
26. Marmor MF, Fulton AB, Holder GE, Miyake Y, Brigell M, Bach M. ISCEV Standard for full-field clinical electroretinography (2008 update). Documenta ophthalmologica Advances in ophthalmology 2009;118:69-77.
27. Holopigian K, Hood DC. Electrophysiology. Ophthalmology clinics of North America 2003;16:237-51.
28. Ventura LM, Porciatti V. Pattern electroretinogram in glaucoma. Curr Opin Ophthalmol 2006;17:196-202.
29. Ventura LM, Porciatti V, Ishida K, Feuer WJ, Parrish RK, 2nd. Pattern electroretinogram abnormality and glaucoma. Ophthalmology 2005;112:10-9.
30. Bach M, Unsoeld AS, Philippin H, et al. Pattern ERG as an early glaucoma indicator in ocular hypertension: a long-term, prospective study. Invest Ophthalmol Vis Sci 2006;47:4881-7.
31. Ventura LM, Sorokac N, De Los Santos R, Feuer WJ, Porciatti V. The relationship between retinal ganglion cell function and retinal nerve fiber thickness in early glaucoma. Invest Ophthalmol Vis Sci 2006;47:3904-11.
32. Hood DC, Frishman LJ, Viswanathan S, Robson JG, Ahmed J. Evidence for a ganglion cell contribution to the primate electroretinogram (ERG): effects of TTX on the multifocal ERG in macaque. Vis Neurosci 1999;16:411-6.
33. Hasegawa S, Takagi M, Usui T, Takada R, Abe H. Waveform changes of the first-order multifocal electroretinogram in patients with glaucoma. Invest Ophthalmol Vis Sci 2000;41:1597-603.
34. Hood DC, Greenstein VC, Holopigian K, et al. An attempt to detect glaucomatous damage to the inner retina with the multifocal ERG. Invest Ophthalmol Vis Sci 2000;41:1570-9.
35. Kaneko M, Machida S, Hoshi Y, Kurosaka D. Alterations of Photopic Negative Response of Multifocal Electroretinogram in Patients with Glaucoma. Curr Eye Res 2014:1-10.
36. Bach M, Poloschek CM. Electrophysiology and glaucoma: current status and future challenges. Cell and tissue research 2013;353.
37. Viswanathan S, Frishman LJ, Robson JG, Harwerth RS, Smith EL, 3rd. The photopic negative response of the macaque electroretinogram: reduction by experimental glaucoma. Invest Ophthalmol Vis Sci 1999;40:1124-36.
38. Viswanathan S, Frishman LJ, Robson JG, Walters JW. The photopic negative response of the flash electroretinogram in primary open angle glaucoma. Invest Ophthalmol Vis Sci 2001;42:514-22.
39. Tamada K, Machida S, Oikawa T, Miyamoto H, Nishimura T, Kurosaka D. Correlation between photopic negative response of focal electroretinograms and local loss of retinal neurons in glaucoma. Curr Eye Res 2010;35:155-64.
40. Machida S, Kaneko M, Kurosaka D. Regional Variations in Correlation between Photopic Negative Response of Focal Electoretinograms and Ganglion Cell Complex in Glaucoma. Curr Eye Res 2014:1-11.
41. Towle VL, Moskowitz A, Sokol S, Schwartz B. The visual evoked potential in glaucoma and ocular hypertension: effects of check size, field size, and stimulation rate. Invest Ophthalmol Vis Sci 1983;24:175-83.
42. Schmeisser ET, Smith TJ. High-frequency flicker visual-evoked potential losses in glaucoma. Ophthalmology 1989;96:620-3.
43. Korth M, Nguyen NX, Junemann A, Martus P, Jonas JB. VEP test of the blue-sensitive pathway in glaucoma. Invest Ophthalmol Vis Sci 1994;35:2599-610.
44. Levin L.A. NS, Ver Hoeve J., Miao-Sin Wu S., Kaufman P.L., Alm A. Adler's Physiology of the Eye: Elsevier - Health Sciences Division; 2011.
45. Klistorner A, Arvind H, Nguyen T, et al. Axonal loss and myelin in early ON loss in postacute optic neuritis. Annals of Neurology 2008;64:325-31.

46. Klistorner A, Arvind H, Nguyen T, et al. Multifocal VEP and OCT in optic neuritis: a topographical study of the structure–function relationship. Documenta Ophthalmologica 2009;118:129-37.
47. Graham SL, Klistorner AI, Goldberg I. Clinical Application of Objective Perimetry Using Multifocal Visual Evoked Potentials in Glaucoma Practice. Arch Ophthalmol 2005;123:729-39.
48. Klistorner A, Graham SL, Martins A, et al. Multifocal blue-on-yellow visual evoked potentials in early glaucoma. Ophthalmology 2007;114:1613-21.
49. Arvind H, Graham S, Leaney J, et al. Identifying Preperimetric Functional Loss in Glaucoma: A Blue-on-Yellow Multifocal Visual Evoked Potentials Study. Ophthalmology 2009;116:1134-41.
50. Arvind H, Klistorner A, Grigg J, Graham SL. Low-luminance contrast stimulation is optimal for early detection of glaucoma using multifocal visual evoked potentials. Investigative Ophthalmology & Visual Science 2011;52:3744-50.
51. Hood DC, Greenstein VC. Multifocal VEP and ganglion cell damage: applications and limitations for the study of glaucoma. Progress in Retinal & Eye Research 2003;22:201-51.
52. Klistorner AI, Graham SL. Electroencephalogram-based scaling of multifocal visual evoked potentials: effect on intersubject amplitude variability. Investigative ophthalmology & visual science 2001;42.
53. Fortune B, Demirel S, Zhang X, et al. Repeatability of normal multifocal VEP: implications for detecting progression. Journal of Glaucoma 2006;15:131-41.
54. Hood DC, Thienprasiddhi P, Greenstein VC, et al. Detecting early to mild glaucomatous damage: a comparison of the multifocal VEP and automated perimetry. Investigative Ophthalmology & Visual Science 2004;45:492-8.
55. Klistorner A, Crewther DP, Crewther SG. Separate magnocellular and parvocellular contributions from temporal analysis of the multifocal VEP. Vision Research 1997;37:2161-9.
56. Klistorner AI, Graham SL, Grigg JR, Billson FA. Electrode position and the multi-focal visual-evoked potential: role in objective visual field assessment. Australian & New Zealand Journal of Ophthalmology 1998;26 Suppl 1:S91-4.
57. Winn BJ, Shin E, Odel JG, Greenstein VC, Hood DC. Interpreting the multifocal visual evoked potential: the effects of refractive errors, cataracts, and fixation errors. British Journal of Ophthalmology 2005;89:340-4.
58. Baseler HA, Sutter EE, Klein SA, Carney T. The topography of visual evoked response properties across the visual field. Electroencephalography & Clinical Neurophysiology 1994;90:65-81.
59. Martins A, Klistorner A, Graham S, Billson F. Effect of fixation tasks on multifocal visual evoked potentials. Clinical & Experimental Ophthalmology 2005;33:499-504.
60. Martins A, Klistorner A, Graham S, Billson F. Effect of check size and stimulation rate on blue-yellow multifocal visual evoked potentials. Clinical & Experimental Ophthalmology 2004;32:270-4.
61. James AC. The Pattern-Pulse Multifocal Visual Evoked Potential. Invest Ophthalmol Vis Sci 2003;44:879-90.
62. James AC, Ruseckaite R, Maddess T, James AC, Ruseckaite R, Maddess T. Effect of temporal sparseness and dichoptic presentation on multifocal visual evoked potentials. Visual Neuroscience 2005;22:45-54.
63. Hood DC, Zhang X, Hong JE, Chen CS. Quantifying the benefits of additional channels of multifocal VEP recording. Documenta ophthalmologica Advances in ophthalmology 2002;104:303-20.
64. Goldberg I, Graham SL, Klistorner AI. Multifocal objective perimetry in the detection of glaucomatous field loss. Am J Ophthalmol 2002;133.
65. Rovamo J, Virsu V. An estimation and application of the human cortical magnification factor. Experimental brain research Experimentelle Hirnforschung Experimentation cerebrale 1979;37.
66. Hood DC, Greenstein VC. Multifocal VEP and ganglion cell damage: applications and limitations for the study of glaucoma. Progress in Retinal and Eye Research 2003;22:201-51.
67. Graham S, Klistorner Al, Grigg JR, Bilson FA. Objective VEP perimetry in glaucoma : asymmetry analysis to identify early deficits. Journal of Glaucoma 2000;9:10-9.
68. Hood DC, Zhang X, Greenstein VC, et al. An interocular comparison of the multifocal VEP: a possible technique for detecting local damage to the optic nerve. Investigative Ophthalmology & Visual Science 2000;41:1580-7.

69. Graham SL, Klistorner AI, Grigg JR, Billson FA. Objective VEP perimetry in glaucoma: asymmetry analysis to identify early deficits. Journal of Glaucoma 2000;9:10-9.
70. Lennerstrand G. BINOCULAR INTERACTION STUDIED WITH VISUAL EVOKED RESPONSES (VER) IN HUMANS WITH NORMAL OR IMPAIRED BINOCULAR VISION. Acta Ophthalmologica 1978;56:628-37.
71. Lennerstrand G. SOME OBSERVATIONS ON VISUAL EVOKED RESPONSES (VER) TO DICHOPTIC STIMULATION. Acta Ophthalmologica 1978;56:638-47.
72. Maddess T, James AC, Bowman EA. Contrast response of temporally sparse dichoptic multifocal visual evoked potentials. Visual Neuroscience 2005;22:153-62.
73. Arvind H, Klistorner A, Graham S, Grigg J. Multifocal Visual Evoked Responses to Dichoptic Stimulation Using Virtual Reality Goggles: Multifocal VER to Dichoptic Stimulation. Documenta Ophthalmologica 2006;112:189-99.
74. Sato E TM, Mizota A, Adachi-Usami E. Binocular interaction reflected in visually evoked cortical potentials

as studied with pseudorandom stimuli. Invest Ophthalmol Vis Sci 2002;43: 3355–58.
75. Arvind H KA, Graham S, Grigg J, , Goldberg I KA, Billson F A. Dichoptic Stimulation Improves Detection of Glaucoma with Multifocal Visual Evoked Potentials. IOVS 2007;48:4590-6.
76. Graham S. Binocular Multifocal VEP Using Virtual Reality Goggles Enhances Inter-Eye Asymmetry and Improves Detection of Early Glaucoma,. ARVO presentation (219/B835) 2007.
77. Graham SL, Klistorner AI, Goldberg I. Clinical application of objective perimetry using multifocal visual evoked potentials in glaucoma practice. Arch Ophthalmol 2005;123:729-39.
78. Fortune B, Demirel S, Zhang X, Hood DC, Johnson CA. Repeatability of normal multifocal VEP: implications for detecting progression. J Glaucoma 2006;15:131-41.
79. Atebara NH. Clinical Optics: AAO; 2007.
80. Malik R, Swanson WH, Garway-Heath DF. 'Structure-function relationship' in glaucoma: past thinking and current concepts. Clin Experiment Ophthalmol 2012;40:369-80.
81. M. DS. The disc and the field in glaucoma. Ophthalmology 1978;85:209-14.
82. Sommer A ea. Clinically detectable nerve fiber atrophy precedes the onset of glaucomatous field loss. Arch Ophthalmol 1991;109:77-83.
83. Leung CK, Ye C, Weinreb RN, et al. Retinal nerve fiber layer imaging with spectral-domain optical coherence tomography a study on diagnostic agreement with Heidelberg Retinal Tomograph. Ophthalmology 2010;117:267-74.
84. Healey PR, Lee AJ, Aung T, et al. Diagnostic accuracy of the Heidelberg Retina Tomograph for glaucoma a population-based assessment. Ophthalmology 2010;117:1667-73.
85. Medeiros FA, Zangwill LM, Bowd C, Sample PA, Weinreb RN. Influence of disease severity and optic disc size on the diagnostic performance of imaging instruments in glaucoma. Invest Ophthalmol Vis Sci 2006;47:1008-15.
86. Bowd C, Zangwill LM, Medeiros FA, et al. Structure–Function Relationships Using Confocal Scanning Laser Ophthalmoscopy, Optical Coherence Tomography, and Scanning Laser Polarimetry. Investigative Ophthalmology & Visual Science 2006;47:2889-95.
87. Rao HL, Leite MT, Weinreb RN, et al. Effect of disease severity and optic disc size on diagnostic accuracy of RTVue spectral domain Optical Coherence Tomograph in glaucoma. Invest Ophthalmol Vis Sci 2010;52:1290-6.
88. Saito H, Tsutsumi T, Iwase A, Tomidokoro A, Araie M. Correlation of Disc Morphology Quantified on Stereophotographs to Results by Heidelberg Retina Tomograph II, GDx Variable Corneal Compensation, and Visual Field Tests. Ophthalmology 2010;117:282-9.
89. Harwerth RS, Wheat JL, Fredette MJ, Anderson DR. Linking structure and function in glaucoma. Progress in Retinal and Eye Research 2010;In Press, Corrected Proof.
90. Aptel F, Sayous R, Fortoul V, Beccat S, Denis P. Structure-function relationships using spectral-domain optical coherence tomography: comparison with scanning laser polarimetry. Am J Ophthalmol 2010;150:825-33.e1.
91. Miglior S, Riva I, Guareschi M, et al. Retinal Sensitivity and Retinal Nerve Fiber Layer Thickness Measured by Optical Coherence Tomography in Glaucoma. Am J Ophthalmol 2007;144:733-40.

92. Strouthidis NG, Vinciotti V, Tucker AJ, Gardiner SK, Crabb DP, Garway-Heath DF. Structure and Function in Glaucoma: The Relationship between a Functional Visual Field Map and an Anatomic Retinal Map. Invest Ophthalmol Vis Sci 2006;47:5356-62.
93. Kanamori A, Naka M, Nagai-Kusuhara A, Yamada Y, Nakamura M, Negi A. Regional Relationship Between Retinal Nerve Fiber Layer Thickness and Corresponding Visual Field Sensitivity in Glaucomatous Eyes. Arch Ophthalmol 2008;126:1500-6.
94. Boland M, Quigley H. Evaluation of a combined index of optic nerve structure and function for glaucoma diagnosis. BMC Ophthalmology 2011;11:6.
95. Gardiner SK, Johnson CA, Cioffi GA. Evaluation of the Structure-Function Relationship in Glaucoma. Invest Ophthalmol Vis Sci 2005;46:3712-7.
96. Hood DC, Anderson SC, Wall M, Kardon RH. Structure versus Function in Glaucoma: An Application of a Linear Model. Invest Ophthalmol Vis Sci 2007;48:3662-8.
97. Hood DC, Kardon RH. A framework for comparing structural and functional measures of glaucomatous damage. Progress in Retinal & Eye Research 2007;26:688-710.
98. Zhu H, Crabb DP, Schlottmann PG, et al. Predicting Visual Function from the Measurements of Retinal Nerve Fibre Layer Structure. Invest Ophthalmol Vis Sci 2010;51:5657-66.
99. Hood DC, Anderson SC, Wall M, Raza AS, Kardon RH. A Test of a Linear Model of Glaucomatous Structure-Function Loss Reveals Sources of Variability in Retinal Nerve Fiber and Visual Field Measurements. Invest Ophthalmol Vis Sci 2009;50:4254-66.
100. Gonzalez-Hernandez M, Pablo LE, Armas-Dominguez K, de la Vega RR, Ferreras A, de la Rosa MG. Structure-function relationship depends on glaucoma severity. British Journal of Ophthalmology 2009;93:1195-9.
101. Grewal DS, Sehi M, Greenfield DS. Diffuse Glaucomatous Structural and Functional Damage in the Hemifield Without Significant Pattern Loss. Arch Ophthalmol 2009;127:1442-8.
102. Hood DC, Greenstein VC, Odel JG, et al. Visual field defects and multifocal visual evoked potentials: evidence of a linear relationship. Archives of Ophthalmology 2002;120:1672-81.
103. Laron M, Cheng H, Zhang B, Schiffman JS, Tang RA, Frishman LJ. Comparison of multifocal visual evoked potential, standard automated perimetry and optical coherence tomography in assessing visual pathway in multiple sclerosis patients. Multiple sclerosis (Houndmills, Basingstoke, England) 2010;16.
104. Balachandran C, Graham SL, Klistorner A, Goldberg I. Comparison of objective diagnostic tests in glaucoma: Heidelberg retinal tomography and multifocal visual evoked potentials. Journal of Glaucoma 2006;15:110-6.
105. Shapley R. Visual sensitivity and parallel retinocortical channels. Annual review of psychology 1990;41.
106. Lee BB, Pokorny J, Smith VC, Martin PR, Valberg A. Luminance and chromatic modulation sensitivity of macaque ganglion cells and human observers. Journal of the Optical Society of America A, Optics and image science 1990;7.
107. Dacey DM, Petersen MR. DENDRITIC FIELD SIZE AND MORPHOLOGY OF MIDGET AND PARASOL GANGLION-CELLS OF THE HUMAN RETINA. Proceedings of the National Academy of Sciences of the United States of America 1992;89:9666-70.
108. Sengpiel F, Blakemore C, Harrad R. Interocular suppression in the primary visual cortex: a possible neural basis of binocular rivalry. Vision Research 1995;35:179-95.
109. Sengpiel F, Bonhoeffer T, Freeman TCB, Blakemore C. On the Relationship Between Interocular Suppression in the Primary Visual Cortex and Binocular Rivalry. Brain and Mind 2001;2:39-54.
110. Baker DH, Meese TS, Summers RJ. Psychophysical evidence for two routes to suppression before binocular summation of signals in human vision. Neuroscience 2007;146:435-48.
111. Meese TS, Challinor KL, Summers RJ, Meese TS, Challinor KL, Summers RJ. A common contrast pooling rule for suppression within and between the eyes. Visual Neuroscience 2008;25:585-601.
112. Johnson CA, Adams AJ, Casson EJ, Brandt JD. Progression of early glaucomatous visual field loss as detected by blue-on-yellow and standard white-on-white automated perimetry. Arch Ophthalmol 1993;111:651-6.

113. Sample PA, Irak I, Martinez GA, Yamagishi N. Asymmetries in the normal short-wavelength visual field: implications for short-wavelength automated perimetry. Am J Ophthalmol 1997;124:46-52.
114. Thomas R, Bhat S, Muliyil JP, Parikh R, George R. Frequency doubling perimetry in glaucoma. J Glaucoma 2002;11:46-50.
115. Medeiros FA, Sample PA, Weinreb RN. Frequency doubling technology perimetry abnormalities as predictors of glaucomatous visual field loss. Am J Ophthalmol 2004;137:863-71.
116. Solomon SG, Lee BB, White AJR, Ruttiger L, Martin PR. Chromatic organization of ganglion cell receptive fields in the peripheral retina. The Journal of neuroscience : the official journal of the Society for Neuroscience 2005;25.
117. Holopigian K, Bach M. A primer on common statistical errors in clinical ophthalmology. Documenta ophthalmologica Advances in ophthalmology 2010;121:215-22.
118. Garway-Heath DF, Holder GE, Fitzke FW, Hitchings RA. Relationship between Electrophysiological, Psychophysical, and Anatomical Measurements in Glaucoma. Invest Ophthalmol Vis Sci 2002;43:2213-20.
119. Hood DC, Chen JY, Yang EB, et al. The role of the multifocal visual evoked potemtial (mfvep) latency in understanding optic nerve and retinal diseases. Trans Am Ophthalmol Soc 2006;104:71-7.
120. Klistorner A GS. Objective perimetry in glaucoma. Opthalmology 2000;107:2283-99.
121. Ruseckaite R, T M, G D, CJ L, AC J. Sparse multifocal stimuli for the detection of multiple sclerosis. Annals of Neurology 2005;57:904-13.
122. Maddess T, James AC, Bowman EA. Contrast response of temporally sparse dichoptic multifocal visual evoked potentials. Visual Neuroscience 2005;22:153-62.
123. Lennerstrand G. Binocular Interaction studied with visual

evoked responses (VER) in humans with normal or

impaired binocular vision. Acta Ophthalmol (Copenh) 1978;56: 628–37.
124. Arvind H, Klistorner A, Graham SL, Grigg JR. Multifocal visual evoked responses to dichoptic stimulation using virtual reality goggles. Documenta Ophthalmologica 2006;112:189-99.
125. Arden GB, Barnard WM, Mushin AS. Visual evoked responses in amblyopia. Br J Ophthalmol 1974;58:18-192.
126. Lennerstrand G. Some observations on visual evoked responses to dichoptic stimulation. Acta Ophthalmol (Copenh) 1978;56:638-47.
127. Lennerstrand G. Binocular interaction studied with visual evoked responses in human with normal or impaired binocular vision. Acta Ophthalmol (Copenh) 1978;56:628-37.
128. Winn BJ, Shin E, Odel JG, Greenstein VC, Hood DC. Interpreting the multifocal visual evoked potential: the effect of refractive errors, cataracts and fixation errors. Br J Ophthalmol 2005;89:340-4.
129. Cowey A, Polls ET. Human cortical magnification factor and its relation to visual acuity. Brain Research 1974;21:447-54.
130. Klistorner A, Graham SL. Electroencephalogram-based scaling of multifocal visual evoked potentials: Effect on intersubject amplitude variability. Invest Ophthalmol Vis Sci 2001;42:2145-52.
131. Goldberg I, Graham SL, Klistorner AI. Multifocal objective perimetry in the detection of glaucomatous field loss. Am J Ophthalmol 2002;133:29-39.
132. Sengpiel F, Bonhoeffer T, Freeman TCB, Blakemore C. On the relationship between interocular suppression in the primary visual cortex and binocular rivary. Brain Mind 2001;2:39-54.
133. Foster KH, Gaska JP, Nagler M, Pollen DA. Spatial and temporal frequency selectivity of neurons in visual cortical areas V1 and V2 of the macaque monkey. J Physiol 1977;365:331-63.
134. Maunsell JH. Functional Visual Streams. Current Opinion in Neurobiology 1992:506-10.
135. Lee BB, Pokorny J, Smith VC, Martin PR, Valberg A. Luminance and chromatic modulation sensitivity of macaque ganglion cells and human observers. J Opt Soc Am, A 1990;7: 2223-36.
136. Dacey DM, Petersen MR. Dendritic field size and morphology of midget and parasol ganglion cell of the human retina. Proc Natl Acad Sci USA 1992;89:9666-70.
137. LeVay S, Nelson SB. Columnar organisation of the visual cortex. The neural basis of visual function, Leventhal, A, Macmillian Press, Houndmills 1991:226-315.

138. Solomon S.G. WAJR, Martin P.R. Temporal contrast sensitivity in the lateral geniculate nucleous of a New World monkey, the marmoset Callithrix jacchus. Journal of Physiology 1999;517:907-17.
139. Wisowaty J.J. BRM. Temporal modulation sensitivity of the blue mechanism : measurements made without chromatic adaptation. . Vision Res 1980;20:895-909.
140. Landers JA, Goldberg I, Graham SL. Detection of Early Visual Field Loss in Glaucoma Using Frequency-Doubling Perimetry and Short-Wavelength Automated Perimetry. Arch Ophthalmol 2003;121:1705-10.
141. Foster DH, Mason RJ. Interaction between rod and cone systems in dichoptic visual masking. Neuroscience letters 1977;4.
142. Leaney J, Klistorner A, Arvind H, Graham SL. Dichoptic Suppression of mfVEP Amplitude: Effect of Retinal Eccentricity and Simulated Unilateral Visual Impairment. Investigative Ophthalmology & Visual Science 2010;51:6549-55.
143. Peterson BB, Dacey DM. Morphology of wide-field, monostratified ganglion cells of the human retina. Visual neuroscience 1999;16.
144. Percival KA, Martin PR, Grunert U. Organisation of koniocellular-projecting ganglion cells and diffuse bipolar cells in the primate fovea. The European journal of neuroscience 2013;37.
145. Livingstone MS HD. Anatomy and physiology of a color system in the primate visual cortex. J Neurosci 1984;4:309-56.
146. Hubel DH WT. Receptive fields and functional architecture of monkey striate cortex. J Physiol (Lond) 1968;195:215-43.
147. GF P. Processing of stereoscopic information in monkey visual cortex. In: Edelman GM GW, Cowan WH, ed. Dynamic Aspects of Neocortical Function. New York: Wiley; 1984:613-35.
148. Hollins M. The effect of contrast on the completeness of binocular rivalry suppression. Perception & Psychophysics 1980;27:550-6.
149. Harter MR, Seiple WH, Musso M. Binocular summation and suppression: Visually evoked cortical responses to dichoptically presented patterns of different spatial frequencies. Vision Research 1974;14:1169-80.
150. Ruseckaite R, Maddess T, Danta G, Lueck CJ, James AC. Sparse multifocal stimuli for the detection of multiple sclerosis. Annals of Neurology 2005;57:904-13.
151. Yücel YH, Zhang Q, Weinreb RN, Kaufman PL, Gupta N. Effects of retinal ganglion cell loss on magno-, parvo-, koniocellular pathways in the lateral geniculate nucleus and visual cortex in glaucoma. Progress in Retinal and Eye Research 2003;22:465-81.
152. Adams AJ, Rodic R, Husted R, Stamper R. Spectral sensitivity and color discrimination changes in glaucoma and glaucoma-suspect patients. Investigative ophthalmology & visual science 1982;23.
153. Anderson DR, Normal Tension Glaucoma S. Collaborative normal tension glaucoma study. Current opinion in ophthalmology 2003;14.
154. Chauhan BC, McCormick TA, Nicolela MT, LeBlanc RP. Optic disc and visual field changes in a prospective longitudinal study of patients with glaucoma: comparison of scanning laser tomography with conventional perimetry and optic disc photography. Archives of Ophthalmology 2001;119:1492-9.
155. Cowey A, Polls, E.T. Human cortical magnification factor and its relation to visual acuity. Brain Res 1974;21:447-54.
156. Boland MV, Zhang L, Broman AT, Jampel HD, Quigley HA. Comparison of optic nerve head topography and visual field in eyes with open-angle and angle-closure glaucoma. Ophthalmology 2008;115:239-45.e2.
157. Healey PR, Anne JL, Tin A, Tien YW, Paul M. Diagnostic Accuracy of the Heidelberg Retina Tomograph for Glaucoma: A Population-Based Assessment. Ophthalmology 2010;117:1667-73.
158. Schlottmann PG, De Cilla S, Greenfield DS, Caprioli J, Garway-Heath DF. Relationship between Visual Field Sensitivity and Retinal Nerve Fiber Layer Thickness as Measured by Scanning Laser Polarimetry. Invest Ophthalmol Vis Sci 2004;45:1823-9.
159. Ferreras A, Pablo LE, Garway-Heath DF, Fogagnolo P, Garcia-Feijoo J. Mapping Standard Automated Perimetry to the Peripapillary Retinal Nerve Fiber Layer in Glaucoma. Invest Ophthalmol Vis Sci 2008;49:3018-25.

160. Mills RP, Budenz DL, Lee PP, et al. Categorizing the stage of glaucoma from pre-diagnosis to end-stage disease. Am J Ophthalmol 2006;141:24-30.
161. Garway-Heath DF, Caprioli J, Fitzke FW, Hitchings RA. Scaling the hill of vision: the physiological relationship between light sensitivity and ganglion cell numbers. Investigative Ophthalmology & Visual Science 2000;41:1774-82.
162. Oddone F, Centofanti M, Iester M, et al. Sector-based analysis with the Heidelberg Retinal Tomograph 3 across disc sizes and glaucoma stages: a multicenter study. Ophthalmology 2009;116:1106-11.
163. Leung CK-s, Chong KK-L, Chan W-m, et al. Comparative Study of Retinal Nerve Fiber Layer Measurement by StratusOCT and GDx VCC, II: Structure/Function Regression Analysis in Glaucoma. Invest Ophthalmol Vis Sci 2005;46:3702-11.
164. Artes PH, O'Leary N, Hutchison DM, et al. Properties of the Statpac Visual Field Index. Investigative Ophthalmology & Visual Science 2011;52:4030-8.
165. Horn FK, Mardin CY, Laemmer R, et al. Correlation between Local Glaucomatous Visual Field Defects and Loss of Nerve Fiber Layer Thickness Measured with Polarimetry and Spectral Domain OCT. Invest Ophthalmol Vis Sci 2009;50:1971-7.
166. Moreno-Montanes JMDP, Anton AMDP, Garcia ND, Olmo NMD, Morilla AP, Fallon MD. Comparison of Retinal Nerve Fiber Layer Thickness Values Using Stratus Optical Coherence Tomography and Heidelberg Retina Tomograph-III. Journal of Glaucoma 2009;18:528-34.
167. Sato S, Hirooka K, Baba T, et al. Correlation between retinal nerve fibre layer thickness and retinal sensitivity. Acta Opthalmologica 2008;86:609-13.
168. Kim N, Lee ES, Seong GJ, Kim JH, An HG, Chan YK. Structure-function Relationship and Diagnostic Value of Macular Ganglion Cell Complex Measurement using Fourier-domain OCT in Glaucoma. Invest Ophthalmol Vis Sci 2010;51:4646-51.
169. Danesh-Meyer HV, Ku JYF, Papchenko TL, Jayasundera T, Hsiang JC, Gamble GD. Regional Correlation of Structure and Function in Glaucoma, Using the Disc Damage Likelihood Scale, Heidelberg Retina Tomograph, and Visual Fields. Ophthalmology 2006;113:603-11.
170. Ford BA, Artes PH, McCormick TA, Nicolela MT, LeBlanc RP, Chauhan BC. Comparison of data analysis tools for detection of glaucoma with the heidelberg retina tomograph. Ophthalmology 2003;110:1145-50.
171. Zangwill LM, Jain S, Racette L, et al. The Effect of Disc Size and Severity of Disease on the Diagnostic Accuracy of the Heidelberg Retina Tomograph Glaucoma Probability Score. Invest Ophthalmol Vis Sci 2007;48:2653-60.
172. Vessani RM, Moritz R, Batis L, et al. Comparison of quantitative imaging devices and subjective optic nerve head assessment by general ophthalmologists to differentiate normal from glaucomatous eyes. Journal of Glaucoma 2009;18:253-61.
173. Bowd C, Zangwill LM, Medeiros FA, et al. Structure-Function Relationships Using Confocal Scanning Laser Ophthalmoscopy, Optical Coherence Tomography, and Scanning Laser Polarimetry. Invest Ophthalmol Vis Sci 2006;47:2889-95.
174. Wheat JLR, N.V. Harwerth, R.S. Correlating RNFL Thickness by OCT With Perimetric Sensitivity in Glaucoma Patients. J Glaucoma 2011;17:17.
175. Klistorner A, Fraser C, Garrick R, et al. Correlation between full-field and multifocal VEPs in optic neuritis. Documenta Ophthalmologica 2008;116:19-27.
176. Klistorner A, Arvind H, Garrick R, Graham SL, Paine M, Yiannikas C. Interrelationship of Optical Coherence Tomography and Multifocal Visual-Evoked Potentials after Optic Neuritis. Investigative Ophthalmology & Visual Science 2010;51:2770-7.
177. Leaney J, Healey PR, Lee M, Graham SL. Correlation of structural retinal nerve fibre layer parameters and functional measures using Heidelberg Retinal Tomography and Spectralis spectral domain optical coherence tomography at different levels of glaucoma severity. Clinical & Experimental Ophthalmology 2012;40:802-12.